

**Catalysis by Nanocrystalline Ceria  
Modified with  
Transition Metals**

*Thesis submitted to the  
Cochin University of Science & Technology  
in partial fulfilment of the requirements for the Degree of*

**Doctor of Philosophy  
in  
Chemistry  
  
in the Faculty of Science**

*By  
Fincy Jose P*

**Department of Applied Chemistry  
Cochin University of Science and Technology  
Kochi-682 022  
December 2004**

*...To My Parents, Husband and Son*

## CERTIFICATE

This is to certify that the work “**Catalysis by Nanocrystalline Ceria Modified with Transition Metals**” submitted by Ms. Fincy Jose P is a bonafide work record of research work carried out by her under my supervision at the Department of Applied Chemistry, Cochin University of Science and Technology in partial fulfilment of the requirements for the degree of Doctor of Philosophy in Chemistry, and further that no part there of has been included before for the award of any other Degree.



Professor Dr. S. Sugunan  
(Supervising Guide)

Department of Applied Chemistry  
Cochin University of Science & Technology  
Kochi-22

Kochi-22  
15-12-2004

## DECLARATION

I hereby declare that the work “**Catalysis by Nanocrystalline Ceria Modified with Transition Metals**” is based on my original work done under the guidance of Dr. S. Sugunan, Professor in Physical Chemistry, Department of Applied Chemistry, Cochin University of Science and Technology and has not been included in any other thesis submitted previously for the award of any other degree.



Fincy Jose P

Kochi-22

15-12-2004

## Preface

---

The development in catalysis has made a significant impact on the rapid growth of chemical industry in all sectors. In recent years catalysis is also looked upon as a solution to eliminate or replace polluting processes due to the inherent characteristics of most catalytic processes as clean technologies.

Rare earth oxides have been widely investigated as structural and electronic promoters to improve the activity, selectivity and thermal stability of catalysts. The most significant of the oxides of rare earth elements in industrial catalysis is  $\text{CeO}_2$ . Its use in catalysis has attracted considerable attention, particularly in applications like environmental catalysis, where ceria has shown great potential. There are several emerging processes for which cerium oxide is currently being actively investigated, specifically in the field of three way catalysts, Fluid Catalytic Cracking etc.

The objective of the present work is to improve the textural and structural properties of cerium oxide by the incorporation of transition metals as well as sulphate ions. We have incorporated tungsten, molybdenum and chromium oxide into pure as well as sulphated cerium oxide and the catalytic systems thus prepared were characterised using various techniques. Industrially important reactions such as acetalization and deacetalization, oxidative dehydrogenation of ethylbenzene, MTBE synthesis and Beckmann rearrangement of cinnamaldoxime and salicylaldoxime have been selected for the measurement of the catalytic activity of the systems.

The work is presented in eight chapters; the last chapter gives the summary of the work done during the research period. The results of the present work indicates that the prepared systems can act as versatile catalysts for the protection and deprotection of functional groups in organic synthesis. The catalytic systems are also proved to be efficient for the production of benzoxazole and isoquinoline by the Beckmann rearrangement of salicylaldoxime and cinnamaldoxime. Furthermore, the materials show considerable activities during oxidative dehydrogenation of ethyl benzene and MTBE synthesis.

## ***ACKNOWLEDGEMENT***

My sincerest thanks and gratitude are due to the efforts of many, whose valuable contributions and services have helped me in the realization of this research work. At the outset I thank God Almighty, without whose blessings I would never have been able to complete this Herculean task.

I take this opportunity to express my heart felt gratitude to Professor Dr. S. Sugunan, my guide, who planted the seed of research interest in me. He has been inspiring and dedicated in a very scholarly way and my gratitude to him is that of a humble sishya to a reverend Guru. I would like to thank Professor Prathapachandra Kurup, Head, Dept. of Applied Chemistry, CUSAT, for the timely help and support extended during the tenure of my research. I am gratefully indebted to Dr. S. Prathapan, who had been instrumental in proposing the mechanisms of various reactions. I extend a special word of thanks to all the teaching and non teaching staff, research scholars and students of this department for their help and support.

I am happy to acknowledge the assistance extended to me by my lab mates without whose help I wouldn't have fulfilled this great ambition. My sincere thanks to Dr. Renuka, Dr. Ramankutty, Dr. Rehna, Dr. Sreejarani, Dr. Nisha, Dr. Suja and Dr. Deepa. I also extend my whole hearted thanks to my present lab mates Smitha, Sanjay, Sunaja, Maya, Radhika, Shali, Binitha, Ramanathan, Kochurani, Ajitha and Shalini. My special thanks to Manju and Bejoy, whose timely help and support has more than once turned the tide in my favour. My sincere thanks are also due to Mr. Gopi Menon, Mr. Joshi, Dept. of USIC and to Mr. Suresh, service engineer, Chemito for their technical assistance.

On this occasion I cuddle the fond memories of my parents who have inspired me and strengthened my mind to face the realities in this competitive world of research. I am bound by love to admit the help extended by my in-laws towards the completion of this doctoral work. This acknowledgement would be incomplete without mentioning my aunts and uncles who loved me and cared for my family while I was steeped in my research work. I thank my husband, who has been with me in every ups and downs, consoling me and fortifying me. Without his love and support this research would never have been complete. Last of all I recall how much I have missed my little baby who has adjusted so much even in his tender years, so that I could complete my dream work decently.

The financial support offered by CSIR-New Delhi is herewith acknowledged with gratitude.

# Contents

## 1. Introduction and Literature Survey

Abstract

1.1 Introduction	2
1.2 Structural properties of cerium oxide	3
1.3 Preparation methods for cerium oxide	4
1.4 Significance of cerium oxide in catalysis	7
1.5 Tungsten, molybdenum and chromium based catalysts	8
1.6 Surface acidity of metal oxides and its measurements	9
1.7 Reactions selected for the present study	10
1.8 Major objectives of the present work	17
References	18

## 2. Materials and Methods

Abstract

2.1 Introduction	28
2.2 Catalyst preparation	28
2.3 Catalyst notations	30
2.4 Characterisation techniques	30
I. Powder X-Ray Diffraction (PXRD) Analysis	31
II. Scanning Electron Microscopy (SEM)	33
III. Energy Dispersive X-ray (EDX) Analysis	33
IV. BET Surface Area and Pore Volume Measurements	34
V. Thermo Gravimetric Analysis (TGA)	35
VI. Infrared (IR) Spectroscopy	36
VII. Diffuse Reflectance UV-vis (DR UV-vis) Spectroscopy	37

2.5 Surface acid amount determination studies	37
I. Adsorption Techniques	38
a) <i>Temperature Programmed Desorption (TPD) of Ammonia</i>	38
b) <i>Perylene Adsorption Studies</i>	39
c) <i>TGA of 2, 6-dimethyl pyridine Adsorbed Samples</i>	39
II. Test reactions for acidity	40
a) <i>Vapour phase Cumene Cracking Reaction</i>	40
b) <i>Vapour phase Cyclohexanol Decomposition Reaction</i>	41
2.6 Catalytic activity measurements	41
I. Liquid - Phase Reactions	42
<i>Acetalization of Cyclohexanone and Hydrolysis of Dimethyl acetal</i>	42
II. Vapour – Phase Reactions	43
a) <i>Oxidative Dehydrogenation of Ethylbenzene</i>	43
b) <i>Methyl Tertiary Butyl Ether Synthesis</i>	44
c) <i>Beckmann Rearrangement of Salicylaldoxime and Cinnamaldoxime</i>	44
References	45
<b>3. Physico-Chemical Characterisation</b>	
Abstract	
3.1 Introduction	48
3.2 Physical characterisation	49
I. <i>BET Surface Area and Pore Volume measurements</i>	49
II. <i>Energy Dispersive X-ray Fluorescence Analysis (EDX)</i>	53
III. <i>X-ray Diffraction analysis (XRD)</i>	55
IV. <i>Scanning Electron Microscopy (SEM)</i>	61
V. <i>Thermogravimetric Analysis (TGA)</i>	64

VI. <i>Fourier Transform Infrared Spectroscopy (FTIR)</i>	67
VII. <i>Ultraviolet -Visible Diffuse Reflectance Spectroscopy (UV - DRS)</i>	71
3.3 Surface acidity measurements	
a) <i>Temperature Programmed Desorption of Ammonia (TPD-NH<sub>3</sub>)</i>	76
b) <i>Perylene Adsorption Studies</i>	80
c) <i>Thermodesorption studies of adsorbed 2,6-dimethylpyridine</i>	83
3.4 Vapour- phase cumene cracking reaction	87
3.5 Effect of reaction variables	87
3.6 Catalytic activity of various systems	89
3.7 Vapour-phase cyclohexanol decomposition reaction	94
3.8 Effect of reaction variables	94
3.9 Catalytic activity of different systems	97
3.10 Conclusions	99
References	100
<b>4. Acetalization and De-acetalization of Functional Groups</b>	
Abstract	
4.1 Introduction	106
4.2 Protection reaction (Acetalization of cyclohexanone)	111
4.3 Effect of reaction variables	111
4.4 Catalytic activity of different catalyst systems	116
4.5 De-protection reaction (Hydrolysis of dimethoxy cyclohexane)	122
4.6 Activity of different catalytic systems	122
4.7 Conclusions	125
References	126

## **5. Oxidative Dehydrogenation of Ethylbenzene**

Abstract

5.1 Introduction	130
5.2 Oxidative dehydrogenation of ethylbenzene	131
5.3 Process optimisation	132
5.4 Catalytic activity of different systems	137
5.5 Mechanism of the reaction	143
5.6 Conclusions	146
References	146

## **6. Beckmann Rearrangements**

Abstract

### Section 1

#### Beckmann Rearrangement of Salicylaldoxime

6.1 Introduction	150
6.2 Beckmann rearrangement of salicylaldoxime	152
6.3 Process optimisation	153
6.4 Activity of different catalytic systems	157
6.5 Conclusions	162

### Section 2

#### Beckmann Rearrangement of Cinnamaldoxime

6.6 Introduction	163
6.7 Beckmann rearrangement of cinnamaldoxime	164
6.8 Process optimisation	165
6.9 Performance of different catalyst systems	168
6.10 Conclusions	173
References	173

## **7. Methyl Tert-Butyl Ether Synthesis**

Abstract

7.1 Introduction	178
7.2 Methyl tertiary butyl ether synthesis	180
7.3 Process optimisation	181
7.4 Catalytic efficiency of different systems	186
7.5 Conclusions	192
References	193

## **8. Summary and Conclusions**

Abstract

8.1 Introduction	197
8.2 Summary	197
8.3 Conclusions	199
Future Outlook	201

## ***Introduction And Literature Survey***

### **Abstract**

---

*Progress towards environmentally friendly processing is marked by the elimination of waste and by-product generation and reduced dependence on hazardous chemicals. The key to both is often provided by the use of heterogeneous catalysis. This area long established in bulk-chemical processing, is beginning to make inroads into the fine-chemical industry also. Much interest is aroused in the field of metal oxide catalysts as they have well defined physical properties and catalytic activities. The use of CeO<sub>2</sub> based materials in catalysis has attracted considerable attention in recent years, particularly in applications like environmental catalysis, where ceria has shown great potential. In the present research work emphasis is given to the enhancement of surface acidity of cerium oxide and its subsequent application in some industrially important reactions. This chapter deals with the general introduction and literature survey on the components of the catalytic systems developed and the various reactions performed for the activity measurements.*

---

## **1.1 Introduction**

Catalysis has wide ranging applications in chemical industry and has a major impact on the quality of human life as well as economic development. In recent years catalysis is also looked upon as a solution to eliminate or replace polluting processes due to the inherent characteristics of most catalytic processes as clean technologies. The catalytic reactions are generally classified as homogeneous and heterogeneous depending on the physical state of the catalyst. Both the categories have their advantages and disadvantages, though heterogeneous catalysis has been more widely applied, as it is more environmentally benign.

Heterogeneous catalysis has been the basis for most of the commercial processes in petroleum and petrochemical industry, where the solid catalysts are often used in vapour phase gas-solid or gas-liquid-solid or liquid- solid reactions. The solid catalysed reactions have a major advantage of easy separation and of using on continuous modes and hence followed in very large scale manufacture. Solid acid catalysts are appealing since the nature of acid sites is known and their chemical behaviour in acid catalysed reactions can be rationalised by means of existing theories and models. It is possible to modify the acid properties of these materials by adopting various synthesis and post synthesis routes. In addition, it is possible to confirm these modifications by the available techniques.

There exists a large variety of solid acids: natural clay minerals, mounted acids, cation-exchange resins, metal oxides and mixtures of metal oxides and zeolites. The studies on catalysis by solid acids are extremely numerous<sup>1-2</sup>. Several reviews have recently been published dealing with the use of solid acids as heterogeneous catalysts for the preparation of fine chemicals<sup>3-6</sup>. In recent years much attention has been centered on the use of solid acids such as metal oxides, mixed metal oxides and supported metal oxides as they form a highly versatile class of catalysts in industrially important reactions.

Rare earth oxides have been widely investigated as structural and electronic promoters to improve the activity, selectivity and thermal stability of catalysts. The

most significant of the oxides of rare-earth elements in industrial catalysis is certainly  $\text{CeO}_2$ . Its use in catalysis has attracted in recent years, especially for those applications, such as oxidation and dehydrogenation reactions, where ceria has shown great potential.

## 1.2 Structural properties of cerium oxide

Cerium with a  $4f^25d^06s^2$  electronic configuration can exhibit both the +3 and +4 oxidation states, and intermediate oxides whose composition is in the range  $\text{Ce}_2\text{O}_3$ - $\text{CeO}_2$  can also be formed. Thermodynamic data indicate that cerium metal is unstable in the presence of oxygen and that  $\text{Ce}_2\text{O}_3$  and  $\text{CeO}_2$  are easily formed<sup>7</sup>. The final stoichiometry is strongly dependent on temperature and oxygen pressure.

The dioxide  $\text{CeO}_2$  crystallises in fluorite structure, which is named after the mineral form of calcium fluoride. It has a face centered cubic unit cell (f. c. c) with space group  $\text{Fm}\bar{3}\text{m}$  ( $a = 0.54113$  nm). In this structure, each cerium cation is coordinated by eight equivalent nearest neighbour oxygen anions at the corner of a cube, each anion being tetrahedrally coordinated by four cations. In early days the oxides of cerium in the range  $\text{Ce}_2\text{O}_3$ - $\text{CeO}_2$  were treated using the classical point defect model of non-stoichiometry, in which oxygen-vacant sites were considered to be present in the lattice in a random fashion, in conformity with the law of statistical thermodynamics. Later on, increasing evidence was accumulated to indicate the formation of stoichiometric phases at low temperature originating from the fluorite lattice by removal of oxygen ions and ordering of the vacancies formed. It is from the pioneering work of Bevan, Brauer and co-workers that a first reliable picture of the structural behaviour of reduced ceria was developed<sup>8-11</sup>. This was later refined by the structural studies of Eyring and Ray et al. and has recently been rationalised by the development of geometric models for defect ordering which allow the description of all known structures and also the prediction of possible phases<sup>12-16</sup>.

### 1.3. Preparation methods for cerium oxide

#### a) Precursor method

Ceria based oxides can be obtained by the decomposition of some compound precursors, such as hydroxide, nitrate, halides, sulfates, carbonates and acetates<sup>17</sup>. Nanosize or porous cerium oxide particles have been prepared at low temperatures by pyrolysis of amorphous citrates, which is prepared by the evaporation of the solvent from the aqueous solution containing cerium nitrate and citric acid<sup>18-19</sup>.

#### b) Precipitation and co-precipitation method

Chemical precipitation is a widely used method for synthesising solid materials from solution. This method utilizes a liquid-phase reaction to prepare insoluble compounds that are crystalline or amorphous precipitates. Usually, ceria preparation is carried out by calcination of the hydroxide or oxalate precipitated using the reaction of aqueous solution of inorganic cerium salt [ $\text{Ce}(\text{NO}_3)_3$ ,  $\text{CeCl}_3$ ,  $\text{CeSO}_4$  and  $(\text{NH}_4)_2\text{Ce}(\text{NO}_3)_6$ ] with alkali solution (NaOH,  $\text{NH}_4\text{OH}$  etc) or oxalic acid solution<sup>20-22</sup>. In the synthesis of mixed oxides, the co-precipitation method is the most commonly used wet-chemical process. Salts of the several metals are dissolved in the same solvent (water is the most popular one). A quantitative and simultaneous precipitation of all the cations occurs without segregation of any particular constituents in the precipitates. Plenty of ceria based mixed oxides such as  $\text{CeO}_2\text{-MnO}_x$ <sup>23-24</sup>,  $\text{CeO}_2\text{-La}_2\text{O}_3$ <sup>25</sup>,  $\text{CeO}_2\text{-TbO}_x$ <sup>26</sup> and  $\text{CeO}_2\text{-ZrO}_2$ <sup>27-30</sup> have been prepared by this method.

#### c) Hydrothermal and solvothermal synthesis

In preparing fine particles of inorganic metal oxides, the hydrothermal method consists of three types of processes: hydrothermal synthesis, hydrothermal oxidation and hydrothermal crystallisation. Of these the hydrothermal crystallisation is the most popular technique in preparing ceria-based nanoparticles. Precipitation from aqueous solutions under elevated temperature and high pressure are involved in the process. In this method particle size is found to depend on the reaction temperature and the starting materials used.

#### d) Sol-gel method

This method is especially used for the synthesis of ultrafine oxide materials at relatively low temperatures. For the preparation of ceria based oxides, cerium isopropoxide, cerium acetylacetonate, cerium nitrate are used as the precursors. The water necessary for the hydrolysis reaction is brought in by adding directly or by the hydrated cerium nitrate. Using this method,  $\text{CeO}_2$ <sup>31</sup>,  $\text{CeO}_2\text{-PrO}_x$ <sup>32</sup>,  $\text{CeO}_2\text{-ZrO}_2$ <sup>33-34</sup> and  $\text{CeO}_2\text{-TiO}_2$ <sup>35</sup> particles have been synthesised.

#### e) Surfactant assisted method

The use of templating techniques has recently opened up new opportunities in the design of novel high surface area materials for catalytic applications<sup>36</sup>. In the present work, this method is used for the preparation of cerium oxides, since the conventional hydroxide method yielded samples with low surface area and textural properties. This method involves the reaction of cerium salts (cerium nitrate) under basic conditions with ammonia at room temperature, leading to the formation of gelatinous, hydrous cerium oxide. If the reaction is conducted in the presence of cationic surfactants (cetyltrimethylammonium bromide), hydrous cerium oxide can incorporate the organic molecule by exchange with surface OH groups<sup>37</sup>. The hydrous oxides can exchange either cations or anions depending on the pH of the medium. If the pH is higher than that of the isoelectric point of hydrous cerium oxide, incorporation of the cationic surfactant takes place according to the equilibrium depicted below:

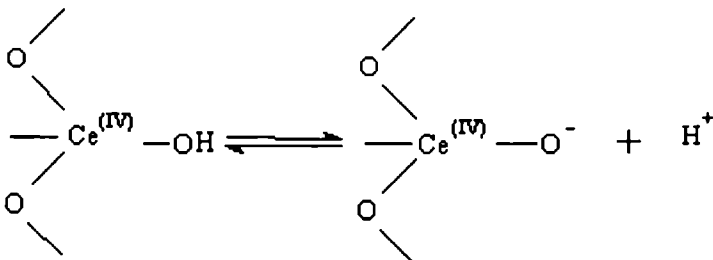


Figure 1.1  
Equilibrium involved in the incorporation of surfactant

The pH of the isoelectric point for hydrous cerium oxide is in the range 6.75-8.00, depending on the environment, and under highly basic conditions (pH > 9), the equilibrium shifts to the right with a negative charge on the surface<sup>38</sup>. The surfactant interacts with hydrous Ce (IV) oxide which has already been formed during the precipitation stage. This implies that oxidation of  $Ce^{3+}$  takes place during the reaction of  $Ce(NO_3)_3$  with ammonium hydroxide. The driving force for the oxidation of  $Ce^{3+}$  is related to the basicity of the reaction medium. According to the definition of basicity,  $Ce^{3+}$  can be regarded as Lewis base while  $Ce^{4+}$  is a Lewis acid. Basic solutions, therefore, favour the formation of  $Ce^{4+}$ . Because of the lower basicity and higher charge,  $Ce^{4+}$  ions are easily hydrated to form complexes with  $OH^-$  and  $H_2O$  [ $Ce(H_2O)_x(OH)_y^{(4-y)^+}$ ]. Further polymerisation and precipitation of these hydroxides to give hydrous oxides and then to the oxide is strongly favoured under basic conditions and in the presence of the surfactant. The hydrated complex thus formed then incorporates the surfactant in accordance with the reaction II. This step can also be viewed as the formation of polymeric hydrous oxide, which then reacts with the alkyl ammonium salt (steps II a and II b) at a pH well above that of the isoelectric point of cerium oxide. Under these conditions, an exchange between the deprotonated hydroxy group of the oxide and the alkyl ammonium cation takes place with the formation of an inorganic/organic composite which upon drying and calcination give cerium oxide with high surface area. The steps involved during the preparation are given in Figure I.2

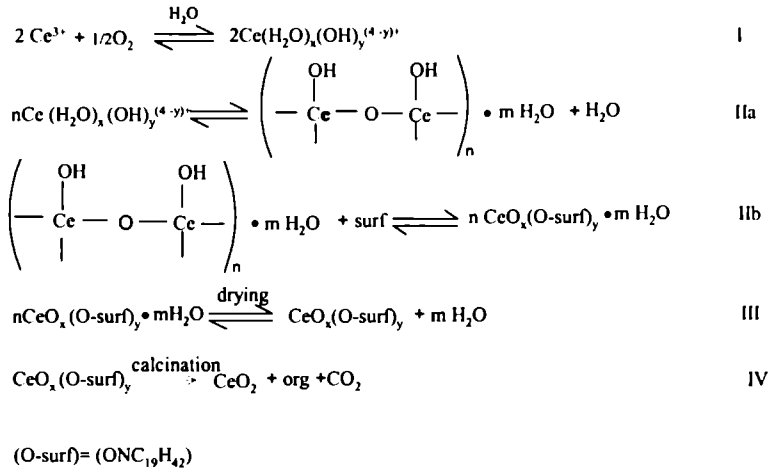


Figure 1.2  
Steps involved in the preparation method

#### 1.4. Significance of cerium oxide in catalysis

Huge amounts of catalysts are consumed for refinery operations to convert crude oil into lower molecular weight fractions (fluid catalytic cracking). Many of the catalyst compositions available contain lanthanides including cerium<sup>39</sup>. CeO<sub>2</sub>-based materials are extensively studied for their wide range of applications in fuel cells<sup>40</sup> gas sensors<sup>41</sup> and as a promoter in three-way catalyst for automotive exhaust control<sup>42</sup>. The properties like the promotion of noble metal dispersion, promotion of water gas shift (WGS) reaction, thermal stability and, most importantly, its oxygen storage capacity (OSC) make it an ideal promoter in TWC formations<sup>43</sup>. The key to oxygen storage capacity of CeO<sub>2</sub>-based materials is due to its ability to shift between Ce<sup>4+</sup> and Ce<sup>3+</sup> state, stable fluorite structure which in fact allows release and transport of O<sup>2-</sup> ions. It is reported that the incorporation of zirconium in the lattice of CeO<sub>2</sub> enhances further OSC by creating lattice defects and hence facilitating O<sup>2-</sup> ion mobility<sup>44</sup>. The ability of cerium oxide to act as an oxidizing agent underlies the

potential use of various cerium derivatives as additives to aid combustion.

The control of sulfur oxide emissions is becoming more important. Several catalyst additives containing cerium and/ or lanthanides can act as the  $\text{SO}_x$  control agent<sup>45</sup>. Cerium also has minor use in other commercial catalysts<sup>46</sup>. The dominant catalyst for the production of styrene from ethyl benzene is an alkali-promoted iron oxide based material. The addition of a few percent of cerium oxide to this system improves activity for styrene formation. The ammoxidation of propylene to produce acrylonitrile is carried out over catalytically active complex molybdates. Cerium, a component of several patented compositions supports this chemical reaction<sup>47</sup>.

One of the most important catalytic properties of ceria is its ability for total oxidation of hydrocarbons along with carbon monoxide and hydrogen. For these latter reasons, ceria may be used as electrode in the fuel cell process, one of the most difficult challenge for next years to come. The oxidation property of ceria is related to the  $\text{Ce}^{4+}/\text{Ce}^{3+}$  electrochemical potential. According to the electrode potential  $\text{Ce}^{4+}$  species are strong oxidising agents<sup>48</sup>. According to its ability to “deliver” oxygen  $\text{CeO}_2$  is considered as a n-type semiconductor.

### **1.5 Tungsten, molybdenum and chromium based catalysts**

Tungsten-based catalysts supported on oxides have been used in various processes, namely hydrodesulphurisation<sup>49-50</sup>, selective catalytic reduction of  $\text{NO}_x$ <sup>51</sup> and olefin metathesis<sup>52-53</sup>. The small and highly charged  $\text{W}^{+6}$  cations are found in several solid acids: heteropoly-oxoanion compounds such as 12-tungstophosphoric acid<sup>54</sup>, oxygen-modified tungsten carbides<sup>55</sup> and  $\text{WO}_x$  dispersed on  $\gamma\text{-Al}_2\text{O}_3$ <sup>56</sup> and  $\text{ZrO}_2$ <sup>57-60</sup>. Acid properties of tungsten based catalysts have also been employed to improve alkane isomerization, a very important step in the synthesis of high octane rating petrol<sup>61-64</sup>. The properties of bulk tungsten oxides were studied in hexane reforming<sup>65-66</sup> and heptane hydrocracking<sup>67</sup>.

Supported molybdenum oxide catalysts are widely used in various catalytic

processes<sup>68</sup>. The molecular structures of the surface molybdenum oxide species on different oxide supports have been extensively investigated by various techniques<sup>69</sup>. The conclusion is that the structures of the surface molybdenum oxide species are related to the nature, in particular the surface structure, of the support; the extent of surface hydration; the loading amount of molybdenum oxide; and the calcination temperatures<sup>70-71</sup>. The structures of molybdenum oxide supported on  $\gamma$ -Al<sub>2</sub>O<sub>3</sub> have been extensively studied under ambient conditions<sup>72-74</sup>. Raman spectral results have demonstrated that at least three different molybdenum oxide species, tetrahedrally and octahedrally coordinated surface species as well as the crystalline MoO<sub>3</sub> phase might be present on the surface of  $\gamma$ -Al<sub>2</sub>O<sub>3</sub> and that their relative amounts depend on the loading of molybdenum oxide<sup>75-76</sup>. It has been reported that zirconia supported Mo catalysts have higher activities in the HDS reaction of thiophene and in the hydrogenation of Co than the alumina supported Mo catalysts<sup>77</sup>, and for the partial oxidation of methanol<sup>78</sup> and ethanol<sup>79</sup> the high activities of catalysts of MoO<sub>3</sub> highly dispersed on ZrO<sub>2</sub> support have also been noted. Supported chromium oxide catalysts are being used for the polymerisation, hydrogenation, and oxidation-reduction reactions between environmentally important molecules such as CO and NO<sup>80-85</sup>.

## 1.6 Surface acidity of metal oxides and its measurements

In reactions occurring by acid catalysis, the activity, stability and selectivity of solid acids are determined to a large extent by their surface acidity (the number, nature, strength, and density of their acid sites). The acidity required for transformation of reactants into valuable products or into by products can be quite different. Indeed certain reactions demand very strong acid sites while others can be catalysed by very weak acid sites. The dependence of the catalytic properties on the acid properties of solid catalysts demand accurate methods for the acidity measurements<sup>86</sup>.

Temperature programmed desorption (TPD) of basic molecules is a popular method for the determination of acid amount of solid catalysts as well as acid strength because it is an easy and reproducible method<sup>87-88</sup>. Ammonia is used frequently as a

probe molecule because of its small molecular size, stability and strong basic strength.

Since ammonia and pyridine adsorb on both Brønsted (B) and Lewis (L) acid sites, the determination of B and L sites is impossible upon using only  $\text{NH}_3$ -TPD and Py-TPD studies. Brønsted and Lewis acid sites play different roles in various types of catalytic reactions, and the strength of respective acid sites strongly affects the catalytic performance<sup>3</sup>. It has been reported that 2, 6-dimethyl pyridine is a useful probe molecule for the selective determination of the Brønsted acid sites. Benesi suggested that 2, 6-dimethylpyridine (2, 6-DMP) can be used as a proton specific probe<sup>89</sup>.

Stone and Rase used thermal analysis techniques to measure the heat change, which is an indication of the acid strength, accompanying adsorption of bases like piperidine, ammonia and pyridine by means of DTA they examined the correlation between the catalytic activity and acid strength of the solid catalysts<sup>90</sup>. The most direct method for the measurement of surface acidity is to perform some model reactions, which are known to be acid catalysed. The most widely used model reactions include decomposition of alcohols<sup>91-92</sup>, cracking of aromatic hydrocarbons<sup>93-95</sup> and isomerization of alkenes<sup>96</sup>. From the nature of the products formed during these reactions, one can get a knowledge about the nature of the acid sites present in the catalyst.

## **1.7 Reactions selected for the present study**

Among various catalysts in use, acid catalysts account for a majority of applications both in terms of volume and economy. The catalytic role of acids has been known since the time of Berzelius. Since the incorporation of transition metals and sulphate ions into pure cerium oxide led to an enhancement in surface acidity, we have carried out some industrially important acid catalysed reactions. At the same time the oxidation capacity of cerium oxide is also taken into account. We have selected reactions such as acetalization and de-acetalization of cyclohexanone, oxidative dehydrogenation of ethyl benzene, methyl tertiary butyl ether synthesis and Beckmann

rearrangements for our present study.

### I. Acetalization and de-acetalization of cyclohexanone

The acetalization of aldehydes or ketones is a reaction of synthetic interest in organic chemistry. The reaction is highly effective in synthesizing enantiomerically pure compounds<sup>97</sup>. It finds practical application in the fields of synthetic carbohydrates<sup>98</sup>, steroids<sup>99</sup>, pharmaceuticals and fragrance<sup>100</sup>, and polymers<sup>101</sup>. Various kinds of acids are well known to catalyze the reaction in homogeneous and heterogeneous phases<sup>102</sup>. Several problems, however, remain to be solved. For example, the formation of dimethylacetals is frequently carried out using trimethyl orthoformate as the reagent, but use of methanol for the reaction is more desirable. In the case of the typical methanol/HCl system, various by-products are produced because of the strong acidity of HCl. On the other hand, some solid acid catalysts such as silica gel, alumina<sup>103</sup>, zeolite<sup>104</sup>, resins<sup>105-106</sup>, clays<sup>107-108</sup>, hydrous zirconium oxide<sup>109</sup> and mesoporous aluminosilicate<sup>110</sup> have been proved to be active for the reaction.

Sulfated metal oxides can also act as effective catalysts for these reactions. Lin et al. reported that sulfated metal oxides such as sulfated oxides of  $ZrO_2$ ,  $TiO_2$ ,  $Fe_2O_3$ ,  $SnO_2$ ,  $Al_2O_3$ ,  $HfO_2$  and  $SiO_2$  can effectively catalyze the reaction between carbonyl compounds and trimethylorthoformate producing dimethylacetals at room temperature<sup>111</sup>. The highly acidic sulfated zirconia has been proposed for the synthesis of acetals from aldehydes and ketones with 2, 2-dimethyl-1, 3-propanediol<sup>112</sup>. The regeneration of carbonyl compounds from their acetals is also performed under acidic conditions. The general scheme of the reaction can be represented as in Figure 1.3.

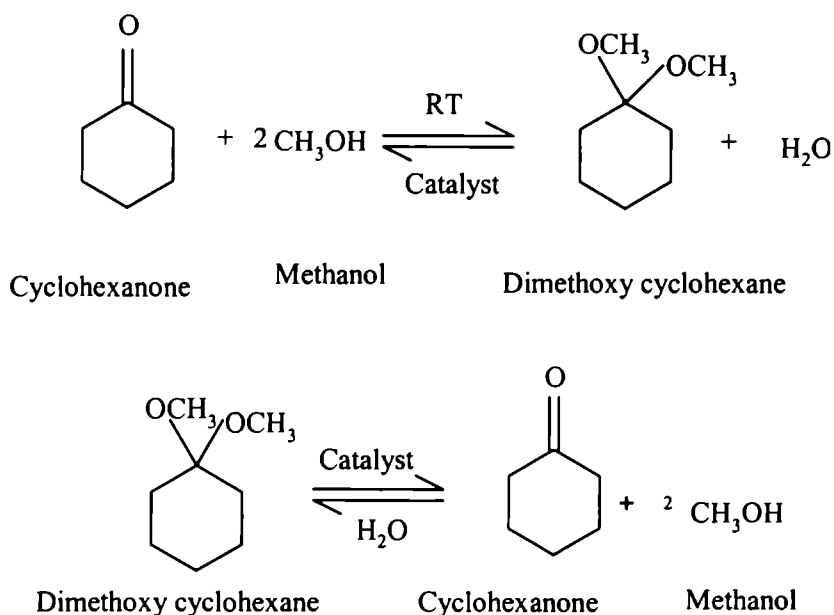


Figure 1.3

Reaction scheme for acetalization and de-acetalization reaction

### 11. Oxidative dehydrogenation of ethylbenzene

The catalytic dehydrogenation of ethylbenzene is of industrial importance in the manufacture of styrene as it is extensively used as an intermediate for the manufacture of polystyrene and numerous thermoplastics. Styrene is commercially manufactured by the catalytic dehydrogenation of ethylbenzene over iron oxide promoted by alkali metal ions<sup>113-115</sup>. Since this direct dehydrogenation is limited by thermodynamic equilibrium, high reactor temperatures (>600°C) are required and typical conversions are low. Also, the high temperatures required to give favourable conversion bring about severe cracking in the more complex alkyl benzenes.

The oxydehydrogenation reaction is a potential alternative for the manufacture of styrene at lower temperatures, without thermodynamic restrictions on the yield<sup>116</sup>. Various catalysts have been reported as efficient catalysts for the oxidative dehydrogenation of ethylbenzene<sup>117-118</sup>. Turco et al. investigated the catalytic proper-

ties of zirconium- tin mixed phosphates and observed that mixed zirconium- tin phosphates give much higher ethylbenzene conversion with respect to pure Zr and Sn phosphates, the selectivity to styrene being likewise high. They concluded that surface acidity of medium-high strength plays a relevant role in the reaction through the formation of a catalytically active coke<sup>119</sup>. Ferrites, a subgroup of spinels is highly active for the oxydehydrogenation reactions<sup>120</sup>. The catalytic effectiveness of ferrites for many such reactions arises because of the ease with which iron can change its oxidation state between 2 and 3. Rare earth oxides especially  $\text{CeO}_2$  is used as a component in new catalyst reformulations for the oxidative dehydrogenation of paraffins and ethylbenzene<sup>121</sup>.

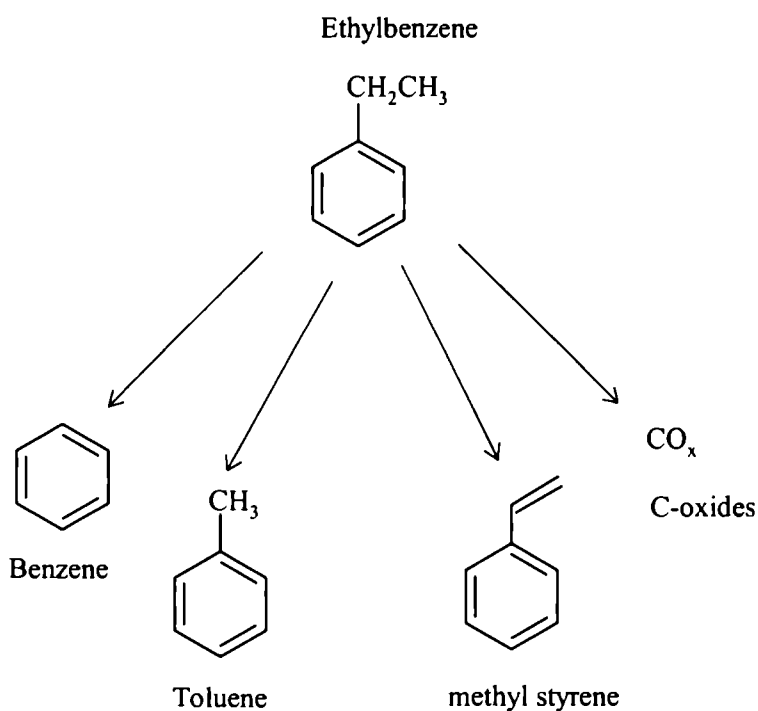


Figure 1.4  
Reaction scheme for oxidative dehydrogenation of ethylbenzene

### **III. Methyl tertiary butyl ether synthesis**

Pollution from motor vehicles is responsible in industrialised nations for ozone forming smog, hazardous carbon monoxide pollution, and other toxic air pollutants. Methyl tert-butyl ether (MTBE) is widely used as an oxygenate because of its good antiknocking properties, outstanding physical properties such as volatility, miscibility in gasoline, and help in the reduction of hazardous emissions<sup>122</sup>. The current commercial MTBE synthesis is a liquid-phase reaction of methanol and isobutene over sulphonated ion-exchange resins at low temperatures (30-100° C) and moderately high pressures (usually upto 2.0 Mpa). Although the resin catalysts are very active, they have some major drawbacks such as thermal fragility, sensitivity to methanol-to-isobutene ratios, and corrosive problems<sup>123-125</sup>. In addition, the deactivated resin catalyst cannot be regenerated and must be properly disposed under current environmental regulations<sup>126</sup>. Another problem concerning MTBE production from isobutene is that the source of isobutene is limited to catalytic cracking and steam cracking fractions of petroleum refining.

Inorganic solid acid catalysts such as micro porous zeolites<sup>127-128</sup>, heteropoly acids (HPA's)<sup>129-131</sup> and inorganic oxides such as Nb<sub>2</sub>O<sub>5</sub>, TiO<sub>2</sub>, ZrO<sub>2</sub>, SiO<sub>2</sub><sup>132</sup> are now considered to be potential alternative catalysts for MTBE synthesis and other etherification reactions. Zeolites have been investigated as efficient catalysts for MTBE formation<sup>133-135</sup>. We have investigated the possibility of using transition metals incorporated pure ceria and its sulphated analogues for the gas phase MTBE synthesis from methanol and tertiary butyl alcohol (TBA). Since, the general mechanism of the reaction suggests that etherification takes place via the intermediate formation of the corresponding tertiary carbocation followed by the nucleophilic attack of the methanol molecules<sup>136-138</sup>, it is assumed that an enhancement of surface acidity will favour the processes.



ever these catalysts are highly corrosive and some of them are hygroscopic nature, which makes their handling very difficult. These problems can be better overcome by the use of heterogeneous catalysts. Not much literature is available on the application of heterogeneous catalysts towards the synthesis of isoquinoline and benzoxazole.

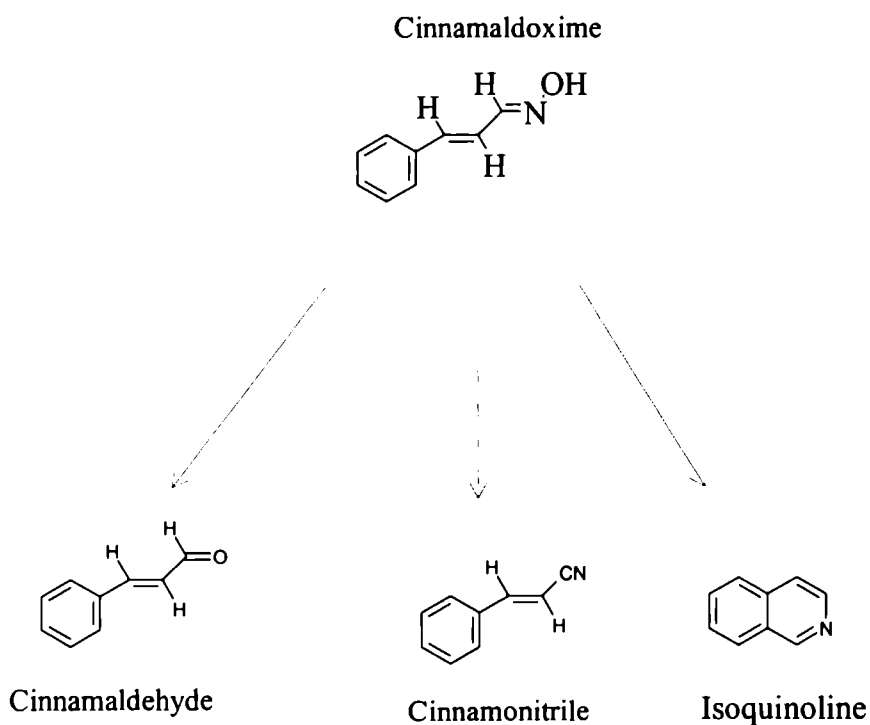


Figure 1.6

Reaction scheme for Beckmann rearrangement of cinnamaldoxime.

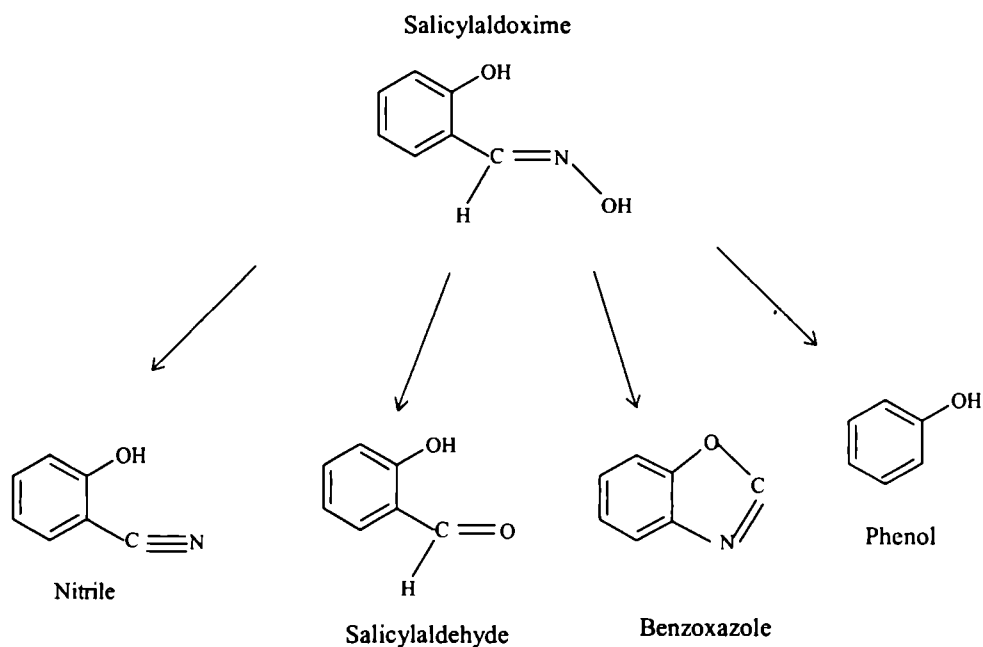


Figure 1.7  
Reaction scheme for Beckmann  
rearrangement of salicylaldoxime

### 1.8. Major objectives of the present work

Major objectives of the present work includes:-

- \* To prepare cerium oxide by “Pseudo-template” method and modify the prepared system with different percentages of transition metals (W, Mo & Cr) as well as by sulphate ions by the wet impregnation method.
- \* To investigate the surface properties of the systems by techniques such as BET surface area and porevolume measurements, EDX, XRD, FTIR, UV-vis DRS, SEM etc.
- \* To examine the surface acidic properties of the catalytic systems using various independent techniques such as TPD of ammonia, perylene adsorption studies, TGA of adsorbed 2, 6-DMP and test reactions like cumene

cracking and cyclohexanol decomposition reaction.

- \* To explore the catalytic activity of the systems towards acetalization and de-acetalization of cyclohexanone.
- \* To test the catalytic efficiency of the systems in oxidative dehydrogenation of ethylbenzene and methyl tertiary butyl ether synthesis.
- \* To evaluate the catalytic performance of the prepared systems in Beckmann rearrangement of salicylaldehyde and cinnamaldehyde.

## References

1. K. Tanabe, "Solid Acids and Bases." Kodansha, Tokyo; Academic Press, New York, 1970.
2. M. R. Guisnet, *Acc. Chem. Res.*, 23 (1990) 392.
3. A. Corma, *Chem. Rev.*, 95 (1995) 559.
4. P. B. Venuto, *Microporous Mater.*, 2 (1994) 297.
5. S. Feast and J. A. Lercher, *Stud. Surf. Sci. Catal.*, 75 (1993) 127.
6. J. Weitkamp and U. Weiss, *Stud. Surf. Sci. Catal.*, 94 (1995) 363.
7. L. R. Morss, *Hand book on the Physics and Chemistry of Rare earths*, Elsevier Science: New York, 1994; vol.18, pp.239.
8. D. J. M. Bevan and J. Kordis, *J. Inorg. Nucl. Chem.*, 26 (1964) 1509.
9. D. J. M. Bevan, *J. Inorg. Nucl. Chem.*, 1 (1955) 49.
10. G. Brauer and K. A. Gingeich, *J. Inorg. Nucl. Chem.*, 16 (1960) 87.
11. G. Brauer and U. Z. Holtschmidt, *Anorg. Allg. Chem.*, 265 (1951) 105.
12. P. Knappe and L. Eyring, *J. Solid State Chem.*, 58 (1985) 312.
13. S. P. Ray, A. S. Nowick and D. E. Cox, *J. Solid. State Chem.*, 15 (1975) 344.
14. S. P. Ray and D. E. Cox, *J. Solid. State Chem.*, 15 (1975) 333.
15. B. F. Hoskins and L. R. Martin, *Aust. J. Chem.*, 48 (1995) 709.
16. Z. C. Kang, J. Zhang and L. Z. Eyring, *Anorg. Allg. Chem.*, 622 (1996) 465.
17. G. Adachi and N. Imanaka, *Chem. Rev.*, 98 (1998) 1479.

18. B. R. Powell, R. L. Bloink and C. C. Eickel, *J. Am. Ceram. Soc.*, 71 (1988) 104
19. X. Dong, G. Hong, D. Yu and D. Yu, *J. Mater. Sci. Technol.*, 13 (1997) 113.
20. C. de Leitenburg, A. Trovarelli and J. Kaspar, *J. Catal.*, 166 (1997) 98.
21. N. Audebrand, J. P. Ayffredic and D. Louer, *Chem. Mater.*, 12 (2000) 1791.
22. S. Nakane, T. Tachi, M. Yoshinaka, K. Hirota and O. Yamaguchi., *J. am. Ceram. Soc.*, 80 (1999) 3221.
23. M. Machida, M. Uto, D. Kurogi and T. Kijima, *Chem. Mater.*, 12 (2000) 3158.
24. M. Machida, M. Uto, D. Kurogi and T. Kijima, *Chem. Mater.*, 11 (2001) 900.
25. G. Colon, J. A. Navio, R. Monaci and I. Ferino, *Phys. Chem. Chem. Phys.*, 2 (2000) 4453.
26. S. Bernal, G. Blanco, M. A. Cauqui, P. Corchado, J. M. Pintodo and J. M. Rodoriguez-Izuquierdo, *Chem. Comm.*, (1997) 1545.
27. A. Kawabata, S. Hirano, M. Yoshinaka, K. Hirota and O. Yamaguchi, *J. Mater. Sci.*, 31 (1996) 4945.
28. N. Seregent, J. F. Lamonier and A. Aboukais, *Chem. Mater.*, 12 (2000) 3830.
29. C. Bozo, N. Guihaume, E. Garbowski, M. Primet, *Catal. Today.*, 59 (2000) 33.
30. T. Masui, Y. Peng, K. Machida and G. Adachi, *Chem. Mater.*, 10 (1998) 4005.
31. F. Imoto, T. Nanataki and S. Kaneko, *Ceram. Trans.*, 1 (1988) 204.
32. C. K. Narula, L. P. Haack, W. Chun, H. W. Jen and G. W. Graham, *J. Phys. Chem.*, 103 (1991) 3634.
33. S. H. Overbury, D. R. Huntley, D. R. Mullins and G. N. Glavee, *Catal. Lett.*, 51 (1998) 133.
34. S. Rossgnol, F. Gerard and D. Dupez, *J. Mater. Chem.*, 9 (1999) 1615.
35. J. Rynkowski, J. Farbotko, R. Touroude and L. Hilaire, *Appl. Catal. A. Gen.*,

- 203 (2000) 335.
36. C. T. Kresge, M. E. Leonowicz, W. J. Roth, J. C. Vartuli and J. S. Beck, *Nature.*, 359 (1992) 710.
  37. D. Terribile, A. Trovarelli, J. Llorca, C. de Leitenburg and G. Dolcetti, *J. Catal.*, 178 (1998) 299.
  38. G. A. Parks, *Chem. Rev.*, 65 (1965) 177.
  39. W. Wachtere, V. Nguyen, U. S. Patent 6, 022, 471, 8 February 2000.
  40. A. Cabanas, J. W. Darr, E. Lester, M. Martyn, *J. Mater. Chem.*, 11 (2001) 561.
  41. S. Rossignol, Y. Madier, D. Duprez, *Catal. Today.*, 50 (1999) 261.
  42. G. Colon. M. Pijolat, F. Valdivieso, J. Kaspar, E. Finocchio, M. Daturi. C. Binet, J. C. Lavalley, R. T. Baker and S. Bernal, *J. Chem. Soc. Faraday Trans.*, 94 (1998) 3717.
  43. A. Trovalli, C. Leitenburg, G. Dolcetti, *Chemtech.*, (1997) 32.
  44. S. Rossignol, F. Gerard, D. Dupez, *J. Mater. Chem.*, 9 (1999) 1615.
  45. G. Kim, U. S. Patent 5, 627, 123, 6 May 1995.
  46. B. T. Kilbourn, *J. Less Common Metals.*, 126 (1986) 101.
  47. J. F. Brazil and R. K. Graselli, *J. Catal.*, 79 (1983) 104.
  48. R. J. Ackermann and E. G. Rauh, *J. Chem. Therm.*, 3 (1971) 609.
  49. J. Ramirez and A. G. Alejandre, *J. Catal.*, 170 (1997) 108.
  50. R. Thomas, E. M. Van Obers, V. H. J. De Beer, J. Medema and J. A. Moulijn, *J. Catal.*, 76 (1982) 241.
  51. L. Lietti, J. Svachula, P. Forzatti, G. Busca, G. Ramis and F. Breganic, *Catal. Today.*, 17 (1993) 131.
  52. W. Grunert, E. S. Shpiro, R. Feldhaus, K. Anders, G. V. Antoshin and K. M. Minachev, *J. Catal.*, 107 (1987) 522.
  53. I. Rodriguez-Ramos, A. Guerrero-Ruiz, N. Homos, Ramirez de la Piscina, P and J. L. G. Fierro, *J. Mol. Catal. A: Chemical.*, 95 (1995) 147.

54. M. Misono, *Catal. Rev. Sci. Eng.*, 29 (1987) 269.
55. F. H. Ribeiro, M. Boudart, R. A Dalla-Betta and E. Iglesia, *J. Catal.*, 130 (1991) 498.
56. S. L. Soled, G. B. McVicker, L. L. Murrell, L. G. Sherman, N. C. Dispenziere, S. L. Hsu and D. Waldman, *J. Catal.*, 111 (1988) 286.
57. K. Arata and M. Hino, in "Proceedings, 9<sup>th</sup> International Congress on Catalysis. Calgary, 1988" (M.J. Phillips and M. Ternan, Eds.), p.1727. Chem. Institute of Canada, Ottawa, 1988.
58. M. Hino and K. Arata, *Chem. Lett.*, 971 (1989).
59. S. L. Soled, N. Dispenziere and R. Saleh, in "Progress in Catalysis" (K.J. \ Smith and E.C. Sanford, Eds.), p.77. Elsevier, Amsterdam, 1992.
60. C. D. Chang, J. G. Santiesteban and D. L. Stern, Mobil Oil Corp., U. S. Patent, 5, 345, 026, 1994.
61. B. G. Baker and N. J. Clark, *Stud. Surf. Sci. Catal.*, 30 (1987) 483.
62. L. H. Gielgens, M. G. H. Van Kampen, M. M. Broek, R. Van Hardeveld and B. Ponc, *J. Catal.*, 154 (1995) 201.
63. V. M. Benitez, C. A. Querini, N. S. Figoli and R. A. Comelli, *Appl. Catal. A. Gen.*, 178 (1999) 205.
64. V. Logie, G. Maire, D. Michel and J. L. Vignes, *J. Catal.*, 188 (1999) 90.
65. A. Katrib, V. Logie, N. Saurel, P. Wehrer, L. Hilaire and G. Maire, *Surf. Sci.*, 30 (1997) 754.
66. V. Logie, P. Wehrer, A. Katrib and G. Maire, *J. Catal.*, 189 (2000) 438.
67. E. Ogata, Y. Camiya and N. Ohta, *J. Catal.*, 29 (1973) 296.
68. J. Haber, "The Role of Molybdenum in Catalysis", Climax Molybdenum Co., Ann Arbor, MI, 1981.
69. K. Segawa and I. E. Wachs, in "Characterization of Catalytic Materials" (I. E. Wachs, Ed.) p.72. Butterworth Heinemann, Boston, 1992.
70. O. H. Han, C. Y. Lin, N. Sustache, M. McMillan, J. D. Carruthers, K. W. Zilm

and G.L. Haller, *Appl. Catal. A. Gen.*, 98 (1993) 195.

71. J. M. Stencel, in "Raman Spectroscopy for Catalysis", p.51. Van Nostrand Reinhold, New York, 1990.
72. H. Jeziorowski and H. Knözinger, *J. Phys. Chem.*, 83 (1979) 1166.
73. L. Wang and W. K. Hall, *J. Catal.*, 83 (1983) 242.
74. S. D. Kohler, J. G. Ekerdt, D. S. Kim and I. E. Wachs, *Catal. Lett.*, 16 (1992) 231.
75. L. Wang and W. K. Hall, *J. Catal.*, 66 (1980) 251.
76. H. Jeziorowski, H. Knözinger, P. Grange and P. Gajardo, *J. Phys. Chem.*, 84 (1980) 1825.
77. D. Hamon, M. Vrinat, M. Breyse, B. Duyand, M. Jebrouni, M. Roubin, P. Magnoux and T. Des Courieres, *Catal. Today.*, 10 (1991) 613.
78. Y. Matsuoka, M. Niwa and Y. Murakami, *J. Phys. Chem.*, 94 (1990) 1477.
79. T. Ono, H. Miyata and Y. Kubokawa, *J. Chem. Soc. Faraday Trans.*, 83 (1987) 1761.
80. S. Wang, K. Murata, T. Hayakawa, S. Hamakawa and K. Suzuki, *Appl. Catal. A. Gen.*, 196 (2000) 1.
81. D. L. Myers and J. H. Lunsford, *J. Catal.*, 99 (1986) 140.
82. D. W. Flick and M. C. Huff, *Appl. Catal. A. Gen.*, 187 (1999) 13.
83. M. M. R. Feijen Jeurissen, J. J. Joma, B. E. Nieuwenhuys, G. Sinquin, C. Petit and J. P. Hindermann, *Catal. Today.*, 54 (1999) 65.
84. K. Köhler, J. Engweiler, H. Viebrock and A. Baiker, *Langmuir II* (1995) 3423.
85. B. M. Weckhuysen, I. E. Wachs and R. A. Schoonheydt, *Chem. Rev.*, 96 (1996) 3327.
86. M. R. Guisnet, *Acc. Chem. Res.*, 23 (11) (1990) 393.
87. R. J. Cvetanovic, Y. Amenomiya, *Adv. Catal.*, 17 (1967) 103.
88. W. F. Farneth, R. J. Gorte, *Chem. Rev.*, 95 (1995) 615.

89. H. A. Benesi, *J. Catal.*, 28 (1973) 176.
90. L. Stone and H. F. Rase, *Anal. Chem.*, 29 (1957) 1237.
91. M. Ai, *J. Catal.*, 40 (1975) 318.
92. M. Ai, *Bull. Chem Soc. Jpn.*, 50 (1977) 2587.
93. J. W. Ward, *J. Catal.*, 9 (1967) 225.
94. W. Przystajko, R. Fiedoorow and I. G. Dalla Lana, *Appl. Catal. A. Gen.*, 15 (1985) 265.
95. P. M. Boorman, R. A. Kydd, Z. Sarbak and A. Somogyvari, *J. Catal.*, 100 (1986) 287.
96. J. Sabati, F. E. Massoth, M. Tokarz, G. M. Tsai and J. Mc Cauley, *Proc. 8<sup>th</sup> Int. Cong. in Catal. Berlin*, (1984) Vol. VI, p. 735.
97. K. Narasaka, M. Inoue, T. Yamada, J. Sugimori and N. Iwasawa, *Chem. Lett.*, (1987) 2409.
98. D. M. Clode, *Chem. Rev.*, 79 (1979) 491.
99. J. R. Bull, J. Floor and G. J. Kruger, *J. Chem. Res. Synop.*, (1979) 224.
100. K. Bruns, J. Conrad and A. Steigel, *Tetrahedron.*, 35 (1979) 2523.
101. A. J. Elliot, in *1,3-Dioxolane Polymers in Comprehensive Heterocyclic Polymers*, Pergamon Press, Oxford, U.K. 1984, Vol. 6.
102. T. W. Greene, P. G. M. Wuts, *Protective Groups in Organic Synthesis*, (2nd Ed). John Wiley & Sons, New York, (1991) 178.
103. Y. Kamitori, M. Hojo, R. Masuda and T. Yoshida, *Tetrahedron Lett.*, 26 (1985) 4767.
104. A. Corma, M. J. Climent, H. Garcia and J. Primo, *Appl. Catal. A. Gen.*, 59 (1990) 333.
105. G. A. Olah, S. C. Narang, D. Meidar and G. F. Salem, *Synthesis.*, (1981) 282.
106. S. A. Patwardhan and S. Dev, *Synthesis.*, (1974) 348.
107. E. C. Taylor and C. S. Chiang, *Synthesis.*, (1977) 467.
108. J. Tateiwa, H. Horiuchi and S. J. Uemura, *Org. Chem.*, 60 (1995) 4039.

109. M. Shibagki, K. Takahashi, H. Kuno and H. Matsushita, *Bull. Chem. Soc. Jpn.*, 63 (1990) 1258.
110. M. J. Climent, A. Corma, S. Iborra, M. C. Navarro and J. Primo, *J. Catal.*, 161 (1996) 783.
111. K. Arata, *Appl. Catal. A. Gen.*, 146 (1996) 3.
112. A. Sarkar, O. S. Yemul, B. P. Bandgar, N. B. Gaikwad and P. P. Wadgaonkar, *Org. Prep. Proceed. Int.*, 28 (1996) 613.
113. E. H. Lee, *Catal. Rev.*, 8 (1973) 285.
114. B. Delmon, P. A. Jacobs and G. Poncelet, *Preparation of Catalysts II* (Elsevier, Amsterdam, 1979) pp.293-305.
115. D. E. Stobbe, F. R. Van Buren, M. S. Hoogenraad, A. J. van Dillen and J. W. Geus, *J. Chem. Soc. Faraday Trans.*, 87 (1991) 1639.
116. L. E. Cadus, L. A. Arrua, O. F. Gorriz and J. B. Rivarola, *Ind. Eng. Chem. Res.*, 27 (1988) 2241.
117. Y. Yang, J. F. Yu, T. H. Wu and J. Z. Sun, *Chin. J. Catal.*, 18 (1997) 126.
118. B. Gryzbowska-Swierskosz, *Appl. Catal. A. Gen.*, 157 (1997) 409.
119. G. Bagnasco, P. Ciambelli, M. Turco, A. La Ginstra and P. Patrono, *Appl. Catal. A. Gen.*, 68 (1991) 69.
120. T. Mathew, S. Malwadkar, Shivanand, Pai, N. Sharanappa, C. P. Sebastian, C. V. V. Satyanarayana and V. V. Bokade, *Catal. Lett.*, 91 (2003).
121. R. X. Valenzuela, G. Bueno, V. C. Corberan, Y. Xu and C. Chen, *Catal. Today.*, 61 (2000) 43.
122. G. H. Unzelman, *Fuel Reformulation*. 1 (1991) 50.
123. T. Takesono and Y. Fujiwara, US Patent, 4, 182, 913, 1980.
124. Le Van Mao, R. R. Carli, H. Ahlafi and V. Ragaini, *Catal. Lett.*, 6 (1990) 321.
125. P. Chu and G. H. Kuhl, *Ind. Eng. Chem. Res.*, 26 (1987) 365.
126. A Study of the Acid-Catalyzed Synthesis of MTBE on Inorganic Solid

- Acids, Ph.D. Dissertation, University of Pittsburgh, 1995.
127. T. Horwath, M. Seiler and M. Hunger, *Appl. Catal. A Gen.*, 197 (2000) 227.
  128. M. Hunger, T. Horwath and J. Weitkamp, *Microporous and Mesoporous Mater.*, 22 (1998) 357.
  129. J. S. Kim, J. M. Kim, G. Seo, N. C. Park and S. Niiyama, *Appl. Catal. A Gen.*, 37 (1988) 45.
  130. J. M. Adams, K. Martin, R. W. McCabe and S. Murray, *Clays and Clay Miner.*, 34 (1986) 597.
  131. M. E. Quiroga, N. S. Figoli and U. A. Sedran, *J. Chem. Eng.*, 67 (1997) 199.
  132. S. Okazaki and N. Wada, *Catal. Today.*, 16 (1993) 349.
  133. A. Kogelbauer, M. Öcal, A. A. Nikolopoulos, J. G. Goodwin Jr and G. Marcelin, *J. Catal.*, 148 (1994) 157.
  134. A. M. Kazi, J. G. Goodwin Jr, G. Marcelin and R. Oukaci, *Ind. Eng. Chem. Res.*, 34 (1995) 718.
  135. A. A. Nikolopoulos, A. Kogelbauer, J. G. Goodwin, Jr. and G. Marcelin, *J. Catal.*, 158 (1996) 76.
  136. C. P. Nicolaidis, C. J. Stotijn, E. R. A. van der Veen and M. S. Visser, *Appl. Catal. A Gen.*, 103 (1993) 223.
  137. G. J. Hutchings, C. P. Nicolaidis and M. S. Scurrrell, *Catal. Today.*, 15 (1992) 23.
  138. R. Le Van Mao, T. S. Le, M. Fairbairn, A. Muntasar, S. Xiao and G. Denes, *Appl. Catal. A Gen.*, 185 (1999) 41.
  139. A. Reser, L. J. Leyshon, D. Saunders, M. V. Mijovic, A. Bright and J. Bogie, *J. Am. Chem. Soc.*, 94 (1972) 2414.
  140. S. Stendby, *Surfactant Sci. Ser.*, 5 (1981) 729.
  141. U. Claussen and H. Harnisch, *Eur. Pat. Appl.*, 25 (1981) 136.

142. C. Arnold Jr, *J. Polym. Sci., Macromol. Rev.*, 14 (1979) 265.
143. P. E. Cassidy, *Thermally Stable Polymers*: Marcel Dekker: New York, 1980.
144. J. F. Wolfe and F. E. Arnold, *Macromolecules.*, 14 (1981) 909.
145. E. W. Choe and S. N. Kim, *Macromolecules.*, 14 (1981) 920.
146. A. W. Chow, S. P. Bitler, P. E. Penwell, J. J. Osborne and J. R. Wolfe, *Macromolecules.*, 22 (1989) 3514.
147. J. Roussilhe, E. Fargin, A. Lopez, B. Despax and N. Pailous, *J. Org. Chem.*, 48 (1983) 3736.
148. I. N. Houppis, A. Molina, J. Lynch, R. A. Reamer, R. P. Volante and P. J. Reider, *J. Org. Chem.*, 58 (1993) 3176.
149. I. L. Finar, *Organic Chemistry I* ELBS Co. Ltd. 1964.
150. W. M. Whaley and T. R. Givindachari, *Organic Reactions VI* (New York, 1951), p. 74.
151. E. P. Styngach and A. A. Semenov, *Khim. Geterotsikl. Soedin.*, 7 (1971) 621.

\*\*\*\*\*

## Chapter 2

### *Materials and Methods*

#### **Abstract**

---

*In the present chapter the experimental procedures used for catalyst preparation, the characterisation techniques and catalytic activity measurements are described in detail. A thorough investigation of the physico-chemical properties was done using techniques such as XRD, EDX, SEM, BET surface area and pore volume measurements, TG/DTA, FTIR, and diffuse reflectance UV-vis spectroscopy. Ammonia TPD, perylene adsorption studies, adsorption of 2, 6 DMP followed by thermodesorption analysis, and catalytic test reactions like cumene cracking and cyclohexanol decomposition were used for the surface acid amount determination. Reactions of industrial importance such as Beckmann rearrangements, acetalization and deacetalization, MTBE synthesis and oxidative dehydrogenation of ethyl benzene are chosen for the catalytic activity measurements.*

---

## 2.1 Introduction

Catalyst surfaces are very complex and heterogeneous with a broad classification of structurally and chemically different sites. In the process of heterogeneous catalysis some of these sites may behave as particularly “active sites” in the sense that their presence causes a high yield and /or a high selectivity of a desired reaction product<sup>1</sup>. Thus, knowledge about the structure and composition of the surface is critical in determining the reactivity and selectivity of a solid catalyst. This chapter gives a detailed description about the preparation of the catalytic systems, pre-treatment conditions, materials used, the techniques used to characterise the catalysts and measures used for the catalytic activity study.

## 2.2 Catalyst preparation

Cerium oxide was prepared by “Pseudo-template” method. The sulphate modification of the samples was done by the wet impregnation method using 0.5 M H<sub>2</sub>SO<sub>4</sub> (1 mL/g). The pure and sulphated ceria were then doped with transition metals such as tungsten, molybdenum and chromium.

### Materials

The materials used for catalyst preparation are given below:

#### Materials

Cerium nitrate

Cetyl trimethyl ammonium bromide

Tungstic acid

Ammonium heptamolybdate

Chromium nitrate

#### Suppliers

Indian Rare Earth Ltd.

Lancaster

S-D fine chemicals

Merck

S-D fine chemicals

## Methods

The experimental procedure used for the preparation of the catalytic systems is discussed in the following section.

### a) Preparation of ceria

High surface area ceria was prepared by adding an aqueous ammonia solution (25 wt%) drop wise over 3 h to a stirred solution of  $\text{Ce}(\text{NO}_3)_3 \cdot 6 \text{H}_2\text{O}$  containing cetyl trimethyl ammonium bromide as surfactant (1.2 molar ratio of Ce/surfactant). Ammonia was added at 20 °C and the pH of the solution was varied from the initial value of 4.5 to a final value of 11. After the completion of precipitation the solution was placed in a thermostatic bath at 90 °C for 90 hrs under continuous stirring. The mixture was then cooled at room temperature and the precipitate was filtered and washed, first with water (till filtrate was free of nitrate ions – confirmed by performing brown ring test) and then with acetone (250 mL) to remove the excess surfactant. The resulting yellow powder was dried at 60 °C for 24 hrs in an air oven.

### b) Transition metal promoted ceria and sulphated ceria systems

Transition metal promoted ceria systems were prepared from the hydroxide by the incipient wetness method. For tungsten incorporation, tungstic acid, with various percentages of tungsten (5-15) was dissolved in 1:1  $\text{NH}_3$  and then stirred with hydroxide for 4 hrs. Tungsten promoted sulphated ceria systems were prepared from the hydroxide by a single step impregnation using 0.5 M  $\text{H}_2\text{SO}_4$  solution (1 mL/g of hydrous cerium oxide) and tungstic acid ((5-15% W).

For molybdenum doping, ammonium hepta molybdate solution with 5-15 molybdenum percentages was stirred with hydroxide for 4 hrs. Chromium incorporation was performed using chromium nitrate solution (5-15% Cr). The samples were kept over night, evaporated to dryness, and dried at 60 °C. All the samples were then calcined at temperatures from 150 to 500 °C and at 500 °C for 5 hrs with a heating rate of 12 K/min with constant flow of air.

### 2.3 Catalyst notations

The catalyst systems developed for the present study and its notations are given below.

<b>Notation</b>	<b>System</b>
C	- Pure cerium oxide
SC	- Sulphated cerium oxide (using 1 mL/g of 0.5 M H <sub>2</sub> SO <sub>4</sub> ).
CW <sub>x</sub>	- Tungstated ceria with x =5, 10 and 15 wt% of tungsten.
CSW <sub>x</sub>	- Sulphated tungstated ceria with x =5, 10 and 15 wt% of tungsten.
CM <sub>x</sub>	- Molybdated ceria with x =5, 10 and 15 wt% of molybdenum.
CSM <sub>x</sub>	- Sulphated molybdated ceria x =5, 10 and 15 wt% of molybdenum.
CCr <sub>x</sub>	- Chromated ceria with x =5, 10 and 15 wt% of chromium.
CSCr <sub>x</sub>	- Sulphated chromated ceria with x =5, 10 and 15 wt% of chromium.

### 2.4 Characterisation techniques

Different physico-chemical techniques were used to characterise the prepared catalytic systems. The surface characterization was performed by techniques like Powder X-Ray Diffraction (PXRD) analysis, Scanning Electron Microscopy (SEM), Energy Dispersive X-ray (EDX) studies, Surface area measurements by BET method, Thermo Gravimetric Analysis (TGA), Fourier Transform Infrared (FT-IR) Spectroscopy and UV-vis Diffuse Reflectance Spectroscopy (UV-vis DRS). Temperature Programmed Desorption (TPD) of ammonia, electron acceptor adsorption studies using perylene, thermo gravimetric analysis after adsorption of 2, 6-dimethyl pyridine, cumene cracking and cyclohexanol decomposition reactions were adopted for the surface acidity determination.

## Materials

The materials used for catalyst characterisation are:

Materials	Suppliers
Liquid nitrogen	Manorama oxygen Pvt.Ltd.
Magnesium oxide	Merck
Potassium bromide	Merck

## Methods

A brief discussion of the techniques adopted is given below.

### I. Powder X-Ray Diffraction (PXRD) Analysis

PXRD analysis plays a vital role in determining the crystal structure. The size and shape of the unit cell determines the angular positions of the diffraction peaks, and the arrangement of the atoms within the unit cell determines the relative intensities of the peaks. The basic principle underlying the analysis is that the scattered waves from the atoms interfere constructively, if they are in phase (coherent), and diffracted beams are formed in specific directions. These directions are governed by the wavelength of the incident radiation and the nature of the crystalline sample. Bragg's law, formulated by W. L. Bragg in 1913, relates the wavelength of the X-rays to the spacing of the atomic planes by the equation<sup>4</sup>,

$$n\lambda = 2d \sin \theta$$

where:

n	=	Order of reflection
$\lambda$	=	Wavelength of X-rays
$\theta$	=	Bragg angle (angle between incoming X-rays and normal to the reflecting lattice plane)
d	=	Inter planar spacing

In PXRD, fine powder of the sample was loaded into an X-ray holder and the diffraction patterns were recorded using Cu K $\alpha$  radiation in the 2 $\theta$  angular range of 5° to 80°, with a step value of 0.05. The maxima of all the peaks in each diffraction pattern were located using the cursor and the 2 $\theta$  values are listed in an increasing order. Knowledge about the 2 $\theta$  values and the wavelength of X-rays ( $\lambda$ ) allows one to calculate the miller indices (hkl) using the formula,

$$h^2 + k^2 + l^2 = \frac{\text{Sin}^2\theta}{A}$$

The value of 'A' is obtained by dividing the observed sin<sup>2</sup> $\theta$  values for all peaks in the diffraction pattern by the integers 2, 3, 4, 5, 6,..... and choosing the smallest value of sin<sup>2</sup> $\theta$  among the values. But we have  $A = \lambda^2 / 4a^2$ , a constant for any pattern, from which the lattice parameter (a) and subsequently the unit cell volume ( $V = a^3$ ) can be calculated. The Bravais lattice of the crystal system can be identified from the sequence of  $h^2+k^2+l^2$  values in the diffraction pattern. According to the selection rules, the  $h^2+k^2+l^2$  values for the different cubic lattices follow the sequence<sup>5</sup>

Primitive 1, 2, 3, 4, 5, 6, 8, 9, 10, 11, 12, 13, 14, 16,.....

Body centered 2, 4, 6, 8, 10, 12, 14, 16,.....

Face centered 3, 4, 8, 11, 12, 16, 19, 20, 24, 27, 32,.....

Crystallite size was estimated by the modified Scherrer relationship<sup>6</sup>,

$$t = 0.9 \lambda / \beta \text{ Cos}\theta$$

where:

- t = Crystallite size (A°)
- $\lambda$  = Wavelength of Cu K $\alpha$  radiation
- $\theta$  = Bragg angle
- $\beta$  = Full width at half maximum (FWHM) of the peak which have maximum intensity.

XRD patterns were recorded in a *Rigaku D-max C* X-ray diffractometer using Ni filtered Cu K $\alpha$  radiation ( $\lambda = 1.5406 \text{ \AA}$ ). The crystalline phases were iden-

tified by comparison with the standard JCPDS data file<sup>7</sup>.

## II. Scanning Electron Microscopy (SEM)

Scanning electron microscopy (SEM) is used to analyze the surface of specimens over a wide range of magnifications. The interaction of a beam of electrons with the specimen results in the generation of secondary electrons, backscattered electrons, auger electrons, characteristic X-rays, and photons of various energies. Secondary electrons and backscattered electrons are collected by their respective detectors and their signals are amplified. Secondary electrons mainly provide surface topographic imaging and backscattered electrons can form both images and supply atomic number information about the sample. Hence, some qualitative elemental information can be obtained. In SEM analysis finely powdered sample was poured on to a double sided carbon tape placed on a metal stub. The stub was then inverted in such a manner that the free side of the carbon tape gently picked up a small amount of the sample, thereby creating a thin coating. It was then sputtered with a thin layer of gold to obtain better contrast and provide improved cohesion<sup>8</sup>.

A serious drawback of the analysis is the charging of the particles and also the result need not be the representative of the whole sample. This can be overcome by making analysis at different locations of the sample particles and for many catalyst particles. The scanning electron microscopy of the samples were carried out in a *JEOL JSM 840 A* (Oxford make) model 16211 SEM analyzer with a resolution of 1.3 eV.

## III. Energy Dispersive X-ray (EDX) Analysis

EDX is an analytical tool that allows non-destructive elemental analysis of the sample. By this method both qualitative as well as quantitative analysis of the elements is possible. A quantitative analysis can be performed by a standard or standard less analysis. A standard analysis is carried out by comparison with a known

compound, whereas a standard less analysis quantifies the elements by calculating the area under the peak of each identified element and after taking account for the accelerating voltage of the beam to produce the spectrum. It also performs calculations to create sensitivity factors that will convert the area under the peak into weight or atomic percent.

The fundamental principle underlying this method is that, when the incident beam bounces through the sample creating secondary electrons, it leaves thousands of sample atoms with vacancies in the electron shells. If these “vacancies” are in inner shells, the atoms are not in a stable state. To stabilize the atoms, electrons from outer shells will drop into the inner shells, however, because the outer shells are at a higher energy state, to do so the atom must lose some energy. Energy is lost in the form of X-rays. The X-rays emitted from the sample atoms are characteristic in energy/wavelength of the element. The EDX analysis of the samples was made in a *JEOL JSM –840A* EDX analyzer.

#### **IV. BET Surface Area and Pore Volume Measurements**

The surface area measurements can be used as an effective method of assessing the efficiency of catalyst supports and promoters. This method can provide information regarding the deactivation of the catalyst, which may occur either due to poisoning or sintering. Of the several methods for the estimation of surface area, BET method is the most widely accepted one now<sup>9</sup>. This method is based on the extension of the Langmuir theory to multilayer adsorption. The basic equation to find out surface area can be written as

$$p / [V_{\text{ads}} (p_0 - p)] = [1 / (V_m C)] + [(C-1) / V_m C] (p/p_0)$$

where :

$p$  - Adsorption equilibrium pressure

$p_0$  - Saturated vapour pressure of the adsorbent

$V_{\text{ads}}$  - Volume at STP occupied by molecules adsorbed at pressure  $P$

- $V_m$  - Volume of adsorbate required for monolayer coverage  
 $C$  - Constant related to heat of adsorption.

According to BET method, a plot of  $p / [V_{ads} (p_0 - p)]$  Vs  $p/p_0$  is a straight line with slope  $S = (C-1)/V_m C$  and intercept  $I = 1/V_m C$ . Knowing the slope (S) and intercept (I)  $V_m$  can be calculated, which is used in calculating the surface area of the catalyst by the following equation.

$$\text{Specific surface area (m}^2 \text{ g}^{-1} \text{ cat)} = V_m N_A A_m / 22414 \times Wt .$$

where :

$V_m$  - Monolayer volume in mL at STP

$N_A$  - Avagadro number

Wt - Weight of the catalyst sample (g)

$A_m$  - Mean cross sectional area occupied by adsorbate molecule (0.162 nm<sup>2</sup> for N<sub>2</sub> )

In BET method, adsorption of N<sub>2</sub> is carried out at liquid nitrogen temperature. Prior to the experiments, activated samples were out gassed at 400 °C under N<sub>2</sub> for four hours and then brought to -196 °C using liquid nitrogen, for adsorbing nitrogen gas at various pressures. The analysis was carried out in a *Micromeritics Gemini* surface area analyser.

## V. Thermo Gravimetric Analysis (TGA)

Thermal analysis is defined as a group of methods based on the determination of changes in chemical or physical properties of a material as a function of temperature in a controlled atmosphere. Thermo Gravimetric Analysis (TGA) is a thermal analysis technique used to measure changes in the weight (mass) of a sample as a function of temperature and/or time. The measurements provide basic information about the thermal stability of a chemical and its composition.

In TGA, the sample is placed into a tared TGA sample pan, which is attached to a sensitive microbalance assembly. The sample holder portion of the TGA balance assembly is subsequently placed into a high temperature furnace. The balance assembly measures the initial sample weight at room temperature and then continuously monitors changes in sample weight (losses or gains) as heat is applied to the sample. TGA tests may be run in a heating mode at some controlled heating rate, or isothermally. Typical weight loss profiles are analysed for the amount or percent of weight loss at any given temperature, the amount or percent of non-combusted residue at some final temperature, and the temperatures of various sample degradation processes. The measurement is typically carried out on milligram size samples in a *TGAQ V2.34* thermal analyser with a heating rate of 20 °C/min from 20 to 700 °C in nitrogen atmosphere.

## **VI. Infrared Spectroscopy**

Infrared spectroscopy is a widely used technique in catalysis as it can give information on the catalyst structure, its surface properties, the sorbate-sorbent interactions, and intermediates<sup>10-11</sup>. It is one of the few techniques capable of exploring a catalyst, both in its bulk and its surface, and under the actual reaction conditions. In cases of some simple reactions it has been possible to identify the active intermediates formed during the course of a reaction.

IR spectroscopy also plays an important role in the identification of acid sites present in the catalyst. Adsorption of certain weakly basic molecular probes and the subsequent IR analysis of the samples serve as an excellent method to identify the nature of acid sites and also to determine their strength. The measurement of the intensity of IR bands due to adsorbed pyridine at a particular temperature enables one to calculate the concentration of the individual Brønsted and Lewis acid sites in a catalyst sample.

The FTIR spectrum of the sample was recorded on a *Nicolet Impact 4000*

spectrometer using the KBr pellet method (from 400 - 4000  $\text{cm}^{-1}$ ).

## VII. Diffuse Reflectance UV-vis (DR UV-vis) Spectroscopy

The diffuse reflectance UV-vis spectroscopy is known to be a very sensitive probe for the identification and characterisation of metal ion coordination. It allows the study of electronic transitions between orbitals or bands in the case of atoms, ions and molecules in gas, liquid or solid state. Electronic transitions are of two types and involve orbitals or levels localized either on the same metal atom or on two adjacent atoms. The first class includes the metal centered transitions[ d-d, (n-1)d-ns, f-f] , and the second class involves charge transfer (CT) transitions from an occupied level centered on a donor atom to a vacant one centered on an acceptor. The CT transitions are intense since they are Laporte-allowed and are sensitive to the nature of donor and acceptor atoms<sup>12</sup>.

Diffuse reflectance UV-vis spectra of the samples were recorded using *Ocean Optics –2000* spectrophotometer with CCD detector. Magnesium oxide was used as the reference material.

### 2.5 Surface acid amount determination studies

Quantification and characterization of surface acid sites forms an important aspect of the characterization of catalysts<sup>13</sup>. Several qualitative, semi-quantitative and quantitative methods have been employed to study the acid amount of catalysts in the last several years<sup>14</sup>. Here we used adsorption techniques such as Temperature Programmed Desorption (TPD) of Ammonia, perylene adsorption studies, adsorption of 2, 6 - dimethyl pyridine and subsequent thermo gravimetric (TG) analysis for the measurement of acid amount. Cumene cracking and cyclohexanol decomposition were also performed as test catalytic reactions for acid amount determination.

**Materials**

The materials used for surface acidity measurements are given below.

<b>Materials</b>	<b>Suppliers</b>
Perylene	Merck
Cumene	Aldrich
Benzene	Qualigens
H <sub>2</sub> SO <sub>4</sub>	Merck
Ammonia	Merck

**2.5.1 Adsorption techniques**

The chemisorption of bases such as pyridine, piperidine, ammonia, quinoline and aliphatic amines is frequently used to characterize solid acid catalysts and to correlate their catalytic activity with the concentration of a particular type of acid site<sup>15</sup>. Pyridine and ammonia, because of their capability of interacting with both Brönsted and Lewis sites, are widely used to get the total acid amount of the systems. Sterically hindered dimethyl and tertiary butyl pyridines are useful to characterize specifically the protonic centers<sup>16</sup>.

**a) Temperature Programmed Desorption (TPD) of Ammonia**

Ammonia is an excellent probe molecule for the measurement of acid property by TPD, because it can be stabilized on acid sites and can penetrate into pores due to its strong basicity and small size. It is possible to get the acid site distribution as well as total acidity from TPD values. TPD tests were carried out in a conventional flow apparatus. The sample (0.4 g) was activated at 300 °C in nitrogen flow for half an hour. After cooling to room temperature, it was saturated with ammonia gas in the absence of nitrogen flow and the system was allowed to attain equilibrium. The excess and physisorbed ammonia was flushed out by a current of nitrogen. Ammonia

was then desorbed at different temperatures (100-500 °C) with a heating rate of 20 °C / minute in the same atmosphere and was trapped in H<sub>2</sub>SO<sub>4</sub>. The amount of ammonia desorbed at each temperature, which is measure of the acid amount at that temperature, was found out by conventional method.

Although this method is helpful in giving an indication about the acid amount of the systems, it suffers from two disadvantages: a) ammonia weakly held on non acidic sites, eg: hydrogen- bonded on ammonium cation, confuses the TPD spectrum and (b) the readsorption of NH<sub>3</sub> affects the peak maximum temperature<sup>17</sup>.

#### **b) Perylene adsorption studies**

Perylene adsorption studies give information regarding the Lewis acid amount in presence of Brönsted acid amount<sup>18</sup>. The principle is based on the ability of the catalyst surface acid sites to accept electron from an electron donor, like perylene to form charge transfer complexes<sup>19</sup>. In this method, the experiments were carried out by stirring a weighed amount of the catalyst with different concentrations of perylene in benzene solvent. The amount of perylene adsorbed was determined by measuring the absorbance of the solution in a UV-vis spectrophotometer (*Shimadzu UV-160 A*) at  $\lambda_{\max}$  439 nm before and after adsorption. From the Langmuir plots, the limiting amount of perylene adsorbed over the catalyst surface, which is a measure of the Lewis acid amount of the system, is obtained. The chemical interaction between the adsorbate and the sample may be described by the Langmuir adsorption isotherm,  $C/X = 1/BX_m + C/X_m$

where, C is the concentration of perylene solution, B, a constant and X<sub>m</sub> is the limiting amount of perylene adsorbed, which corresponds to the theoretical amount of the adsorbate required to cover all the active sites for base adsorption.

#### **c) TGA of 2, 6-dimethyl pyridine adsorbed samples**

2, 6-dimethyl pyridine is a useful probe molecule for the selective determi-

nation of the Brønsted acid sites (BAS). Benesi suggested that 2, 6-dimethylpyridine (2, 6-DMP) can be used as a proton specific probe<sup>16</sup>. The catalyst samples activated at 500 °C were kept in a desiccator saturated with vapors of 2, 6-DMP for 48 h. The weight loss of the adsorbed samples was measured by thermo gravimetric analysis operating between 40 to 600 °C at a heating rate of 20 °C/minute. The amount of 2, 6-DMP adsorption was strongly dependent on the purging temperature, and it was found that the coordinately adsorbed 2, 6-DMP on Lewis acid sites could be eliminated by purging at temperatures above 300 °C<sup>20</sup>. The weight loss between 301-400 °C, 401-500 °C and 501-600 °C are considered to be measures of weak, medium and strong acid sites, respectively.

### 2.5.2 Test reactions for acidity

Catalytic cumene cracking and cyclohexanol decomposition reactions were performed as test reactions for acidity.

#### a) Vapour phase cumene cracking reaction

Vapour phase cumene cracking reaction is a model reaction for identifying the Lewis/ Brønsted acid ratio of a catalyst. The major reactions taking place during the cracking of cumene are dealkylation to give benzene and propene over BAS and dehydrogenation to give  $\alpha$ -methyl styrene over LAS<sup>21</sup>. A comparison of the amount of benzene and  $\alpha$ -methyl styrene gives an idea about the BAS and LAS possessed by the catalyst.

The vapour phase cumene cracking reaction was carried out in a fixed bed, down flow vertical glass reactor (1 cm diameter, 40 cm length) inside a double zone furnace. 0.5 g of the catalyst activated at 500 °C for 2 hrs was immobilized inside the reactor using glass wool. Cumene was fed into the reactor at a flow rate of 4 mL/h. The temperature of the reaction bed was kept at 400 °C. The product analysis was achieved gas chromatographically (*Chemito 8610*) by comparison with authentic sam-

ples. The analytical conditions are given in Table 2.1.

### **b) Vapour phase cyclohexanol decomposition reaction**

Cyclohexanol decomposition reaction has been widely studied, as it is a model reaction to determine the functionality of an oxide catalyst. The amphoteric character of the alcohol permits its interaction with both acidic and basic centers. The dehydration of cyclohexanol resulting in the formation of cyclohexene was found to occur with the participation of acidic sites and dehydrogenation leading to cyclohexanone takes place with the intervention of both acidic and basic sites<sup>22-23</sup>.

The vapour phase cyclohexanol decomposition reaction was carried out at atmospheric pressure in a fixed bed down flow glass reactor at a temperature of 300 °C. About 0.5 g of the activated catalyst was sandwiched between silica beads in a glass reactor. The liquid reactant was fed into the reactor with the help of an injection pump at a flow rate of 4 mL/h. The products were analysed by a gas chromatograph (*Chemito 8610*) under the analytical conditions specified in Table 2.1.

## **2.6 Catalytic activity measurements**

To test the catalytic efficiency of the prepared systems, reactions, both in the liquid phase and in the vapour phase have been carried out. The liquid phase reactions conducted were acetalization of cyclohexanone using methanol and the hydrolysis of dimethyl acetal. Oxidative dehydrogenation of ethylbenzene, Methyl Tertiary Butyl Ether (MTBE) synthesis, Beckmann rearrangement of salicylaldehyde and cinnamaldehyde were done in vapour phase.

### **Materials**

The materials used for catalytic activity measurements are given below.

<b>Materials</b>	<b>Suppliers</b>
Toluene	Merck
Benzyl chloride	Merck
Cyclohexanone	Qualigens
Methanol	Merck
Dimethoxy cyclohexane	Sigma aldrich
Tertiary butanol	Merck
Ethylbenzene	Merck
Salicylaldehyde	S-D fine Chemicals
Cinnamaldehyde	Central Drug House

## **Methods**

The experimental procedures adopted for measuring the catalytic activity are described below:

### **I. Liquid - Phase Reactions**

The liquid phase reactions were carried out in a 50 mL double-necked flask fitted with a water condenser. The temperature of the reaction was maintained using an oil bath and a dimmerstat.

#### **Acetalization of cyclohexanone and Hydrolysis of dimethyl acetal**

Single pot acetalization of cyclohexanone using methanol was performed at room temperature. Cyclohexanol and methanol in the specific molar ratio was added to 0.25 g of the catalyst in a R.B flask and magnetically stirred. The products were identified by comparison with authentic samples using a *Chemito 1000* gas chromatograph under the analysis conditions specified in Table 2.1. The products were further analysed by gas chromatography-mass spectrometer (GC-MS) using a *Shimadzu-5050* spectrometer provided with a 30 m HP-30 capillary column of cross linked 5%

phenylmethylsilicone. The MS detector voltage was 1 kV. (Column temperature was adjusted between 50-260 °C with heating rate of 10 K/minute, injector: 240 °C and detector: 290 °C). Hydrolysis of the dimethyl acetal was done using 1:20 mixture of water and acetone as solvent. Here also the analysis was performed by *Chemito1000* gas chromatograph with a capillary SE-30 column. The GC analysis conditions are discussed in Table 2.1.

To have an optimum conversion of cyclohexanone, reaction conditions such as temperature of the reaction, cyclohexanone to methanol molar ratio, duration of reaction and the amount of the catalyst were studied in depth. To understand the true heterogeneous nature of the reaction metal leaching studies were also carried out.

## II. Vapour – Phase Reactions

The vapour phase reactions were conducted at atmospheric pressure in the presence of N<sub>2</sub> (oxygen was used in ODH reactions) in a fixed bed, vertical, down-flow reactor inserted into a double-zone furnace. The catalyst in powdered form (0.5 g) was placed in a catalyst bed of glass wool and sandwiched between inert silica beads. A thermocouple positioned near the catalyst bed monitored the reaction temperature. A temperature controller was used to maintain the temperature of the reaction. The reactant was fed into the reactor with the help of a syringe pump at a controlled flow rate. The condensed reaction mixture was collected downstream from the reactor in a receiver connected through a cold-water circulating condenser. The products were collected at regular intervals and analysed gas chromatographically.

### a) Oxidative dehydrogenation of ethylbenzene

Vapour-phase oxydehydrogenation of ethylbenzene was performed in presence of oxygen. A detailed investigation of various reaction parameters was also done. A soap bubble meter was used to check the flow of air. About 0.5 g of the activated catalyst was placed in the catalyst bed and 15 mL of air flow per minute

along with ethylbenzene was passed through the reactor at a temperature of 500 °C. The products were analysed by gas chromatography (*Chemito GC 8610*, flame ionisation detector, FFAP column-2 m length). Table 2.1 gives the analysis conditions of the product mixture. A blank run was carried out at 500 °C, which indicated negligible thermal reaction.

#### **b) Methyl tertiary butyl ether synthesis**

MTBE synthesis was carried out by passing a mixture of methanol and tertiary butanol in the specific molar ratio through 0.5 g of the catalyst placed at the center of the reactor. The reaction was done in nitrogen atmosphere at a reaction temperature of 150 °C and the effluents from the reactor were analyzed by GC (*Chemito GC 1000*, flame ionisation detector) equipped with a SE-30 capillary column under the analysis conditions given in Table 2.1. The products were further analysed by gas chromatography-mass spectrometer (GC-MS) using a *Shimadzu-5050* spectrometer provided with a 30 m HP-30 capillary column of cross linked 5% phenylmethylsilicone. The influence of reaction temperature, feed rate and methanol to tertiarybutanol molar ratio were also investigated.

#### **c) Beckmann rearrangement of salicylaldoxime and cinnamaldoxime**

0.5 g of the catalyst was kept at the center of the reactor. A solution of salicylaldoxime or cinnamaldoxime (5 wt%) in benzene was introduced to the reactor using a syringe pump at the required flow rate and reaction temperature. Analysis of the products was done by gas chromatograph (*Chemito GC 1000*) and further confirmed by gas chromatograph-mass spectrometer (GC-MS) using a *Shimadzu-5050* spectrometer provided with a 30 m HP-30 capillary column of cross linked 5% phenylmethylsilicone. GC analysis conditions are specified in Table 2.1.

Table 2.1.  
Analysis conditions for various catalytic reactions

Catalytic reaction	Column	Analysis conditions		
		Injector temperature (°C)	Detector temperature (°C)	Temperature programme for the column
Cyclohexanol decomposition	SE-30 capillary	100	100	50°C-isothermal
Cumene cracking	SE - 30	230	230	60°C-isothermal
Acetalization of cyclohexanone	SE-30 capillary	100	100	80°C-2-15°C-230°C*
Hydrolysis of dimethyl acetal	SE-30 capillary	100	100	80°C-2-15°C-230°C*
MTBE synthesis	SE-30 capillary	230	230	70°C
Oxidative dehydrogenation	FFAP	230	230	90°C-isothermal
Beckmann rearrangement				
a) Salicylaldoxime	SE-30 capillary	200	200	80°C-2-20°C-210°C*
b) Cinnamaldoxime	SE-30 capillary	200	200	80°C-2-20°C-210°C*

\* Initial temperature-duration-rate of increase- final temperature.

### References

1. R. F. Howe, R. N. Lamb and K. Wandelt, " Surface Science-Principles and Applications", Springer-Verlag, 1991, p.209.
2. D. Terribile, A. Trovarelli, J. Llorca, C. de Leitenburg and G. Dolcetti, *J. Catal.*, 178 (1998) 299.

3. G. A. Parks, *Chem. Rev.*, 65 (1965) 177.
4. J. W. Niemantsverdriet, "Spectroscopy in Catalysis" Weinheim, New York, 1995.
5. C. Suryanarayana and M. G. Norton, "X-Ray Diffraction- A Practical Approach," Plenum press, New York, 1998.
6. H. P. Klug and L. E. Alexander, "X-ray Diffraction Procedures," Wiley, New York, 1974.
7. H. Lipson and H. Steeple, "Interpretation of X-ray Powder Diffraction Patterns", Macmillan, London, 1970, p.261.
8. V. Yu. Gusev, S. Ruetsch, L. A. Popeko and I. E. Popeko, *J. Phys. Chem B.*, 103 (1999) 6498.
9. S. Brunauer, P. H. Emmette and E. Teller, *J. Am. Chem. Soc.*, 60 (1938) 309.
10. H. Knözinger, *Catal. Today.*, 32 (1996) 71.
11. I. E. Wachs, "Characterization of Catalytic Materials", Butterworth-Heinemann: Manning, 1992.
12. G. Ertl, H. Knozinger and J. Weitkamp, "Handbook of Heterogeneous Catalysis", Vol. 2, VCH, Weinheim, 1997, p.646.
13. L. Forni, *Catal. Rev.*, 8 (1974) 65.
14. H. A. Benesi and B. H. C. Winquist, *Adv. Catal.*, 27 (1978) 97.
15. A. Corma, C. Rodellas and V.Fornes, *J. Catal.*, 88 (1984) 374.
16. H. A. Benesi, *J. Catal.*, 28 (1973) 176.
17. N. Katada, T. Miyamoto, H. A. Begum, N. Naito, and M. Niwa, *J. Phys. Chem. B.*, 104 (2000) 5511.
18. B. D. Flockart, J. A. N. Scott and R. C. Pink, *Trans. Faraday Soc.*, 62 (1966) 730.
19. J. J. Rooney and R. C. Pink, *Proc. Chem. Soc.*, (1961) 70.
20. A. Satsuma, Y. Kamiya, Y. Westi and T. Hattori, *Appl. Catal. A. Gen.*, 194 (2000) 253.
21. S. M. Bradley and R. A. Kydd, *J. Catal.*, 141 (1993) 239.
22. M. Ai, *J. Catal.*, 40 (1975) 318.
23. M. Ai, *Bull. Chem. Soc. Jpn.*, 50 (1977) 2587.

### *Physico-Chemical Characterisation*

#### **Abstract**

---

*Transition metal incorporated pure ceria and its sulphated analogues were successfully prepared via the pseudo-template method using a cationic surfactant. A detailed investigation of the physico-chemical characterisation of the catalytic systems was performed by techniques such as EDX, BET surface area and porevolume measurements, XRD, SEM, Thermogravimetry, FTIR and UV-vis DRS. Surface acidic properties of the systems were obtained from TPD of ammonia, perylene adsorption studies, TGA of adsorbed 2, 6-dimethyl pyridine and catalytic test reactions such as cumene cracking and cyclohexanol decomposition reaction. Characterisation techniques establish that the metal oxide species are highly dispersed on catalyst surface. Acid amount measurements indicate an enhancement in surface acidity especially the Lewis acidity upon modification.*

---

### 3.1 Introduction

In heterogeneous catalysis, the reaction occurs at the surface. Catalysis and catalytic surfaces hence need to be characterised by reference to their physico chemical properties and by their actual performance as a catalyst. The catalytic performance of the catalysts can be better appreciated if one knows as many of its properties as well. A large number of powerful techniques are now available which enable one to characterise the real catalyst, atom by atom, under in situ conditions. A complete knowledge on the exact location, structure and electronic ground state of the active site in the catalyst is essential to establish a basic understanding of the structure-activity correlations and also to improve the efficiency of the catalyst for high selectivity and stability.

The preparation of cerium oxide was performed using “pseudo-template” method. Its modification with various percentages of tungsten, molybdenum and chromium as well as its surface modification by sulphate ions were done using the conventional wet impregnation method. Following catalyst preparation, the surface morphology was obtained from scanning electron microscopy. Chemical composition and surface area of the systems were determined by energy dispersive X-ray analysis and BET surface area measurements respectively. Thermal stability of the systems was analysed using thermo gravimetric analysis. Fourier transform infrared spectroscopy and X-Ray Diffraction (XRD) studies were performed to understand the chemical structure of the prepared systems. UV-vis diffuse reflectance spectroscopy gives an idea about the metal ion coordination.

Since surface acid amount of metal oxides is an important parameter in determining the catalytic efficiency, a detailed investigation of the acid amount of the prepared systems is essential. Therefore, in the present study, adsorption techniques such as Temperature Programmed Desorption of ammonia (TPD-NH<sub>3</sub>), perylene adsorption studies, thermo gravimetric analysis of adsorbed 2, 6-dimethylpyridine were carried out to understand the amount, distribution and strength of the acid sites. Cumene

cracking and cyclohexanol decomposition reactions were also performed as test reactions for acidity.

### 3.2 Physical characterisation

The catalyst samples prepared were characterised by adopting various physical methods such as BET surface area and pore volume measurements, energy dispersive X-ray analysis, X-ray diffraction studies, Fourier transform infrared spectroscopy, scanning electron microscopy, thermogravimetric analysis and diffuse reflectance UV-vis spectroscopy. The observations and the explanations of the results are given below.

#### I. BET Surface Area and Pore Volume measurements

##### a) Tungsten incorporated systems

Table 3.1 presents the surface areas and pore volumes of the tungsten modified ceria systems using the BET method.

Table 3.1  
Surface area and pore volume of tungsten modified ceria systems

Catalyst	Surface area (m <sup>2</sup> /g)		Pore volume* (cm <sup>3</sup> /g)
	BET	Langmuir	
C	148	203	0.211
SC	44	67	0.122
CW <sub>5</sub>	92	141	0.170
CW <sub>10</sub>	72	111	0.152
CW <sub>15</sub>	76	117	0.155
CSW <sub>5</sub>	53	81	0.108
CSW <sub>10</sub>	51	79	0.133
CSW <sub>15</sub>	50	78	0.125

\* Pore volume measured at a  $p/p_0$  of 0.9997

From Table 3.1, it can be observed that the surface area of the support decreases with the introduction of tungsten as well as sulphate ions. Surface area decreases from 148 to 92 m<sup>2</sup>/g, on incorporation of 5 wt% of tungsten into pure ceria. Further incorporation also results in a decrease of surface area for the CW<sub>10</sub> system and a small increase is noticed for the CW<sub>15</sub> system. In the case of sulphated systems, though there is a decrease in the surface area value compared with pure ceria, among tungsten incorporated systems there is no appreciable change with increase in tungsten loading.

The results indicate that the doping of tungsten as well as sulphate ions have a negative effect on surface area and pore volume values. Dong et al. observed that in the case of ceria supported tungsten oxide catalysts, when the concentration of tungsten ions is below the dispersion capacity, highly dispersed tungsten oxide species are formed on the surface of the support presumably by the incorporation of the dispersed tungsten ions into the surface vacant sites of CeO<sub>2</sub><sup>1</sup>. In the present case it can be inferred that the dispersed tungsten species are occupying the surface vacant sites of CeO<sub>2</sub>, which causes pore blockage and subsequent reduction of surface area. Another reason for this decrease of surface area is attributed to the agglomeration of the particles upon modification. The existence of sulphate ions in the acidified solution is reported to be responsible for spherical agglomeration of the nanoparticles<sup>2</sup>. This is supported by SEM analysis of the systems, which show clusters of particles upon incorporation. The crystallite size values obtained from XRD measurements using Scherer equation also show an increase in crystallite size values with loading.

#### **b) Molybdenum incorporated systems**

The surface area and pore volume measurements of molybdenum doped ceria systems are shown in Table 3.2.

Table 3.2  
Surface area and pore volume of molybdenum modified ceria systems

Catalyst	Surface area (m <sup>2</sup> /g)		Pore volume* (cm <sup>3</sup> /g)
	BET	Langmuir	
C	148	203	0.211
SC	44	67	0.122
CM <sub>5</sub>	61	94	0.142
CM <sub>10</sub>	34	52	0.109
CM <sub>15</sub>	26	40	0.085
CSM <sub>5</sub>	37	56	0.099
CSM <sub>10</sub>	22	34	0.078
CSM <sub>15</sub>	16	25	0.056

\* Pore volume measured at a  $p/p_0$  of 0.9997

Surface area of pure ceria was found to decrease with the successive incorporation of sulphate ions as well as molybdenum oxide. Sulphated systems possess lower surface area compared to simple supported systems with the same molybdenum loading. Pore volume values also decrease with the doping of sulphate ions and molybdenum oxide. In simple supported systems with an increase of molybdenum concentration from 5 to 15 wt% the surface area values decreases from 61 to 26 m<sup>2</sup>/g.

The decrease of surface area upon molybdenum doping can be explained by considering the nature of interaction between the support and the metal oxide. Chen et al. reported several models concerning the interactions between molybdena and  $\gamma$ -alumina, which can tentatively divided into two categories:- (a) the dispersed oxide species are spreading on the top of or (b) incorporating into the surface of the support<sup>3</sup>. This indicates that under appropriate conditions, the dispersed molybdena might cover the support with the formation of a monolayer on the top of the surface,

or the dispersed molybdena might incorporate into the vacant sites on the surface of the support. On the basis of the second concept the decrease in surface area with molybdenum loading, can be explained as the plugging of the surface vacant sites of ceria by the incorporated molybdena. As a result of this, the pore volumes of the modified catalysts are found to be lower than the unmodified systems. The decrease may also be due to the agglomeration of the particles as discussed in the case of tungsten modified systems. This type of decrease in surface area upon modification with molybdenum oxide was reported in the case of  $\text{SiO}_2/\text{TiO}_2$  supported molybdena catalysts. Watson et al. observed that from 2 to 20 wt% loading of molybdena, the catalysts showed a general decrease in surface area with increasing amount of molybdenum added to  $\text{SiO}_2/\text{TiO}_2$  support<sup>4</sup>

### c) Chromium incorporated systems

Table 3.3 represents the results obtained for chromium doped ceria systems by BET method.

Table 3.3  
Surface area and pore volume of chromia modified ceria systems

Catalyst	Surface area ( $\text{m}^2/\text{g}$ )		Pore volume* ( $\text{cm}^3/\text{g}$ )
	BET	Langmuir	
C	148	203	0.211
SC	44	67	0.122
CCr <sub>5</sub>	53	81	0.125
CCr <sub>10</sub>	45	68	0.097
CCr <sub>15</sub>	37	57	0.086
CSCr <sub>5</sub>	31	56	0.095
CSCr <sub>10</sub>	24	55	0.078
CSCr <sub>15</sub>	22	52	0.067

\* Pore volume measured at a  $p/p_0$  of 0.9997

Results presented in Table 3.3 indicate that the incorporation of chromium oxide exert a negative influence on the surface area and pore volume values. Surface area of pure ceria is reduced successively with the incorporation of chromium oxide. Similar trend is seen in the case of sulphated series also. In this case also the reduction of surface area can be ascribed to the plugging of the pores by the incorporated metals and the agglomeration of the particles as discussed above. This type of reduction of surface area is reported in the case of other metal ions also. According to Idriss et al. catalytic systems such as Co/CeO<sub>2</sub> and Pd-Co/CeO<sub>2</sub> possess surface areas lower than pure ceria. They attributed this drop to blocking of the micropores of the support by clusters of Co compounds<sup>5</sup>.

## II. Energy Dispersive X-ray Fluorescence (EDX) Analysis

### a) Tungsten incorporated systems

The elemental composition of tungsten incorporated ceria systems as well as the sulphate doped samples determined by EDX analysis is given in Table 3.4. The percentage of tungsten among the oxides is also given.

Table 3.4  
EDX data for tungsten doped ceria and its sulphated analogues

Catalyst	Composition					
	Atom (%)			Oxide (%)		W (%)
	Ce	W	S	CeO <sub>2</sub>	SO <sub>4</sub>	
C	100	-	-	100	-	-
SC	93.1	-	6.9	84.7	15.3	-
CW <sub>5</sub>	94.9	5.1	-	95.8	-	4.2
CW <sub>10</sub>	93.1	6.9	-	94.3	-	5.7
CW <sub>15</sub>	87.6	12.4	-	89.7	-	10.3
CSW <sub>5</sub>	90.3	3.4	6.3	83.2	14.2	2.6
CSW <sub>10</sub>	87.7	6.0	6.3	81.2	14.3	4.5
CSW <sub>15</sub>	83.5	9.8	6.7	77.4	15.2	7.4

EDX results presented in Table 3.4 show that the percentage of tungsten among the oxides in the case of CW<sub>3</sub> system is 4.2, whereas for the sulphated system it is only 2.6. Similar is the case with high loaded samples. In the case of sulphated samples, the amount of sulphate retained in the samples is almost the same, though the percentage of tungsten is varied from 5 to 15 wt%.

### b) Molybdenum incorporated systems

The EDX results obtained for molybdenum incorporated systems is presented in Table 3.5. Here also the percentage of molybdenum among the oxides is given.

Table 3.5

EDX data for pure ceria, sulphated ceria, molybdenum modified ceria and its sulphated analogues

Catalyst	Composition					
	Atom (%)			Oxide (%)		Mo (%)
	Ce	Mo	S	CeO <sub>2</sub>	SO <sub>4</sub>	
C	100	-	-	100	-	-
SC	93.1	-	6.9	84.7	15.3	-
CM <sub>5</sub>	90.9	9.1	-	92.5	-	7.5
CM <sub>10</sub>	82.4	17.6	-	85.2	-	14.8
CM <sub>15</sub>	79.9	20.1	-	83.1	-	16.9
CSM <sub>5</sub>	80.1	10.9	9.0	72.2	19.8	8.0
CSM <sub>10</sub>	76.4	18.6	5.0	73.4	11.7	14.5
CSM <sub>15</sub>	71.1	25.8	3.1	71.3	7.6	21.1

From Table 3.5, it is evident that the percentage of molybdenum present in the sulphated systems is higher than the simple supported ones, even though the same amount of ammoniumheptamolybdate is used for incorporation. The sulphate retaining ability of the samples was found to decrease with increase in the amount of molybdenum.

### c) Chromium incorporated systems

Table 3.6 presents the chemical composition data for chromium doped systems obtained from EDX analysis.

Table 3.6

EDX data for pure ceria, sulphated ceria, chromium modified ceria and its sulphated analogues

Catalyst	Composition					
	Atom (%)			Oxide (%)		Cr (%)
	Ce	Cr	S	CeO <sub>2</sub>	SO <sub>4</sub>	
C	100	-	-	100	-	-
SC	93.1	-	6.9	84.7	15.3	-
CCr <sub>5</sub>	81.2	18.8	-	84.1	-	15.9
CCr <sub>10</sub>	71.9	28.1	-	75.9	-	24.1
CCr <sub>15</sub>	61.3	38.7	-	66.1	-	33.9
CSCr <sub>5</sub>	75.7	16.8	7.5	70.3	17.0	12.7
CSCr <sub>10</sub>	59.1	31.4	9.5	54.8	21.5	23.7
CSCr <sub>15</sub>	51.3	39.7	10.0	48.6	20.8	30.6

Table 3.6 shows that in chromium doped systems, the percentage of chromium is higher for the simple supported systems than the sulphated samples among the oxides. The amount of sulphate retained in the sample is maximum for the CSCr<sub>10</sub> system.

### III. X-Ray Diffraction (XRD) Analysis

#### a) Tungsten incorporated systems

Figure 3.1 shows the XRD patterns of a series of tungsten modified CeO<sub>2</sub> samples with different tungsten loading.

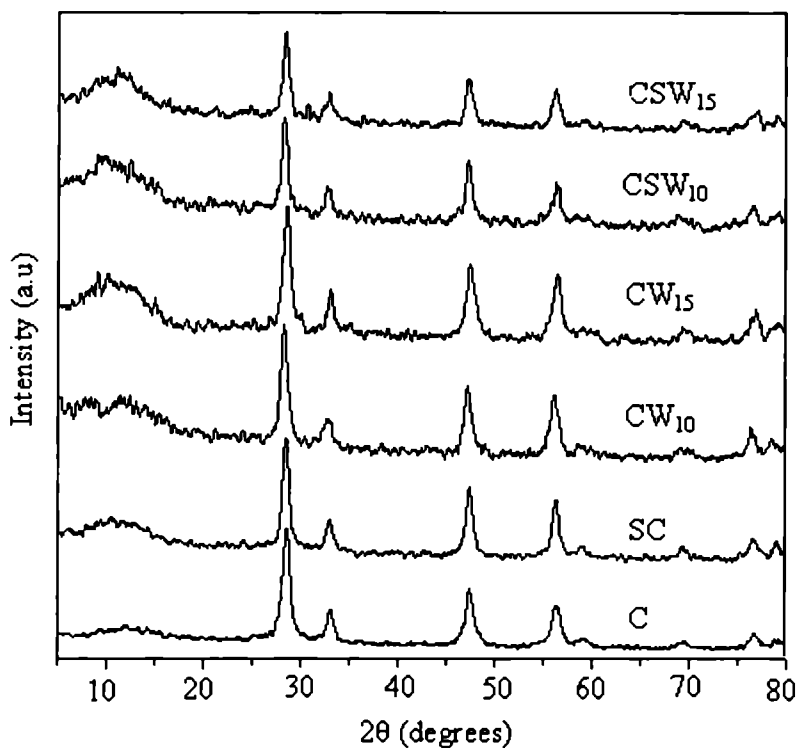


Figure 3.1

## XRD profiles of tungsten modified series

The XRD data of the prepared systems agree well with the standard values given in the JCPDS data cards (34-394), thus confirming the fluorite structure of ceria. The XRD patterns of the modified systems show the peaks corresponding to ceria only. Characteristic peaks of crystalline  $\text{WO}_3$  (typically with  $2\theta = 23.14^\circ$ ,  $23.64^\circ$  and  $24.36^\circ$ ) have not been observed. It is reported that in the case of metal oxides there is a critical value called dispersion capacity, at values lower than which the oxide might become highly dispersed on the support without the formation of its crystalline phase<sup>1</sup>. Since no characteristic peaks corresponding to tungsten oxide species are seen in Figure 3.1, it can be concluded that the tungsten loading is below the dispersion capacity.

Dong et al. studied the surface properties of ceria supported tungsten oxide catalysts and found that at low tungsten loading highly dispersed tungsten oxide species are found on the surface<sup>1</sup>. The characteristic peaks of crystalline  $\text{WO}_3$  is seen only for samples with tungsten loading greater than the dispersion capacity which they found as  $4.6 \text{ W}^{6+} \text{ ions/nm}^2$ . The XRD patterns of tungstated MgO catalysts show a similar observation. Martin et al. studied the properties of a series of tungstates formed in W-Mg-O samples with tungsten content ranging from 5 to 80 wt%<sup>6</sup>. They observed that all X-ray diffraction patterns for samples containing less than 60 wt% of W, calcined at  $450 \text{ }^\circ\text{C}$ , show intense diffraction peaks due to MgO only. The lack of diffraction peaks due to tungsten containing species was explained on the basis of the fact that these species are either amorphous or exist as very small crystallites with  $d < 4 \text{ nm}$ . In the present case the absence of diffraction lines corresponding to tungsten oxide species indicate the high dispersion of these species over the catalyst surface or the existence as small crystallites with  $d < 4 \text{ nm}$  and also the concentration of the tungsten species is below the dispersion capacity. The lack of detection of crystalline  $\text{WO}_3$  is in full agreement with previous studies on  $\text{WO}_3\text{-TiO}_2$  and  $\text{WO}_3\text{-Al}_2\text{O}_3$ <sup>7-12</sup>.

The results obtained on indexing the XRD pattern are given in Table 3.7. The hkl values pointing to the 111 plane of ceria, indicates the fluorite (fcc) structure of  $\text{CeO}_2$ . The crystallite sizes obtained from Scherer equation shows an increase in crystallite size upon modification<sup>13</sup>. This supports the reduction of surface area with the incorporation of tungsten oxide and sulphate ions. Lattice parameter of all the modified systems is found to be around 0.542.

Table 3.7

XRD data for pure ceria, sulphated ceria, tungsten doped ceria and its sulphated analogues

Catalyst	$d_{hkl}$	$h^2+k^2+l^2$	hkl	Lattice parameter (nm)	Unit cell volume (nm <sup>3</sup> )	Crystal structure	Crystallite size (nm)
C	3.129	3	111	0.542	0.159	fcc	8.7
SC	3.146	3	111	0.545	0.162	fcc	10.7
CW <sub>5</sub>	3.151	3	111	0.539	0.157	fcc	8.8
CW <sub>10</sub>	3.157	3	111	0.539	0.157	fcc	9.7
CW <sub>15</sub>	3.129	3	111	0.542	0.159	fcc	9.1
CSW <sub>5</sub>	3.157	3	111	0.538	0.156	fcc	10.9
CSW <sub>10</sub>	3.127	3	111	0.541	0.158	fcc	11.6
CSW <sub>15</sub>	3.151	3	111	0.539	0.157	fcc	11.9

### b) Molybdenum incorporated systems

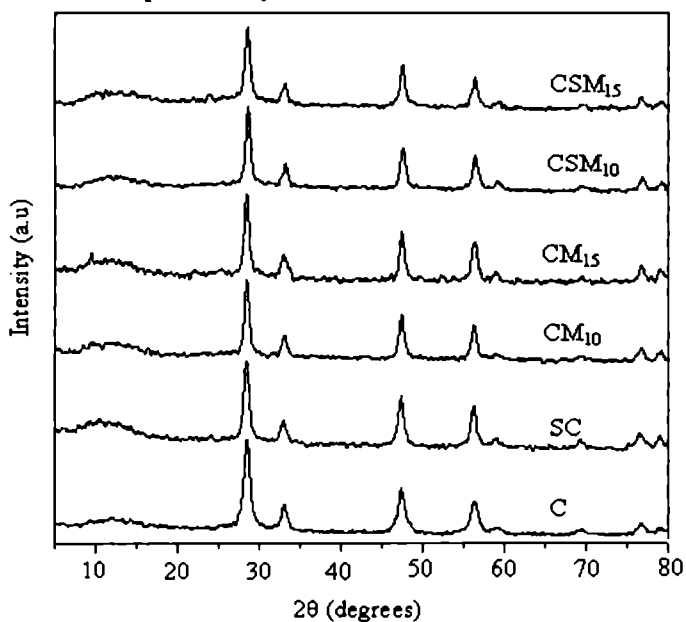


Figure 3.2

XRD patterns of molybdenum doped series

The power X-ray diffraction patterns of the molybdenum loaded catalysts are shown in Figure 3.2. Here also the fluorite structure (space group Fm3m) of ceria is observed in all cases. No characteristic peak of crystalline MoO<sub>3</sub> is observed.

The results presented in Figure 3.2 indicate that the molybdena species are finely dispersed on the catalyst surface, and the concentration is below the dispersion capacity. However, it may be possible for molybdenum oxide to exist as a microcrystalline material below the XRD detection limit. Watson et al. studied the XRD patterns of a series of SiO<sub>2</sub>/TiO<sub>2</sub> supported molybdena catalysts with different molybdenum loading. They observed that molybdena species are finely dispersed showing no MoO<sub>3</sub> diffraction lines up to 15 wt% loading<sup>4</sup>. Similarly in the case of ZrO<sub>2</sub> supported molybdena samples with low MoO<sub>3</sub> concentration (11 wt%) only tetragonal ZrO<sub>2</sub> was observed and crystalline MoO<sub>x</sub> phases were not detected in XRD<sup>14</sup>.

Table 3.8 shows the results of XRD data indexing for the molybdenum modified systems. The results confirm the crystal structure of the systems as fcc. There is an increase in the crystallite size calculated using the Scherer equation upon modification.

Table 3.8

XRD data for pure ceria, sulphated ceria, molybdenum doped ceria and its sulphated analogues

Catalyst	$d_{hkl}$	$h^2+k^2+l^2$	hkl	Lattice Parameter (nm)	Unit cell volume (nm <sup>3</sup> )	Crystal structure	Crystallite size (nm)
C	3.129	3	111	0.542	0.159	fcc	8.7
SC	3.146	3	111	0.545	0.162	fcc	10.7
CM <sub>5</sub>	3.119	3	111	0.541	0.158	fcc	10.3
CM <sub>10</sub>	3.129	3	111	0.542	0.159	fcc	11.1
CM <sub>15</sub>	3.140	3	111	0.543	0.161	fcc	11.8
CSM <sub>5</sub>	3.124	3	111	0.542	0.159	fcc	11.0
CSM <sub>10</sub>	3.124	3	111	0.541	0.158	fcc	11.9
CSM <sub>15</sub>	3.129	3	111	0.541	0.158	fcc	12.0

### c) Chromium incorporated systems

The powder X-ray diffractograms of the pure, supported and sulphate modified systems calcined at 500 °C are given in Figure 3.3. The XRD pattern of pure ceria gives sharp peaks characteristics of the fluorite structure (fcc with  $a = 0.541$  nm) of ceria, which remained intact after modification with chromium oxide. The characteristic peak of crystalline chromium oxide is absent in all cases. This points to the fact that the chromium species are either highly dispersed or exist as microcrystalline material below the XRD detection limit as discussed in the case of tungsten as well as molybdenum oxide incorporated series.

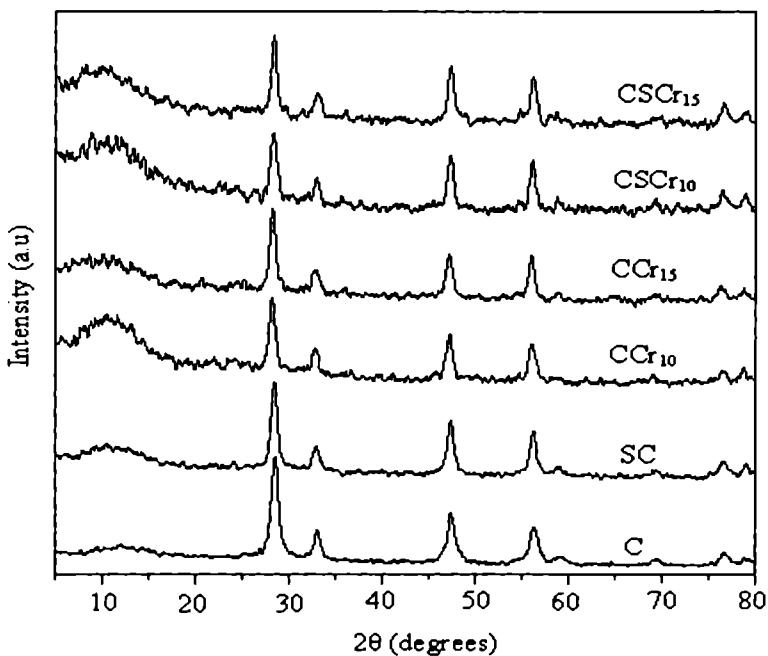


Figure 3.3

XRD patterns of chromium doped series

Table 3.9 represents the XRD data indexing results for chromium doped systems. Here also the crystallite size was increased with modification. The crystal structure is fcc in all the catalytic systems.

Table 3.9  
XRD data for pure ceria, sulphated ceria, chromium doped ceria and its sulphated analogues

Catalyst	$d_{hkl}$	$h^2+k^2+l^2$	hkl	Lattice parameter (nm)	Unit cell volume ( $\text{nm}^3$ )	Crystal structure	Crystallite size (nm)
C	3.129	3	111	0.542	0.159	fcc	8.7
SC	3.146	3	111	0.545	0.162	fcc	10.7
CCr <sub>5</sub>	3.179	3	111	0.542	0.159	fcc	11.1
CCr <sub>10</sub>	3.177	3	111	0.543	0.161	fcc	11.2
CCr <sub>15</sub>	3.162	3	111	0.543	0.161	fcc	11.4
CSCr <sub>5</sub>	3.157	3	111	0.541	0.158	fcc	11.5
CSCr <sub>10</sub>	3.148	3	111	0.542	0.159	fcc	11.8
CSCr <sub>15</sub>	3.140	3	111	0.541	0.158	fcc	12.0

#### IV. Scanning Electron Microscopy (SEM)

##### a) Tungsten incorporated systems

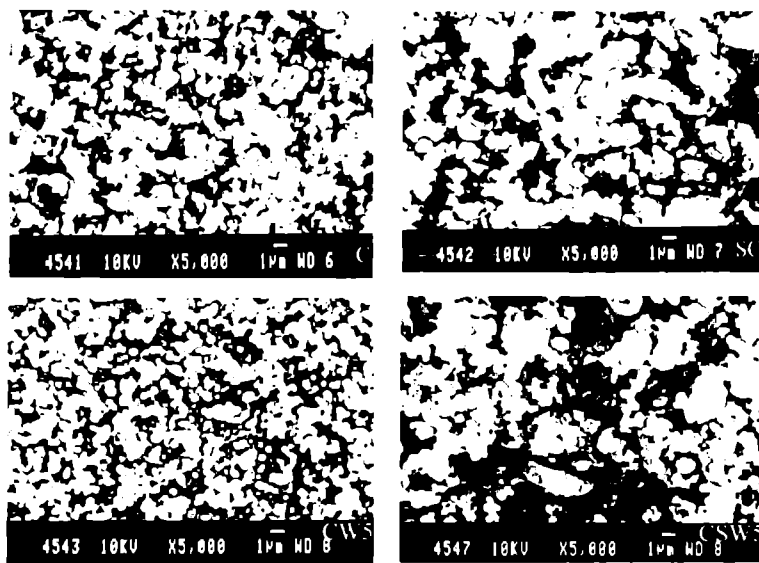


Figure 3.4  
Scanning Electron Micrographs of tungsten doped systems

Scanning electron micrographs of some of the representative systems in the tungsten incorporated series is given in Figure 3.4. The effect of tungsten loading as well as sulphate modification is apparent from the SEM pictures of C, SC, CW<sub>5</sub> and CSW<sub>5</sub>.

Figure 3.4 clearly shows that the particles tend to agglomerate upon modification with tungsten. The particle size is observed to be increasing with the addition of tungsten. Moreover a comparison of the SEM photographs of sulphate incorporated simple and supported systems indicates that the introduction of sulphate anions to the catalyst surface also result in an increase of particle size.

From the results it is found that both the introduction of tungsten oxide as well as sulphate ions results in the agglomeration of the particles leading to the formation of bigger crystallites. Combining the results obtained for surface area analysis and SEM, the decrease of surface area upon modification can be ascribed to the agglomeration of the particles.

#### b) Molybdenum incorporated systems

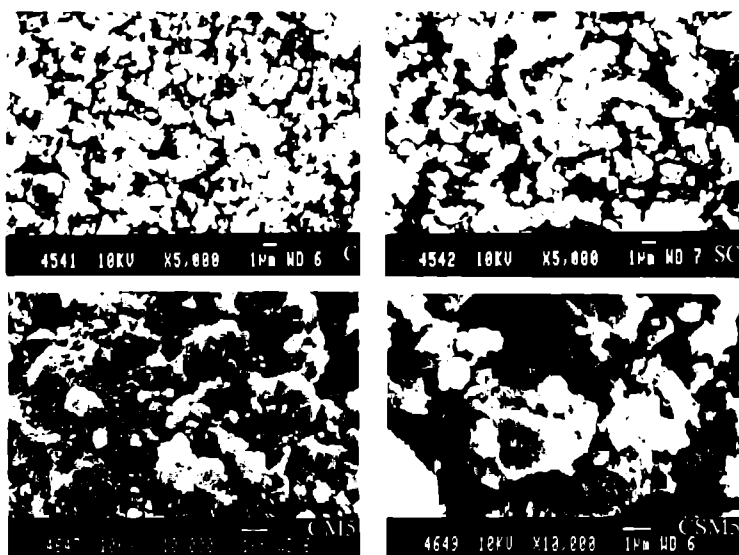


Figure 3.5

Scanning Electron Micrographs of molybdenum doped systems

To examine the effect of molybdenum incorporation and surface sulphate modification on the particle size of the catalysts, SEM pictures of some representative samples were taken and the results are presented in Figure 3.5

The incorporation of molybdena into pure ceria results in the formation of bigger crystallite as evident from the SEM pictures. Sulphate modification further increases the particle size. This increase in the particle size is well supported by the surface area results and also the crystallite sizes obtained from XRD data using the Scherer equation.

### c) Chromium incorporated systems

SEM analysis of the systems gives us an idea about the surface topography of the catalysts. Figure 3.6 presents the SEM pictures of some representative samples among the chromium oxide incorporated series.

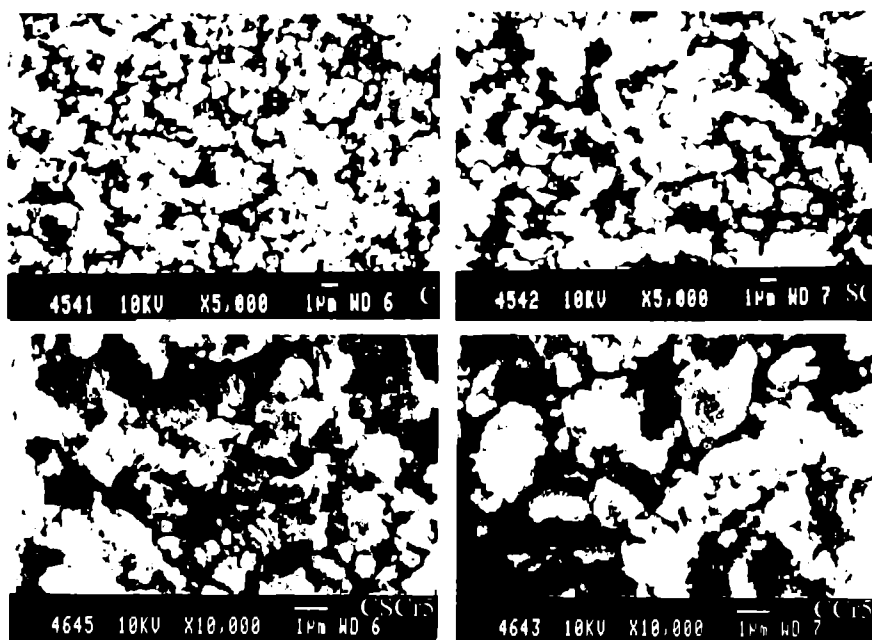


Figure 3.6  
Scanning Electron Micrographs of chromium doped systems

The particle size is observed to be smaller in the case of pure ceria. Modification results in an enhancement in the particle size as clear from the Figure 3.6. The SEM pictures agree well with the BET surface area results. Since particle agglomeration takes place with modification, the modified systems possess lower surface area than the simple systems. Sulphate incorporation was found to further reduce the surface area as evident from the SEM pictures.

### V. Thermogravimetric Analysis (TGA)

To examine the thermal stability of the prepared systems, thermal analysis was carried out and thermogram for pure and tungsten incorporated systems are shown in Figure 3.7.

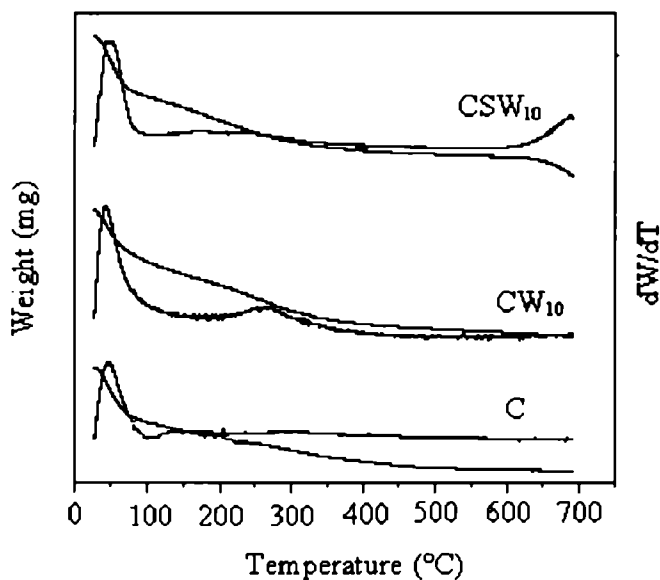


Figure 3.7

TG-DTG curves for pure ceria, tungsten doped ceria and its sulphated analogues

As can be noted from the Figure 3.7, the TG-DTG curve for pure cerium oxide shows two major weight loss. No other weight loss is noticed in the case of

tungsten doped simple systems. In the case of sulphated sample in addition to the weight losses seen in simple systems, another weight loss in the high temperature region is observed. The major weight loss around 100 °C is due to the loss of non-dissociative adsorbed water as well as water held on the surface by hydrogen bonding<sup>15</sup>. The second weight loss peak in the temperature range 125-325 °C could be due to the elimination of organics through oxidation processes<sup>16</sup>. No phase transition is observed here indicating the stability of the cerium oxide fluorite phase. TG-DTG curve of tungsten doped sulphated samples reveals the commencement of decomposition of surface sulphate groups above 650 °C.

#### b) Molybdenum incorporated systems

TG-DTG curves obtained for pure, molybdenum incorporated and sulphate treated samples are given in Figure 3.8.

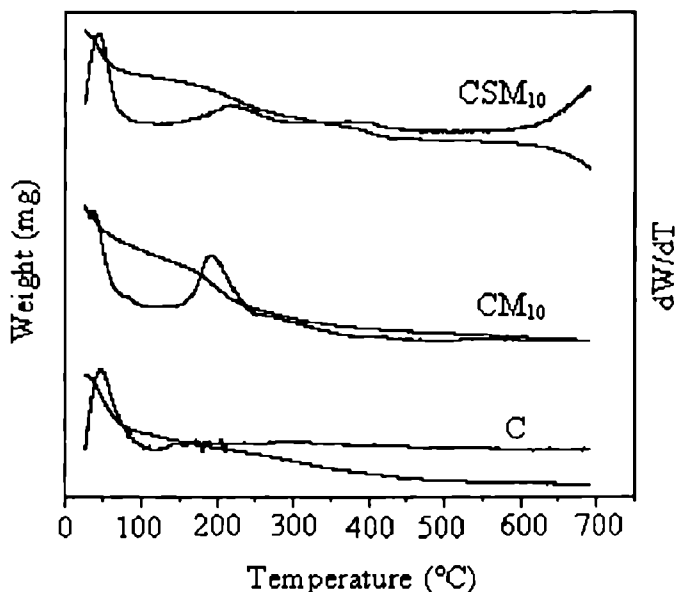


Figure 3.8

TG-DTG curves of pure ceria, molybdenum doped ceria and its sulphated analogues

The TG pattern of the molybdenum doped simple systems show weight losses in the temperature ranges 25-100 °C and 150-250 °C. In sulphated samples an additional weight loss above 625 °C is also observed. The weight loss in the range 25-100 °C corresponds to water loss and another at 150-250 °C corresponds to the elimination of surfactant moiety as discussed earlier. The additional weight loss which is seen in the case of sulphated samples can be ascribed to the decomposition of sulphate group. Sakthivel et al. studied the TG pattern of sulphated zirconia catalysts and observed two major weight losses in the temperature range 50-220 °C and >500 °C. According to them the weight loss in the region 50-220 °C correspond to water loss and the other in the region >500 °C to the decomposition of sulphate ions<sup>17</sup>.

### c) Chromium incorporated systems

The results obtained for thermogravimetric analysis in the case of chromium doped systems are presented in Figure 3.9.

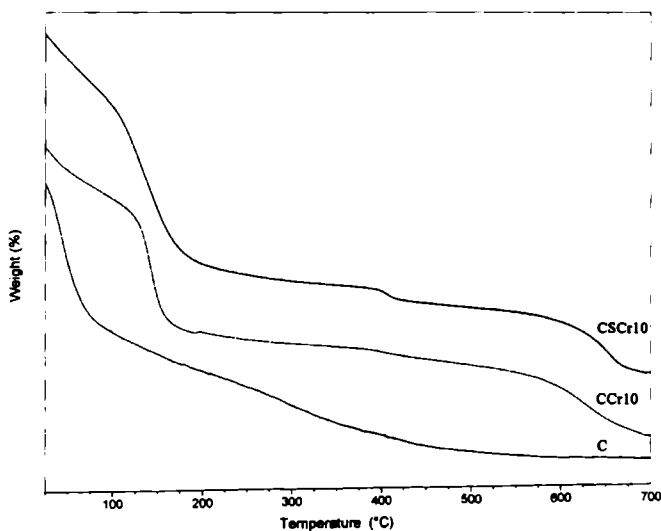


Figure 3.9

TG curves of pure ceria, chromium doped ceria and its sulphated analogues

The TG curve of pure ceria shows weight losses near 100 °C and in the 150-250 °C range, which is ascribed to the loss of physisorbed water and surfactant species from the surface of the catalyst respectively. With the incorporation of chromium no change in the TG pattern of pure ceria is noticed. Further in the case of sulphated sample, an additional weight loss in the high temperature region (above 650 °C) is observed, arising from the decomposition of the sulphate moiety.

## VI. Fourier Transform Infrared Spectroscopy (FTIR)

### a) Tungsten incorporated systems

FTIR spectra of tungsten doped ceria samples and its sulphated analogues are shown in Figure 3.10. The IR spectrum of pure ceria gives two strong absorption bands around 3421 and 1600  $\text{cm}^{-1}$  in addition to the bands at 1352 and 1057  $\text{cm}^{-1}$ . All the tungsten doped systems show characteristic peaks in the range 933-953  $\text{cm}^{-1}$ . The presence of sulphate species in the catalyst is evident from the characteristic peaks around 1200  $\text{cm}^{-1}$ .

The absorption bands centred around 1352 and 1057  $\text{cm}^{-1}$  are assigned to the characteristic peaks of  $\text{CeO}_2$  species<sup>18</sup>. Dong et al. investigated the IR spectra of ceria supported tungsten oxide catalysts with different tungsten loading and observed that the peak around 965  $\text{cm}^{-1}$  arises from the highly dispersed surface tungsten oxide species. According to them when the amount of tungsten oxide is higher than the dispersion capacity an additional broad peak ranging from 650 to 900  $\text{cm}^{-1}$  is noticed which is attributed to the presence of bulk tungsten oxide species<sup>1</sup>.

Based on the above literature it can be inferred that the tungsten oxide species are highly dispersed on the catalyst surface. The absence of peak in the range 650 to 900  $\text{cm}^{-1}$  points to the absence of bulk tungsten oxide species. This conclusion is in good agreement with the XRD results in which the characteristic  $2\theta$  values of crystalline  $\text{WO}_3$  is absent. Hydroxy groups are detected with a large band around 3500  $\text{cm}^{-1}$  corresponding to O-H stretching frequency and a broad band at 1600  $\text{cm}^{-1}$ ,

due to in plane bending vibrations of O-H groups<sup>16</sup>. Sulphate loading has been qualitatively confirmed from the FTIR spectra of the modified samples, which showed bands in the range of 1109-1119  $\text{cm}^{-1}$  for the sulphated samples, but lacked the characteristic band near 1400  $\text{cm}^{-1}$ , which is quoted as a common feature of all super acidic sulphated oxides<sup>19</sup>.

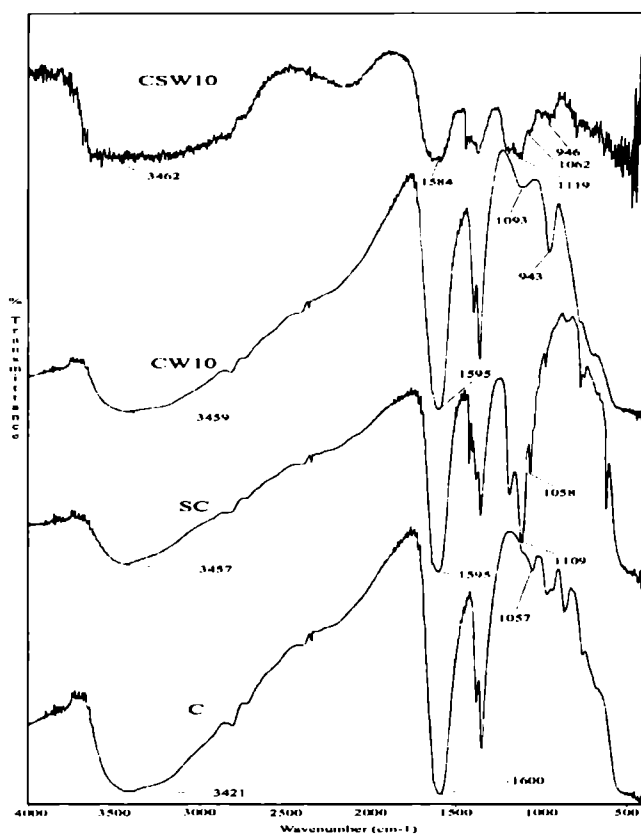


Figure 3.10

FTIR spectra of pure ceria, sulphated ceria, tungsten doped ceria and its sulphated analogues

### b) Molybdenum incorporated systems

Figure 3.11 shows the FTIR spectra of the molybdenum incorporated simple as well as sulphated ceria systems.

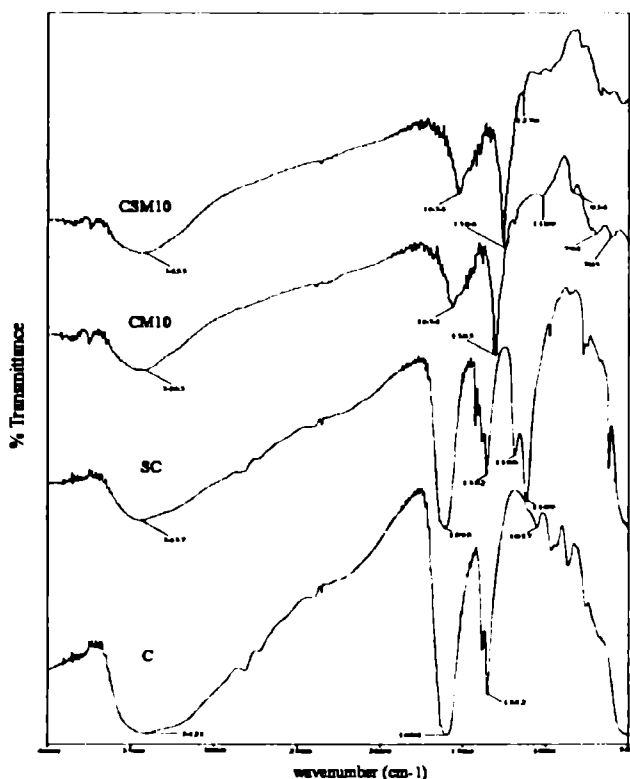


Figure 3.11

FTIR of pure ceria, sulphated ceria, molybdenum doped ceria and its sulphated analogues

The IR spectrum of pure ceria gives two strong absorption bands at 1352 and 1057  $\text{cm}^{-1}$  just as in the case of tungsten incorporated systems. The characteristic absorption bands of hydroxy groups are observed at 3421 and 1600  $\text{cm}^{-1}$ . The spectra of molybdenum doped systems show characteristic bands in the region 1050-900  $\text{cm}^{-1}$  and 850-700  $\text{cm}^{-1}$ . All the sulphated samples show absorption bands around 1270  $\text{cm}^{-1}$  apart from the bands present in the unmodified systems.

The characteristic band around 1352 and 1057  $\text{cm}^{-1}$  which arises from  $\text{CeO}_2$  found to shift towards higher wavenumbers upon modification with molybdenum

ions. The peaks in the region  $1050\text{-}900\text{ cm}^{-1}$  is attributed to terminal Mo=O vibrations and  $850\text{-}700\text{ cm}^{-1}$  is the region of antisymmetric Mo-O-Mo or O-Mo-O stretching vibrations or both<sup>20-22</sup>. The surface OH groups present in the oxide supports give strong IR bands in the  $3421\text{ cm}^{-1}$  and  $1057\text{ cm}^{-1}$  regions. The IR bands in the region  $3421\text{ cm}^{-1}$  is due to the -OH stretching frequency and the bands at  $1057\text{ cm}^{-1}$  to the bending vibrations of the -OH group<sup>23</sup>.

The sulphate loading of the supported system is confirmed by the characteristic peaks in the region  $1200\text{-}1000\text{ cm}^{-1}$ . The IR spectra of all the sulphated samples show a characteristic peak around  $1270\text{ cm}^{-1}$  which can be ascribed to the bidentate sulphate group coordinated to the metal ion. It was reported that the peak around  $1210\text{ cm}^{-1}$  corresponds to the unsymmetrical vibrations the chelate bidentate<sup>24-26</sup>. The IR spectra of sulphated metal oxides such as sulphated oxides of  $\text{ZrO}_2$ ,  $\text{Fe}_2\text{O}_3$  and  $\text{HfO}_2$  have been studied in detail for explaining the superacidity of these catalysts<sup>27-30</sup>. A common feature of all the superacidic sulphated oxides is the presence of a strong band near  $1400\text{ cm}^{-1}$  representing the asymmetric stretching frequency of  $\text{S}=\text{O}$ <sup>31-33</sup>. The absence of this peak suggests the lack of superacidic properties of the catalytic systems.

### **c) Chromium incorporated systems**

FTIR spectra of chromium doped simple and sulphated ceria systems are presented in Figure 3.12

FTIR spectra of chromium doped ceria systems also gives characteristic peaks arising from  $\text{CeO}_2$  species and surface hydroxyl group. The presence of sulphate ions in the catalyst is confirmed by the presence of peaks around  $1200\text{ cm}^{-1}$  region in the FTIR spectrum as discussed in the case of tungsten and molybdenum modified systems. The absence of bands around  $1440\text{ cm}^{-1}$  corresponds to the absence of free  $\text{S}=\text{O}$  group of the sulphate molecule<sup>34-35</sup>. In the case of chromium incorporated systems an additional band around  $620\text{ cm}^{-1}$  is observed which is assumed to be originating from chromia species.

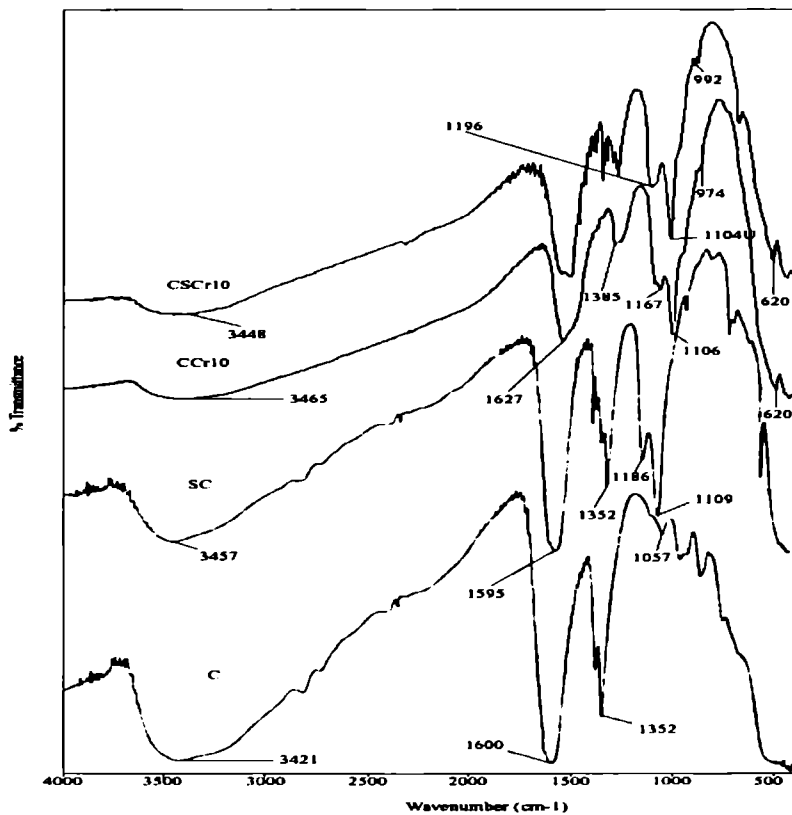


Figure 3.12  
FTIR spectra of chromium incorporated systems

## VII. Ultraviolet -Visible Diffuse Reflectance Spectroscopy (UV - vis - DRS)

### a) Tungsten incorporated systems

The diffuse reflectance UV-vis spectroscopy is known to be a very sensitive technique for the identification and characterisation of metal ion coordination. Figure 3.13 shows UV- vis - DRS profiles of tungsten incorporated ceria systems with different tungsten loading.

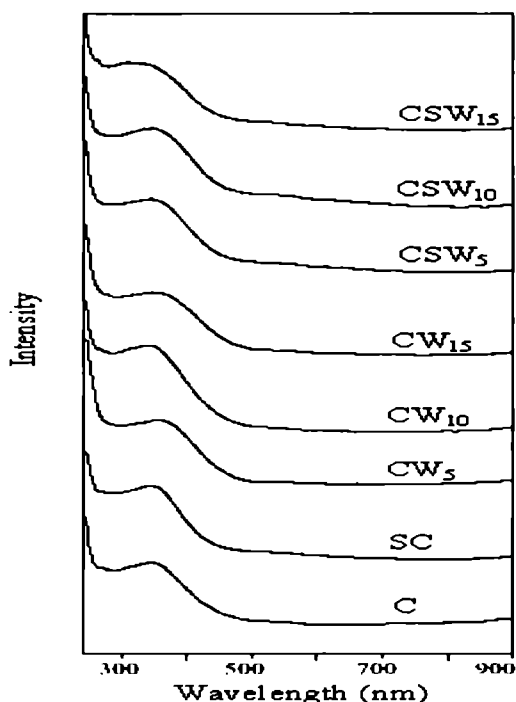


Figure 3.13

#### Diffuse reflectance spectra of tungsten incorporated ceria systems

From Figure 3.13 it is evident that a single characteristic band around 300 nm is present in all the cases. No additional bands are observed with the incorporation of tungsten. The position of ligand to metal charge transfer (LMCT,  $O^{2-} \rightarrow Ce^{4+}$ ) spectra depends on the ligand field symmetry surrounding the Ce center. The electronic transitions from oxygen to cerium require higher energy for a tetra coordinated  $Ce^{4+}$  than for a hexa-coordinated one. It was reported in the case of Ce-MCM-41 samples that the absorption band centered at 300 nm is due to the presence of  $Ce^{4+}$  species in the tetra-coordinated environment, whereas in the case of a silica and ceric oxide mixture and Ce-exchanged MCM-41 samples, two distinct bands, at 300 and 400 nm, corresponds to two different types of  $Ce^{4+}$  species. The absorption at higher wavelength ( $\sim 400$  nm) may be assigned to hexa-coordinated  $Ce^{4+}$  species<sup>36</sup>. In the

present case since the absorption bands are seen around 300 nm, it is assumed that the  $Ce^{4+}$  species is in the tetra coordinated environment.

### b) Molybdenum incorporated systems

The UV-vis DR spectra of molybdenum doped ceria systems are helpful in identifying the structures of molybdenum species dispersed on ceria surface. The UV-vis DR spectra of the various molybdenum modified ceria systems are shown in Figure 3.14.

The spectra clearly shows the characteristic band arising from  $CeO_2$  species around 300 nm. In the case of simple supported systems, at lower molybdenum loading a small peak in the 230-260 nm region is observed, which is found to disappear at higher molybdenum loading. Also the band arising from ceria species broadens as the molybdenum loading increases. The surface modification by sulphate anions does not result in strong changes in the UV-vis DR spectrum, and is characterised by the single peak around 300 nm.

Since Mo (VI) ion has a  $d^0$  electronic configuration, the only absorption band which can occur in the UV-visible range of the electronic spectra is due to the ligand-metal charge transfer transition (LMCT)  $O^{2-} \rightarrow Mo^{6+}$ . This type of band is usually observed in the range of 200-400 nm<sup>37</sup>. The energy of the electronic transitions strongly depends on the ligand field symmetry surrounding the molybdenum center. A more energetic transition is expected for a tetrahedral Mo (VI) than for an octahedral Mo(VI)<sup>38</sup>. It has been reported that the band at 230-260 nm is the characteristic absorption of Mo=O bond of tetrahedral molybdate and the band at about 320 nm is due to the Mo-O-Mo bridge bond of octahedral species<sup>39-51</sup>.  $Ce^{4+}$  species in the tetra coordinated environment is indicated by the absorption band at 300 nm and that in the octahedral environment by the band at 400nm<sup>36</sup>. On the basis of these literature, it can be assumed that in our case the band around 300 nm originates from  $CeO_2$  species in the tetrahedral environment. The absence of band at 400 nm suggests that

octahedral  $\text{CeO}_2$  species is not present in the catalyst. Moreover the band at 230 nm present in the case of  $\text{CM}_5$  and  $\text{CM}_{10}$  system may be assigned to the absorption of Mo=O bond of tetrahedral molybdate. The disappearance of this band at higher molybdenum loading and also in sulphated samples, may be due to the formation of octahedral molybdate species which gets overlapped with the band arising from  $\text{CeO}_2$  species.

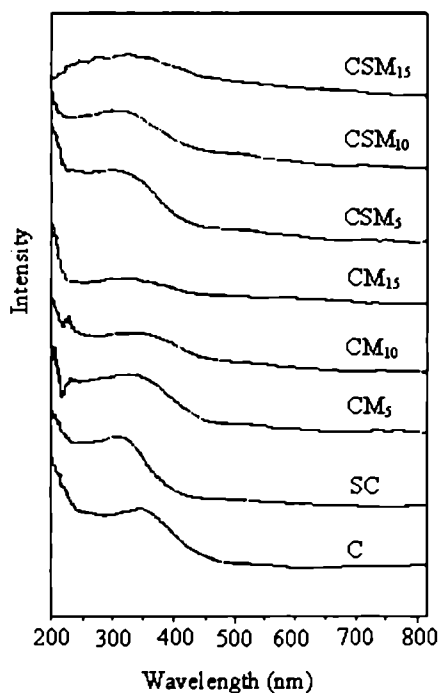


Figure 3.14

Diffuse reflectance spectra of molybdenum incorporated ceria systems

### c) Chromium incorporated systems

UV- vis diffuse reflectance spectroscopy is commonly used to determine the symmetry and the environment of supported transition metal ion catalysts<sup>52-54</sup>. The UV-vis DR spectra of chromium modified ceria systems and their sulphated analogues are presented in Figure 3.15.

From Figure 3.15, it is observed that only a single band is present at 300 nm in the case of pure ceria, sulphated ceria and chromium doped sulphated ceria systems. For chromium doped simple systems, a new band around 230 nm is also observed. Here also the surface modification by sulphate anions does not result in strong changes in the UV-vis spectrum, which is characterised by the bands quite similar to that of the unmodified sample.

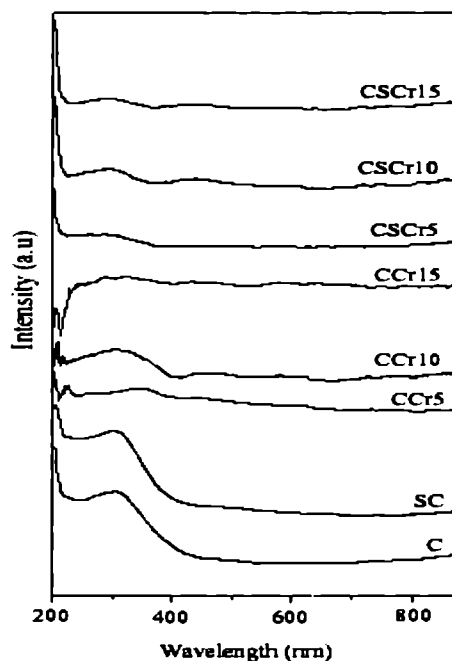


Figure 3.15

Diffuse reflectance spectra of chromium incorporated ceria systems

Just as discussed in the case of tungsten and molybdenum doped systems, the absorption band at 300 nm arises from tetra coordinated  $\text{Ce}^{4+}$  species. More over the absorption band around 230 nm may be from the chromia species and the absence of this band for sulphated samples may due to the broadening of the band corresponding to ceria species.

### **3.3 Surface acidity measurements**

#### **I. Temperature Programmed Desorption of Ammonia (TPD-NH<sub>3</sub>)**

The TPD of ammonia was used to characterise the acid site distribution and furthermore to obtain the quantitative amounts of acid sites in the specified temperature range<sup>55</sup>. Ammonia is an excellent probe molecule as it allows the determination of both the protonic and cationic acid centers. In this method, the interaction of acid sites and basic probe molecule (ammonia) is studied to determine the amount and strengths of acid sites<sup>56</sup>. The acid site distribution pattern can be classified into weak (desorption at 100-200 °C) medium (201-400 °C) and strong (401-600 °C) acid sites. The amount of ammonia desorbed at 100 °C may contain some amount of physisorbed ammonia too.

#### **a) Tungsten incorporated systems**

Table 3.10 gives the distribution of acid sites of pure ceria, tungsten incorporated ceria systems and their sulphated counterparts. Total acidity is also shown as the sum of amount of ammonia desorbed from the entire temperature region.

Table 3.10 reveals that pure cerium oxide possesses lower acidity among the different systems. Considerable enhancement in surface acidity is observed after incorporation of tungsten oxide and sulphate species. Among the simple supported systems CW<sub>10</sub> and CW<sub>15</sub> possesses almost the same amount of acidity. The TPD data of sulphated systems show a considerable enhancement in the weak and medium acid sites compared to simple systems. Among sulphated systems CSW<sub>10</sub> possess maximum acidity. In the case of sulphated systems a regular increase in surface acidity with tungsten loading is not observed.

Table 3.10  
Ammonia TPD studies on tungsten incorporated ceria systems

Catalyst	Amount of ammonia desorbed (mmol/g)			
	Weak (100-200 °C)	Medium (201-400 °C)	Strong (401-600 °C)	Total (100-600 °C)
C	0.17	0.20	0.09	0.46
SC	0.36	0.09	0.03	0.48
CW <sub>5</sub>	0.24	0.15	0.10	0.49
CW <sub>10</sub>	0.22	0.26	0.13	0.61
CW <sub>15</sub>	0.28	0.17	0.17	0.62
CSW <sub>5</sub>	0.29	0.35	0.18	0.82
CSW <sub>10</sub>	0.56	0.36	0.09	1.01
CSW <sub>15</sub>	0.45	0.32	0.15	0.92

The ammonia TPD results indicate that the number of acid sites possessed by pure ceria is less compared with the tungsten incorporated series. The acidity of the sulphated series is considerably higher than the simple supported systems. The pronounced enhancement in the surface acidity upon sulphate modification can be attributed to the increase of the electron accepting properties of the metal cations via the inductive effect of the sulphate anions, which withdraw electron density through the bridging oxygen atom<sup>57</sup>. The electron withdrawing nature of the sulphate group increases the Lewis acidity of the systems<sup>58</sup>.

#### b) Molybdenum incorporated systems

The acid strength distribution of molybdenum incorporated pure and sulphated ceria systems is presented in Table 3.11. The distribution pattern can be classified into weak (desorption at 100-200 °C) medium (201-400 °C) and strong (401-600 °C) acid sites.

Table 3.11  
Ammonia TPD results of molybdenum incorporated ceria systems

Catalyst	Amount of ammonia desorbed (mmol/g)			
	Weak (100-200 °C)	Medium (201-400 °C)	Strong (401-600 °C)	Total (100-600 °C)
C	0.17	0.20	0.09	0.46
SC	0.36	0.09	0.03	0.48
CM <sub>5</sub>	0.51	0.47	0.18	1.16
CM <sub>10</sub>	0.36	0.17	0.15	0.68
CM <sub>15</sub>	0.48	0.21	0.15	0.84
CSM <sub>5</sub>	0.56	0.34	0.21	1.11
CSM <sub>10</sub>	0.34	0.20	0.13	0.67
CSM <sub>15</sub>	0.66	0.41	0.27	1.34

Table 3.11 indicates that pure ceria possess low surface acidity. Upon modification with molybdenum oxide, there is enhancement in the strength and amount of acid sites in the weak, medium and strong regions. Among the simple supported catalysts maximum acidity is possessed by the CM<sub>5</sub> system. The TPD data of the molybdenum doped sulphated systems indicates considerable increase in the surface acid amount than sulphated ceria catalyst. In both cases a regular rise in surface acidity with increase in molybdenum concentration is not observed.

The ammonia desorption studies give an idea about the distribution of acid sites in three temperature ranges; 100-200 °C (weak), 201-400 °C (medium) and 401-600 °C (strong). The results suggest that the surface acid amount of pure ceria is modified to a great extent by the incorporation of molybdenum oxide. Tanabe et al. proposed a mechanism for the generation of acid sites by mixing two oxides<sup>59-60</sup>. They suggest that the acidity generation is caused by an excess of positive charge in a model structure of a binary oxide related to the coordination number of a positive element and a negative element.

### c) Chromium incorporated systems

Table 3.12 represents the acid strength distribution of the simple as well as chromium doped ceria systems.

Table 3.12

Ammonia TPD results of chromium incorporated ceria systems

Catalyst	Amount of ammonia desorbed (mmol/g)			
	Weak (100-200 °C)	Medium (201-400 °C)	Strong (401-600 °C)	Total (100-600 °C)
C	0.17	0.20	0.09	0.46
SC	0.36	0.09	0.03	0.48
CCr <sub>5</sub>	0.46	0.18	0.15	0.79
CCr <sub>10</sub>	0.29	0.17	0.14	0.60
CCr <sub>15</sub>	0.29	0.18	0.15	0.62
CSCr <sub>5</sub>	0.33	0.18	0.15	0.66
CSCr <sub>10</sub>	0.33	0.22	0.15	0.70
CSCr <sub>15</sub>	0.45	0.29	0.23	0.97

The results presented in Table 3.12 describe the distribution of acidity in the three temperature regions namely weak acid sites (100-200 °C), medium acid sites (201-400 °C) and strong acid sites (401-600 °C). Here also pure cerium oxide exhibits lowest surface acidity among the different systems. Considerable enhancement of both strong and weak acid sites is observed after chromium incorporation. Among chromium oxide doped simple systems the total acidity decreases with increase in the concentration of chromium from 5 to 10 wt%. In the case of sulphated series a regular rise in surface acidity is observed with chromium addition. Sohn et al. reported that in the case of chromium oxide supported on zirconia, the surface acidity of the catalytic systems increases abruptly upon the addition of 1 wt% chromium into ZrO<sub>2</sub>,

and then the acidity increase gently with increasing chromium oxide content. According to them the combination of  $ZrO_2$  and  $CrO_x$  probably generates stronger acid sites and more acidity as compared with the separate components<sup>61</sup>. The TPD data of the chromium oxide doped ceria systems points to an increase of strong acid sites and also the surface acidity than the simple system.

## II. Perylene Adsorption Studies

Adsorption studies using perylene as electron donor gives information regarding the Lewis acidity in presence of Brønsted acidity<sup>62-63</sup>. The technique is based on the ability of the catalyst surface site to accept a single electron from an electron donor like perylene to form a charge transfer complexes. The perylene adsorption was done at room temperature from a solution in benzene. Perylene after electron donation gets adsorbed on the catalyst surface as radical cation. The limiting amount of perylene adsorbed, which gives a measure of the Lewis acidity or the electron accepting capacity, was obtained from the Langmuir plot.

### a) Tungsten incorporated systems

The limiting amounts of perylene adsorbed obtained from the langmuir plots for tungsten modified ceria systems are shown in Figure 3.16.

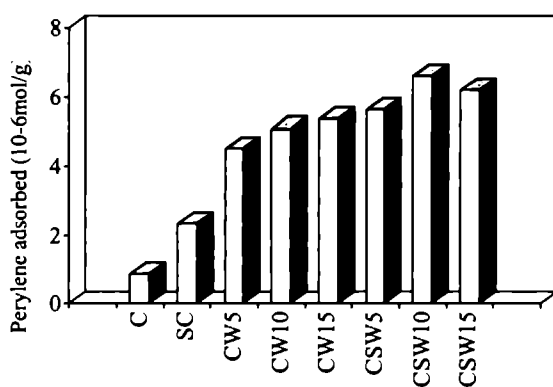


Figure 3.16

Variation in Lewis acidity of tungsten doped ceria systems from perylene adsorption studies.

From Figure 3.16, it is observed that the limiting amount of perylene adsorbed, which gives a measure of the Lewis acidity or the electron accepting capacity, is higher for the tungsten incorporated systems than simple systems. The limiting amount of perylene shows a steady increase with successive addition of tungsten species. In the case of sulphated systems also similar trend is observed, except for the CSW<sub>15</sub> system.

The lower value of limiting amount of perylene in the case of pure ceria indicates comparatively lower electron accepting capacity and hence a lower Lewis acidity compared to the supported systems. Incorporation of tungsten ions influences the acid strength via electronic interactions as evident from the higher values for the limiting amount in the case of tungsten doped systems. In the case of sulphated systems, the Lewis acidity enhancement can be ascribed to the increase in the electron acceptor properties of the cerium cation via the inductive effect of the sulphate anions, which withdraw electron density from the cerium cation through the bridging oxygen atom. This type of enhancement in Lewis acidity upon modification was observed in the case of zirconia catalysts modified with iron as well as sulphate ions<sup>64</sup>. Martin et al. investigated the structure and properties of tungstates formed in W-MgO systems with different tungsten loading and observed that incorporation of tungsten to MgO increases surface acidity and develops Lewis acid sites, the strength of which increases as the W content increases<sup>6</sup>.

#### **b) Molybdenum incorporated systems**

Figure 3.17 represents the results of perylene adsorption studies over molybdenum incorporated ceria and sulphated ceria systems.

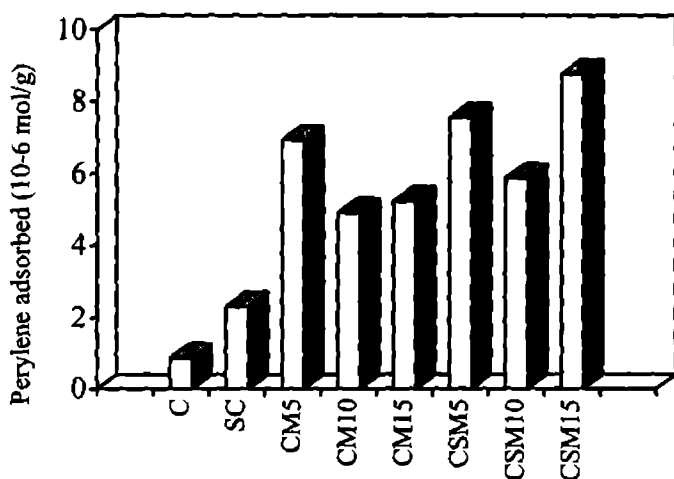


Figure 3.17

Variation in Lewis acidity of molybdenum doped ceria systems from perylene adsorption studies

The results presented in the Figure 3.17 suggest that the addition of molybdenum substantially improves the Lewis acidity. Among the molybdenum doped systems a decreasing trend in Lewis acidity is observed with increase in the concentration of molybdenum from 5 to 10 wt%, and thereafter increases with molybdena concentration. Similar trend is seen in the case of sulphated series. Here also the sulphated samples posses higher Lewis acidity than the simple supported systems.

### c) Chromium incorporated systems

The results of the perylene adsorption studies on different chromium doped ceria systems are presented in Figure 3.18.

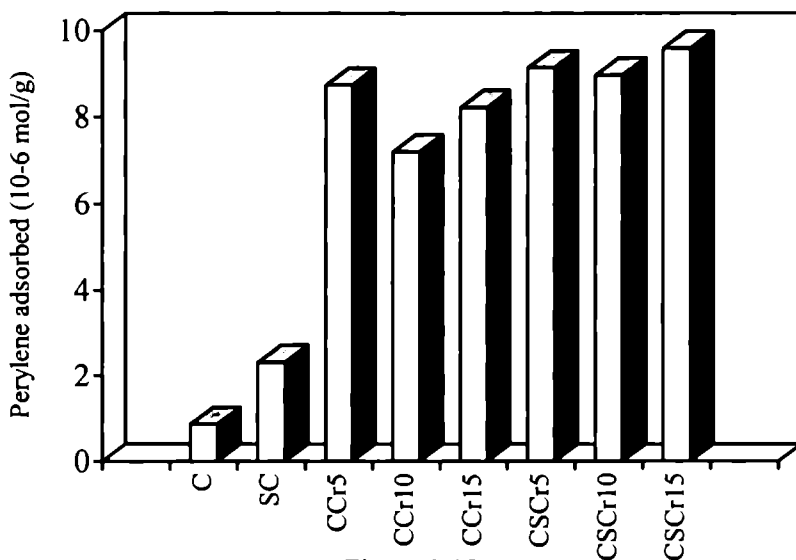


Figure 3.18

Variation in Lewis acidity of chromium doped ceria systems from perylene adsorption studies

As evident from Figure 3.18, the limiting amount of perylene adsorbed is very low in the case of pure cerium oxide. The introduction of chromium as well as sulphate species significantly changes the adsorption properties. In the case of chromium incorporated simple systems, an increase in the percentage of chromium from 5 to 10 wt% results in a decrease of Lewis acidity. However there is a small increase in Lewis acidity for CCr<sub>15</sub> system. Similar trend is seen in the case of sulphated series. The sulphated analogues exhibited higher perylene adsorption capacity than the simple chromium incorporated systems. Here also the enhancement of Lewis acidity on sulphation can be attributed to the increase of electron accepting properties of the surface metal cations by the sulphate anions<sup>65</sup>.

### III. Thermodesorption studies of adsorbed 2, 6-dimethylpyridine

Thermodesorption study of adsorbed basic molecules is a popular method for the determination of acid amount of solid catalyst as it is an easy and reproducible method. 2, 6-dimethylpyridine (2, 6-DMP) is a useful probe molecule for the selective determination of Brönsted acid sites. Though it adsorbs strongly on Brönsted

acid sites, it also forms weak bonds with Lewis acid sites at low temperatures<sup>66</sup>. So an appropriate purging temperature is essential for the selective determination of Brønsted acid sites by 2, 6-DMP. Satsuma et.al reported that the coordinatively adsorbed 2, 6-DMP on Lewis acid sites can be eliminated by employing a purging temperature above 300 °C<sup>67</sup>.

In the present study for the selective determination of the Brønsted acid sites the purging temperature was kept at 300 °C. The number of mmoles of 2, 6-DMP desorbed per gram of the catalyst in the temperature region 301-600 °C is divided into weak (301-400 °C), medium (401-500 °C) and strong (501-600 °C) acid sites. The results obtained for different catalytic systems are discussed in the following section.

#### a) Tungsten incorporated systems

Table 3.13 gives the distribution of Brønsted acid sites of pure ceria, tungsten incorporated ceria systems and its sulphated counterparts determined by TGA of adsorbed 2, 6-DMP.

Table 3.13  
TGA of 2, 6-DMP over tungsten incorporated ceria systems

Catalyst	2, 6-dimethylpyridine desorbed (mmol/g)			
	Weak (301-400 °C)	Medium (401-500 °C)	Strong (501-600 °C)	Total (301-600 °C)
C	0.08	0.05	0.05	0.18
SC	0.05	0.03	0.01	0.09
CW <sub>5</sub>	0.07	0.03	0.02	0.12
CW <sub>10</sub>	0.08	0.01	0.01	0.10
CW <sub>15</sub>	0.08	0.02	0.01	0.11
CSW <sub>5</sub>	0.07	0.03	0.01	0.11
CSW <sub>10</sub>	0.09	0.03	0.03	0.15
CSW <sub>15</sub>	0.08	0.02	0.01	0.11

From Table 3.13 it is clear that the relative amount of Brönsted acid sites is reduced by the incorporation of tungsten as well as sulphate ions. Pure ceria has the highest number of Brönsted acid sites, which amounts to 0.18 mmol /g. Among the simple supported systems, with an increase in tungsten loading the number of Brönsted acid sites first decreases and then increases. All the tungsten incorporated sulphated systems have Brönsted acidity higher than the simple sulphated systems.

### b) Molybdenum incorporated systems

The number of Brönsted acid sites in molybdenum doped ceria systems and its sulphated analogues as obtained from thermodesorption of adsorbed 2, 6-DMP in the temperature range 300-600 °C is given in Table 3.14. The results obtained for pure and sulphated ceria is also given for comparison.

Table 3.14

TGA of 2, 6-DMP over molybdenum incorporated ceria systems

Catalyst	2, 6-dimethylpyridine desorbed (mmol/g)			
	Weak (301-400 °C)	Medium (401-500 °C)	Strong (501-600 °C)	Total (301-600 °C)
C	0.08	0.05	0.05	0.18
SC	0.05	0.03	0.01	0.09
CM <sub>5</sub>	0.06	0.01	0.01	0.08
CM <sub>10</sub>	0.08	0.01	0.01	0.10
CM <sub>15</sub>	0.05	0.01	0.02	0.08
CSM <sub>5</sub>	0.08	0.05	0.01	0.14
CSM <sub>10</sub>	0.08	0.08	0.03	0.18
CSM <sub>15</sub>	0.06	0.09	0.03	0.19

The results clearly show that incorporation of molybdenum oxide reduces the Brönsted acidity of pure ceria. Among the simple supported systems,  $CM_{10}$  shows maximum Brönsted acidity. In the case of sulphated systems,  $CSM_{10}$  and  $CSM_{15}$  possess Brönsted acidity comparable to pure ceria.

### c) Chromium incorporated systems

The results obtained for the thermodesorption analysis of 2, 6-DMP in the case of chromium incorporated systems are presented in Table 3.15.

Table 3.15  
TGA of 2, 6-DMP over chromium incorporated ceria system

Catalyst	2, 6-dimethylpyridine desorbed (mmol/g)			
	Weak (301-400 °C)	Medium (401-500 °C)	Strong (501-600 °C)	Total (301-600 °C)
C	0.08	0.05	0.05	0.18
SC	0.05	0.03	0.01	0.09
CCr <sub>5</sub>	0.07	0.01	0.01	0.09
CCr <sub>10</sub>	0.07	0.01	0.01	0.09
CCr <sub>15</sub>	0.07	0.03	0.02	0.12
CSCr <sub>5</sub>	0.08	0.03	0.01	0.12
CSCr <sub>10</sub>	0.07	0.04	0.01	0.12
CSCr <sub>15</sub>	0.06	0.02	0.01	0.09

It is evident from the Table 3.15 that Brönsted acidity of pure ceria is reduced upon doping with chromium oxide and sulphate ions. The amount of the Brönsted acidity is the same for the systems  $CCr_5$  and  $CCr_{10}$ . Similar is the case with their sulphated analogues also.

### 3.4. Vapour - phase cumene cracking reaction

Model reactions constitute an efficient means for the measurement surface acidity of solids especially in terms of the nature, strength and density of the acid sites. Cumene cracking reaction is a test reaction for the simultaneous determination of Brönsted and Lewis acid sites. In vapour phase cumene cracking reaction,  $\alpha$ -methyl styrene and benzene were obtained as the major products with small amounts of ethylbenzene, styrene and toluene. Here the cracking products such as benzene, toluene, styrene and ethylbenzene are considered together as dealkylated products.

### 3.5 Effect of reaction variables

The reaction conditions are optimised in terms of reaction temperature, flow rate and the amount of the catalyst; the results are presented in the following section. All the reactions are performed over CSW<sub>5</sub> catalyst.

#### I. Effect of Temperature

Table 3.16 demonstrates the effect of temperature on cumene cracking reaction. The results indicate that there is enhancement in catalytic activity with temperature. Selectivity to  $\alpha$ -methyl styrene decreased with temperature with a simultaneous increase in the selectivity of dealkylated products.

Table 3.16

Effect of temperature on cumene cracking reaction

Temperature (°C)	Conversion (%)	Selectivity (%)		Lewis/ Brönsted
		$\alpha$ -methyl styrene	Dealkylation products	
300	1.4	97.0	3.0	32.3
350	5.2	94.2	5.8	16.2
400	19.6	93.1	9.2	10.1
450	24.2	90.5	9.5	9.5
500	26.9	79.7	20.2	4.0

Catalyst- 0.5 g CSW<sub>5</sub>, flow rate-4 mL/h, time on stream-2 h.

## II. Effect of flow rate

The influence of flow rate on catalytic activity as well as selectivity pattern is illustrated in Table 3.17. Increase in flow rate result in a decrease in conversion. Lower the flow rate, higher will be the residing time of the reactants on the catalyst surface, ultimately resulting in an enhancement in catalytic activity. Selectivity to  $\alpha$ -methyl styrene increased with decrease in contact time.

Table 3.17

Effect of flow rate on cumene cracking reaction

Flow rate ( mL / h )	Conversion (%)	Selectivity (%)		
		$\alpha$ -methyl styrene	Dealkylation products	Lewis/ Brönsted
3	20.5	87.9	12.1	7.3
4	19.6	93.1	9.2	10.1
5	9.6	94.9	5.1	18.6
6	8.4	95.9	4.1	23.4

Catalyst- 0.5 g CSW<sub>3</sub>, temperature -400 °C, time on stream-2 h.

## III. Effect of catalyst amount

Table 3.18 shows the influence of catalyst concentration on cumene conversion and product selectivity. The conversion of cumene was found to increase with catalyst concentration. The selectivity to  $\alpha$ -methyl styrene shows a drastic decrease from 95.9 to 77.1%, with an increase of catalyst concentration from 0.25 to 1 g.

Table 3.18

Effect of catalyst concentration

Amount of catalyst (g)	Conversion (%)	Selectivity (%)		
		$\alpha$ -methyl styrene	Dealkylation products	Lewis/ Brönsted
0.25	12.7	95.9	4.1	23.4
0.5	19.6	93.1	9.2	10.1
0.75	20.8	89.8	10.2	8.8
1	21.9	77.1	22.9	3.4

Catalyst-CSW<sub>3</sub>, temperature -400 °C, time on stream-2 h, flow rate-4 mL/h.

#### IV. Effect of time on stream

The lowering of activity with time on stream is a common problem associated with heterogeneous catalysts. To study this, reaction was carried out continuously for 8 hrs over the catalyst CW<sub>5</sub> and the product analysis was done at regular intervals of 60 minutes. The results obtained are presented in Table 3.19. Catalytic activity was found to decline with reaction time. After 4 hrs of reaction there is no noticeable change in  $\alpha$ -methyl styrene selectivity. The decrease of catalytic activity with reaction time is mainly due to coke formation. There is enhancement in Lewis/Brönsted ratio with reaction time.

Table 3.19

Effect of time on stream on cumene cracking reaction

Time on stream (h)	Conversion (%)	Selectivity (%)		Lewis/Brönsted
		$\alpha$ -methyl styrene	Dealkylation products	
1	8.6	78.3	21.7	3.6
2	9.4	93.1	9.2	10.1
3	7.5	93.9	6.1	15.4
4	6.9	95.6	4.3	22.2
5	6.2	97.3	2.7	36.0
6	5.8	97.4	2.6	37.5
7	5.1	97.6	2.4	40.7
8	4.6	97.9	2.1	46.6

Catalyst-0.5 g CW<sub>5</sub>, temperature -400 °C, flow rate-4 mL/h.

#### 3.6 Catalytic activity of various systems

The catalytic activity of different metal incorporated systems along with the selectivity to different products is given in Table 3.20 & Table 3.21.

Table 3.20

Cumene cracking over tungsten and molybdenum modified ceria systems

Catalyst	Conversion (%)	Selectivity (%)		Lewis/ Brönsted
		$\alpha$ -methyl styrene	Dealkyl- ation products	
C	8.4	70.9	29.1	2.4
SC	8.9	75.6	24.4	3.1
CW <sub>5</sub>	9.4	80.5	19.5	4.1
CW <sub>10</sub>	10.3	89.1	10.9	8.2
CW <sub>15</sub>	11.7	90.6	9.4	9.6
CSW <sub>5</sub>	19.6	91.7	8.4	10.9
CSW <sub>10</sub>	21.3	93.1	6.9	13.5
CSW <sub>15</sub>	20.2	93.6	6.4	14.6
CM <sub>5</sub>	11.9	95.2	4.8	19.8
CM <sub>10</sub>	9.8	92.1	7.9	11.7
CM <sub>15</sub>	10.3	93.3	6.7	13.9
CSM <sub>5</sub>	11.2	96.8	3.2	30.3
CSM <sub>10</sub>	9.1	94.1	5.9	15.9
CSM <sub>15</sub>	13.9	97.2	2.8	34.7

Catalyst-0.5 g, temperature -400 °C, flow rate-4 mL/h, time on stream- 2 h.

Table 3.21  
Cumene cracking over chromium modified ceria systems

Catalyst	Conversion (%)	Selectivity (%)		Lewis/ Brönsted
		$\alpha$ -methyl styrene	Dealkyl- ation products	
C	8.4	70.9	29.1	2.4
SC	8.9	75.6	24.4	3.1
CCr <sub>5</sub>	14.8	93.2	6.8	13.7
CCr <sub>10</sub>	10.9	90.8	9.2	9.9
CCr <sub>15</sub>	12.6	92.9	7.1	13.1
CSCr <sub>5</sub>	13.7	94.5	5.5	17.2
CSCr <sub>10</sub>	14.1	93.8	6.2	15.1
CSCr <sub>15</sub>	15.9	95.4	4.6	20.7

Catalyst-0.5 g, temperature -400 °C, flow rate-4 mL/h, time on stream- 2 h

From Tables 3.20 and 3.12, it can be inferred that dehydrogenation of cumene to  $\alpha$ -methyl styrene is the predominant reaction on metal doped ceria and sulphated analogues. The selectivity to  $\alpha$ -methyl styrene is lower for the simple systems. In the case of tungsten loaded samples selectivity to  $\alpha$ -methyl styrene was found to increase with tungsten loading. Among molybdenum loaded systems, selectivity to  $\alpha$ -methyl styrene decreased as the molybdenum loading is changed from 5 to 10 wt%, and increased for the CM<sub>15</sub> system and also maximum selectivity is shown by CSM<sub>15</sub> among sulphated series. The chromium incorporated samples show a different trend towards  $\alpha$ -methyl styrene selectivity. In that case CCr<sub>5</sub> and CSCr<sub>15</sub> shows maximum selectivity among simple and sulphated systems respectively.

The main reactions in cumene cracking are dealkylation and dehydrogenation. Dealkylation reaction, which results in the formation of products such as benzene, toluene, ethylbenzene, is generally attributed to the action of Brönsted acid

sites where as dehydrogenation of cumene giving  $\alpha$ -methyl styrene is due to the Lewis acid sites<sup>68-69</sup>. Boorman et al. investigated the catalytic activity of cobalt, molybdenum and fluoride modified  $\gamma$ -alumina toward the cumene cracking reaction and concluded that the catalytic activity of these systems can be correlated to their surface acidity<sup>70</sup>.

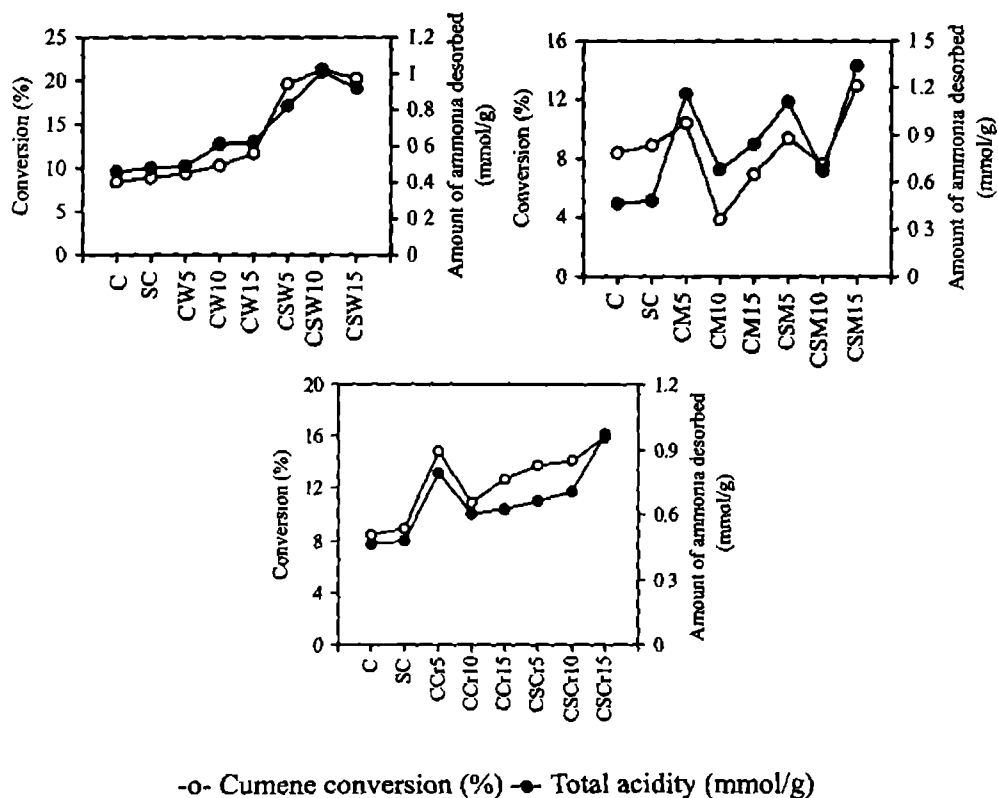


Figure 3.19

Correlation between cumene conversion and total acidity as obtained from TPD of ammonia

Figure 3.19 gives the dependence of the cracking activity upon the surface acidity obtained from TPD of ammonia. One-to-one correlation between the Lewis acidity of the catalytic systems as obtained from perylene adsorption studies and the selectivity towards the formation of  $\alpha$ -methyl styrene is presented in Figure 3.20.

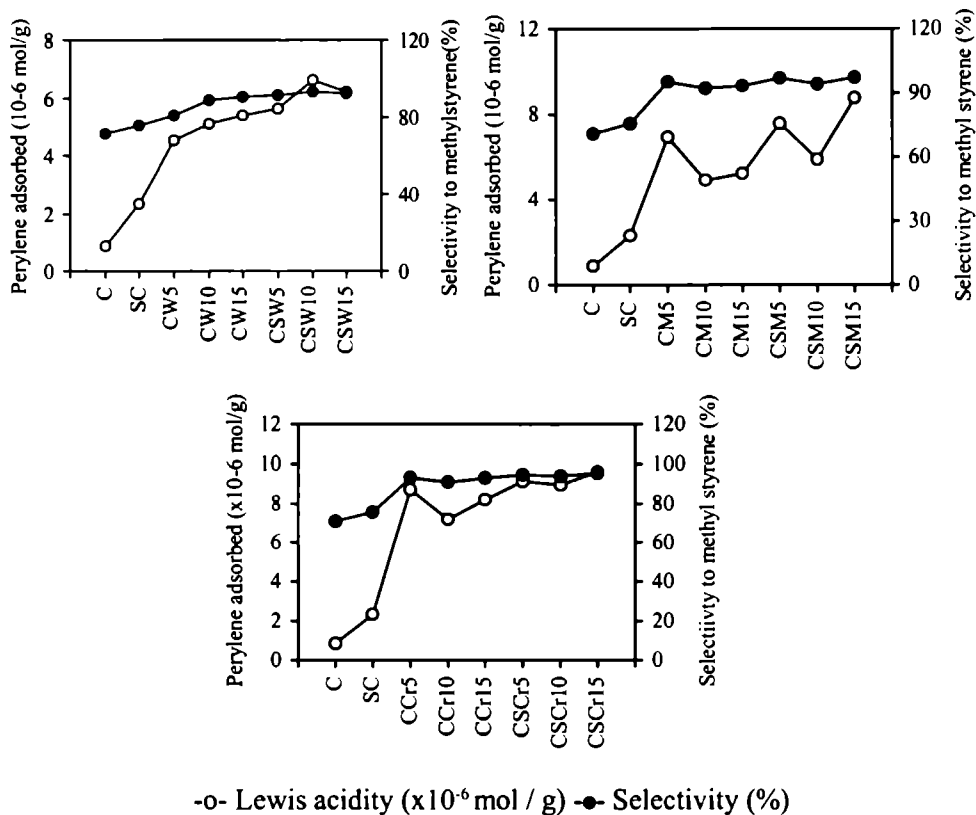


Figure 3.20

One to one comparison of Lewis acidity and  $\alpha$ -methyl styrene selectivity

In the present case the cumene conversion was found to depend on the surface acidity obtained from TPD of ammonia. Modified systems are found to be more active than the simple systems, in accordance with their surface acidity. And also the sulphated systems show higher activity than simple supported systems in most cases. Good correlation is observed between the Lewis acidity and  $\alpha$ -methyl styrene selectivity, supporting the fact that Lewis acid sites are responsible for the dehydrogenation reaction.

### 3.7 Vapour phase cyclohexanol decomposition reaction

In Alcohol decomposition reaction the dehydrogenation reaction usually competes with the dehydration of the starting compound to an olefin, which is produced in a variable proportion depending on the particular catalyst and reaction conditions. The amphoteric nature of the alcohol permits its interaction with both acidic and basic centers. During the reaction the dehydrogenation reaction leading to the formation of cyclohexanone was assumed to takes place with the intervention of both acidic and basic sites whereas, dehydration reaction to cyclohexene takes place with the participation of acidic sites<sup>71-72</sup>. Cyclohexanol decomposition reaction was carried out in vapour-phase at 300 °C for 2 hrs with a flow rate of 4 mL/h. The reaction conditions such as reaction temperature, flow rate and time on stream were investigated in detail. The products detected were cyclohexene, cyclohexanone, phenol, benzene, methyl cyclopentene and cyclohexane. The selectivity was calculated as ‘-ene’ selectivity ( $C=C$ ) and ‘-one’ selectivity ( $C=O$ ). The products such as benzene, methyl cyclopentene and cyclohexane were included in the ‘-ene’ selectivity, and phenol together with cyclohexanone were taken as -one- selectivity since these were formed by the further transformation of cyclohexene and cyclohexanone respectively.

### 3.8 Effect of reaction variables

#### I. Effect of temperature and time on stream

The effect of temperature on the conversion of cyclohexanol and the selectivity to different products is shown in Table 3.22.

Table 3.22  
Effect of temperature in the cyclohexanol decomposition reaction

Temperature (°C)	Conversion (%)	Selectivity (%)	
		-ene-	-one-
250	12.9	82.3	17.7
300	76.8	74.1	25.9
350	94.7	69.9	30.1
400	96.3	57.6	42.4

Catalyst-0.5 g CM<sub>10</sub>, flowrate-3 mL/h, time on stream-2 h.

An increase of temperature from 250 to 350 °C results in an appreciable increase in the conversion of cyclohexanol. When the temperature is increased further to 400 °C, there is not much change in the percentage conversion. At higher temperatures (350 and 400 °C) the selectivity to cyclohexene is lower than at 300 °C. With increase in temperature the cyclohexanone selectivity was found to increase. According to Jebarathinam et al. in the case of copper containing spinel catalysts the conversion of cyclohexanol and the formation of cyclohexanone were increased with increase in temperature from 250 to 370 °C<sup>73</sup>.

Figure 3.21 illustrates the time on stream stability of the catalyst CM<sub>10</sub> at a reaction temperature of 300 °C. After a period of 4 hrs, considerable deactivation was observed, which decreases the conversion of cyclohexanol to a great extent. The decrease in conversion suggests that the catalyst is deactivated as a result of the thermal decomposition of cyclohexanol and cyclohexanone to carbonaceous compounds, or due to the presence of surface oligomers resulting from poly condensation of cyclohexanone as suggested by Lin and Wang<sup>74</sup>. The cyclohexene produced in the reaction also ascribed to have a high capacity for deactivating the catalysts on account of the ease with which they can give rise to surface carbonaceous compounds<sup>75</sup>.

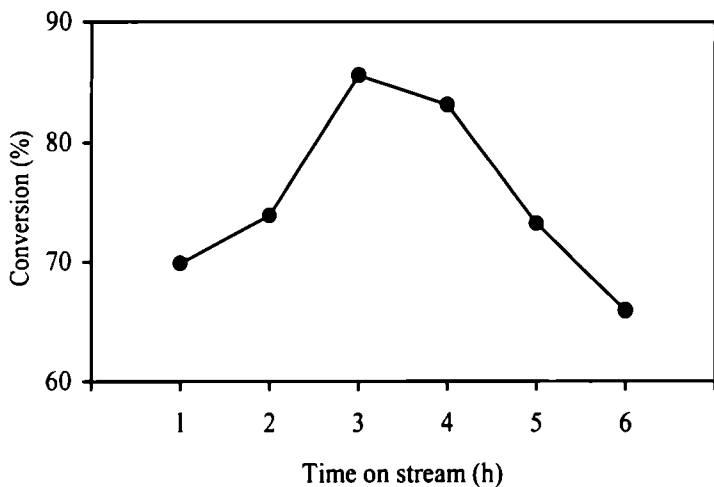


Figure 3.21

Effect of reaction time on cyclohexanol decomposition reaction

Catalyst-0.5 g  $CM_{10}$ , flowrate-4 mL/h, temperature - 300 °C

## II. Effect of flow rate

The effect of flow rate on the cyclohexanol conversion and selectivity to different products is presented in Table 3.23. Here all the reactions are done at a reaction temperature of 300 °C on  $CM_{10}$  catalyst.

Table 3.23

Effect of flow rate on cyclohexanol decomposition reaction

Flow rate (mL/h)	Conversion (%)	Selectivity (%)	
		-ene-	-one-
2	80.7	73.3	26.7
3	76.8	74.1	25.9
4	73.9	76.2	23.8
5	67.4	86.7	13.3

Temperature-300 °C, time on stream-2 h, catalyst-0.5 g  $CM_{10}$

As the flow rate is increased from 2 to 5 mL/h, the percentage conversion decreases from 80.7 to 67.4. Cyclohexene selectivity shows a gradual increase with flow rate upto 4 mL/h. There is a rapid increase in cyclohexene selectivity upon changing the flow rate from 4 to 5 mL/h.

### 3.9 Catalytic activity of different systems

Table 3.24 gives the conversion percentage and product distribution obtained in the vapour phase cyclohexanol decomposition reaction for different transition metal modified ceria systems.

Table 3.24  
Cyclohexanol decomposition reaction over tungsten, molybdenum  
and chromium oxide modified ceria systems

Systems	Conver- sion (%)	Selectivity (%)		Systems	Conver- sion (%)	Selectivity (%)	
		-ene-	-one-			-ene-	-one-
C	93.4	62.3	37.7	CM <sub>15</sub>	84.2	80.7	19.3
SC	98.5	68.8	31.2	CSM <sub>5</sub>	66.1	83.2	16.8
CW <sub>5</sub>	70.7	63.7	36.3	CSM <sub>10</sub>	74.5	78.0	22.0
CW <sub>10</sub>	85.4	79.1	20.9	CSM <sub>15</sub>	93.1	88.1	11.9
CW <sub>15</sub>	54.9	77.8	22.2	CCr <sub>5</sub>	60.9	86.2	13.8
CSW <sub>5</sub>	76.6	82.4	17.5	CCr <sub>10</sub>	64.3	76.2	27.8
CSW <sub>10</sub>	59.2	90.5	9.5	CCr <sub>15</sub>	89.5	72.5	27.5
CSW <sub>15</sub>	94.5	85.2	14.8	CSCr <sub>5</sub>	56.5	77.4	22.6
CM <sub>5</sub>	63.2	86.9	13.1	CSCr <sub>10</sub>	44.4	82.3	17.7
CM <sub>10</sub>	73.9	76.0	24.0	CSCr <sub>15</sub>	95.6	89.9	10.1

Temperature-300 °C, time on stream-2 h, catalyst-0.5 g, flow rate – 4 mL/h

The conversion and selectivity for various products presented in Table 3.24 indicates that dehydration of cyclohexanol is the predominant reaction. All the modified systems show higher selectivity to cyclohexene compared to simple systems. In the case of tungsten doped systems, -ene- selectivity was found to increase with tungsten loading from 5 to 10 wt% and a decrease was observed for CW<sub>15</sub> system. Similar trend is seen with regard to sulphated systems. Compared to tungsten oxide doped systems, reverse trend is seen in the case of molybdenum incorporated systems. Here CM<sub>10</sub> and CSM<sub>10</sub> gives the lowest -ene- selectivity among the series. Among chromium doped simple systems, the -ene- selectivity was found to decrease with chromium loading, whereas a simultaneous increase in -ene-selectivity with chromium loading is observed for the sulphated systems.

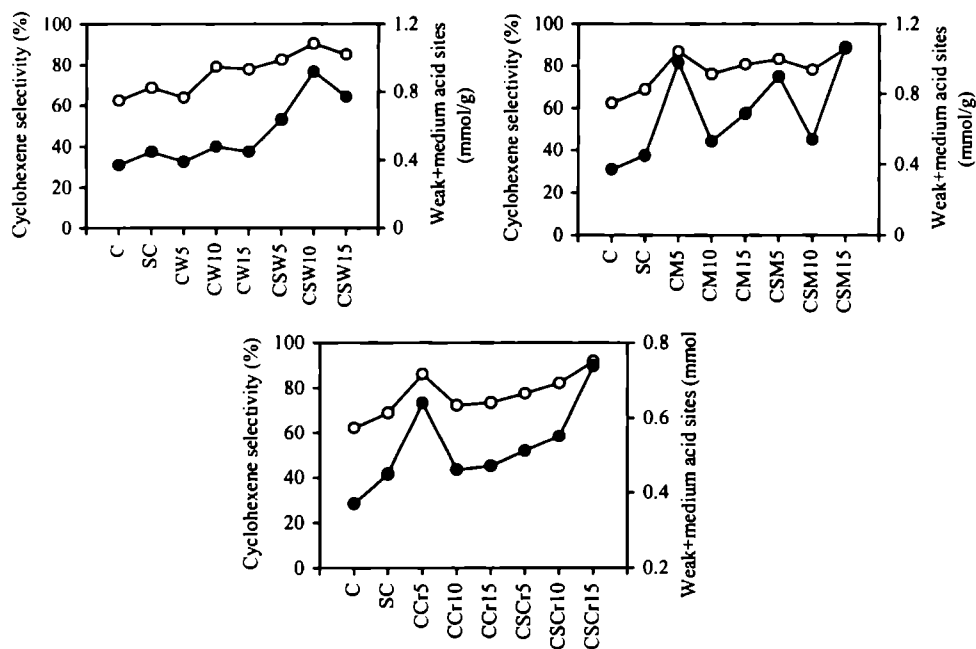


Figure 3.22

Correlation between cyclohexene selectivity and weak+medium acid sites

Figure 3.22 represents the correlation between the amount of weak and medium acid sites and the *-ene-* selectivity. In the case of cyclohexanol decomposition reaction the dehydration activity resulting in the formation of cyclohexene is found to depend on the amount of weak and medium acid sites present in the catalysts. According to Murthy et al. the high catalytic activity of silicoaluminophosphates (SAPOs) in the formation of cyclohexene is probably due to the weak and medium acidic centers<sup>76</sup>. The results presented in the Figure 3.22 supports the fact that the weak and medium acid sites are responsible for the formation of cyclohexene.

### 3.10 Conclusions

The general conclusions drawn from the different surface characterisation techniques as well as surface acidity measurements of the supported ceria catalysts are given below.

- \* The surface area and pore volumes of the modified systems are lower than the simple systems. The reduction of surface area upon modification suggest that the incorporated metal oxides are occupying the surface vacant sites of the support. SEM micrographs of the catalytic systems show agglomeration of the particles upon modification. This agglomeration of the particles together with the plugging of the pores is responsible for the decrease of surface area.
- \* XRD patterns of the catalysts show the presence of fluorite structure of ceria, and no new characteristic phases are observed with the incorporation of transition metal oxides. This points to the fact that the incorporated metal oxides are highly dispersed on the surface of the catalyst.
- \* The TG-DTG analysis of the pure and modified samples reveal high thermal stability of the catalyst system even after 700 °C, while the sulphated samples are stable upto 650 °C.
- \* The characteristic peaks of pure ceria, incorporated metal oxides and sulphate groups are observed in the FTIR spectra of the catalytic systems. Presence of

tetracoordinated  $Ce^{4+}$  species is evident from the UV-vis diffuse reflectance spectroscopy.

- \* The acidity measurements by the three independent techniques namely ammonia TPD, perylene adsorption studies and catalytic test reactions suggest an enhancement in surface acidity especially the Lewis acidity upon incorporation of transition metal oxides.

## REFERENCES

1. L. Dong, Y. Hu, F. Xu, D. Lu, B. Xu, Z. Hu and Y. Chen, *J. Phys. Chem. B.*, 104 (2000) 78.
2. M. Hirano, Y. Fukuda, H. Iwata, Y. Hotta and M. Inagaki, *J. Am. Ceramic Soc.*, 83 (2000).
3. Y. Chen and L. F. Zheng, *Catal. Lett.*, 12 (1992) 51.
4. R. B. Watson and U. S. Ozkan, *J. Catal.*, 208 (2002) 124.
5. H. Idriss, C. Diagne, J. P. Hindermann, A. Kiennemann and M. A. Barteau, *J. Catal.*, 155 (1995) 219.
6. C. Martin, P. Malet, V. Rives and G. Solana, *J. Catal.*, 169 (1997) 516.
7. C. Martin, G. Solana and V. Rives, *Catal. Lett.*, 49 (1997) 235.
8. R. Thomas, E. M. Van Obers, V. H. J. De Beer, J. Medema and J. A. Moulijn, *J. Catal.*, 76 (1982) 241.
9. D. C. Vermaire and P. C. Van Berge, *J. Catal.*, 116 (1989) 309.
10. S. S. Chan, I. E. Wachs and L. L. Murrell, *J. Catal.*, 90 (1984) 150.
11. B. Scheffer, J. J. Heijeinga and J. A. Moulijn, *J. Phys. Chem.*, 91 (1987) 4752.
12. L. Salvati, L. E. Makovsky, J. M. Stencel, F. R. Brown and D. M. Hercules, *J. Phys. Chem.*, 85 (1981) 3700.
13. H. Lipson, H. Steeple: Interpretation of X-ray powder Diffraction Patterns, Macmillan, London, (1970) 261.
14. K. Chen, S. Xie, E. Iglesia and A. T. Bell, *J. Catal.*, 189 (2000) 421.

15. B. M. Reddy and A. Khan, *J. Phys. Chem. B.*, 106 (2002) 10964.
16. D. Terribile, A. Trovarelli, J. Llorca, C. de Leitenburg and G. Dolcetti, *J. Catal.*, 178 (1998) 299.
17. A. Sakthivel, N. Saritha and P. Selvam, *Catal. Lett.*, 72 (2001) 225.
18. N. C. Wu, E.W. Shi, Y. Q. Zheng and W. J. Li, *J. Am. Ceram. Soc.*, 85 (2002) 2462.
19. M. Bensitel, O. Saur, J. C. Lavalley and B. A. Morrow, *Mater. Chem. Phys.*, 19 (1988) 147.
20. H. Knözinger, In Proceeding of the 9<sup>th</sup> International Congress in Catalysis, M. J. Philips, M. Terman, Eds.; Chemical Institute of Canada: Ottawa, 1988; Vol.5, p 20.
21. J. Leyrer, B. Vielhaber, M. I. Zaki, Z. Shuxian, J. Weitkamp and H. Knözinger, *Mater. Chem. Phys.*, 13 (1985) 301.
22. F. Prinetto, G. Cerrato, G. Ghiotti, A. Chioino, M. C. Campa, D. Gazzoli and V. Indovina, *J. Phys. Chem.*, 99 (1995) 5556.
23. H. P. Bochnm and H. Knözinger, "Catalysis", J. R. Anderson and M. Boudart, Eds., vol.4, Springer, Berlin, (1983) Chapter 2.
24. K. Nakamoto, *Infrared and Raman Spectra of Inorganic and Co-ordination compounds*, 4<sup>th</sup> Edn., Wiley, New York, 1986.
25. F. Babou, G. Coudrier and J. C. Vedrine, *J. Catal.*, 152 (1995) 341.
26. T. Yamaguchi, *Appl. Catal. A. Gen.*, 61 (1990) 1.
27. X. Song and A. Sayari, *Catal. Rev. Sci. Eng.*, 38 (1996) 329.
28. M. Ponzi, C. Duschatzky, A. Carraseull and E. Ponzi, *Appl. Catal. A. Gen.*, 169 (1998) 373.
29. B. A. Morrow, R. A. Mc Farlane, M. Lion and J.C. Lavalley, *J. Catal.*, 107 (1987) 232.
30. M. bensitel, O. Saur, J. C. Lavalley and B. A. Morrow, *Mater. Chem. Phys.*, 19 (1988) 147.

31. M. Waquif, J. Bachelier, O. Saur and J. C. Lavalley, *J. Mol. Catal.*, 72 (1992) 127.
32. J. R. Sohn and H. J. Jang, *J. Mol. Catal.*, 64 (1991) 349.
33. C. Miao, W. Hua, J. Chen and Z. Gao, *Catal. Lett.*, 37 (1996) 187.
34. F. Babou, G. Coudurier and J. C. Vedrine, *J. Catal.*, 152 (1995).
35. D. Spielbauer, G. A. H. Mekhemer, M. I. Zaki and H. Knözinger, *Catal. Lett.*, 40 (1996) 71.
36. S. C. Laha, P. Mukherjee, S. R. Sainkar and R. Kumar, *J. Catal.*, 207 (2002) 213.
37. Z. Liu and Y. Chen, *J. Catal.*, 177 (1998) 314.
38. F. A. Cotton and G. Wilkinson, in "Advanced Inorganic Chemistry" 4<sup>th</sup> ed. Wiley, New York, 1980.
39. G. Xiong, Z. Feng, J. Li, Q. Yang, P. Ying, Q. Xin and C. Li, *J. Phys. Chem. B.*, 104 (2000) 3581.
40. H. Jeziorowski and H. Knözinger, *Chem. Phys. Lett.*, 51 (1977) 519.
41. J. H. Ashley and P. C. H. Mitchell, *J. Chem. Soc. A.*, (1968) 2821.
42. J. H. Ashley and P. C. H. Mitchell, *J. Chem. Soc. A.*, (1969) 2730.
43. P. C. H. Mitchell and F.J. Trifiro, *J. Chem. Soc. A.*, (1970) 3183.
44. G. N. Asmolov and O. V. Krylov, *Kinet. Katal.*, 11 (1970) 1028.
45. N. Giordano, J. C. J. Bart, A. Vaghi, A. Castellan and G. Martinotti, *J. Catal.*, 36 (1975) 81.
46. Y. Iwasawa and S. Gasawara, *J. Chem. Soc. Faraday Trans.*, 75 (1979) 1465.
47. P. Gajardo, P. Grange and B. Delmon, *J. Phys. Chem.*, 83 (1979) 1771.
48. L. Wang and W. K. Hall, *J. Catal.*, 77 (1982) 232.
49. Y. Iwasawa and M. J. Yamagushi, *J. Catal.*, 82 (1983) 373.
50. M. Fournier, C. Louis, M. Che, P. Chaquin and D. Masure, *J. Catal.*, 119 (1989) 400.
51. C. C. Williams, J. G. Ekerdt, J. M. Jehng, F. D. Hardcastle, A. M. Turek and I.

- E. Wachs, *J. Phys. Chem.*, 95 (1991) 8781.
52. J. H. Ashley and P. C. H. Mitchell, *J. Chem. Soc. A.*, (1968) 2821.
53. A. Iannibello, S. Marengo, P. Tittarelli, G. Morelli and A. Zecchina, *J. Chem. Soc. Faraday Trans.*, 80 (1984) 2209.
54. C. Louis, M. Che, and F. B. Verduraz, *J. Chim. Phys.*, 79 (1982) 803.
55. F. Arena, R. Dario and A. Paramaliana, *Appl. Catal. A. Gen.*, 170 (1998) 127.
56. F. Lonyi and J. Valyon, *Microporous and Mesoporous Materials.*, 47 (2001) 293.
57. A. Corma, V. Fornes, M. I. Juan Rajadell and J. M. Lopez Nieto, *Appl. Catal. A. Gen.*, 116 (1994) 151.
58. A. Corma and B. W. Wojciechowski, *Catal. Rev. Sci. Eng.*, 24 (1982) 1.
59. K. Tanabe, T. Sumiyoshi, K. Shibata, T. Kiyoura and I. Kitagawa, *Bull. Chem. Soc. Jpn.*, 47 (1974) 1064.
60. K. Tanabe, M. Misono, Y. Ono and H. Hattori, *New Solid Acid and Bases* (Kodansa, Tokyo, 1989) ch.3, p.108.
61. J. R. Sohn and S. G. Ryu, *Catal. Lett.*, 74 (2001) 105.
62. J. Kijenski and A. Baiker, *Catal. Today.*, 5 (1989) 1.
63. B. D. Flockarc, J. A. N. Scott and R. C. Pink, *Trans. Faraday Soc.*, 62 (1966) 730.
64. H. Suja, C.S. Deepa, K. S. Rani and S. Sugunan, *Appl. Catal. A. Gen.*, 230 (2002) 233.
65. G. Busca and J. C. Lavalley, *Spectrochim. Acta.*, 42A (1986) 443.
66. P. A. Jacobs and C. F. Heylen, *J. Catal.*, 34 (1974) 267.
67. A. Satsuma, Y. Kamiya, Y. Westi and T. Hattori, *Appl. Catal. A. Gen.*, 195 (2000) 253.
68. J. W. Ward, *J. Catal.*, 9 (1967) 225
69. W. Przystajko, R. Fiedoorow and I. G. Dalla Lana, *Appl. Catal. A. Gen.*, 15 (1985) 265.

70. P. M. Boorman, R. A. Kydd, Z. Sarbak and A. Somogyvari, *J. Catal.*, 100 (1986) 287.
71. M. Ai, *J. Catal.*, 40 (1975) 318.
72. M. Ai, *Bull. Chem Soc. Jpn.*, 50 (1977) 2587.
73. N. J. Jebarathinam and V. Krishnaswami, *Catalysis: Modern Trends.*, (1995).
74. Y. M. Lin and I. Wang, *Appl. Catal. A. Gen.*, 41 (1988) 53.
75. M. A. Aramendia, V. Borau, C. Jimenez, J. M. Marinas and F. J. Romero, *J. Catal.*, 151 (1995) 44.
76. K. V. V. S. B. S. R. Murthy, B. Srinivas and S. J. Kulkarni, *Catalysis: Modern Trends*, N. M. Gupta and D. K. Chakrabarthy (Eds) 1995.

\*\*\*\*\*

### *Acetalization and Deacetalization of Functional Groups*

#### **Abstract**

---

*The acetalization reaction is widely used in organic synthesis to protect the carbonyl group of aldehydes and ketones. In the present chapter, the catalytic efficiency of the modified ceria systems in the liquid-phase acetalization of cyclohexanone using methanol is analysed in depth. The effect of various reaction parameters like reaction temperature, reaction time, cyclohexanone to methanol molar ratio, catalyst concentration etc. are also investigated. The results suggest that the medium plus strong acid sites play a significant role in determining the catalytic activity. The modified systems are also capable of hydrolysing the dimethoxy cyclohexane formed, thereby acting as versatile catalysts in protecting and deprotecting carbonyl groups during organic synthesis.*

---

#### **4.1 Introduction**

Fine chemicals are complex and multifunctional molecules, often characterized by low volatility and limited thermal stability. Their manufacture is generally based on a multi-step synthesis performed in liquid phase, frequently involving protection - deprotection steps. The use of blocking functions in organic synthesis, developed nearly 100 years back, makes more complex the entire synthetic plan since it requires at least two additional steps. At the same time, environmental and economic considerations have created interest, in both academic and industrial research, in designing synthetic procedures that are clean, selective, high yielding, and easy to manipulate. An extensive application of heterogeneous catalysis in synthetic chemistry can help to achieve new selective reactions, to lower the waste production, and, finally, to render more attractive synthetic process from both the environmental and the economic point of view. This is in agreement to some parameters of the "ideal synthesis" recently presented by Wender <sup>1</sup>.

The heterogeneous catalysis that was originally studied and applied in bulk chemistry with particular interest to petrochemical industry is more recently extended to synthetic organic chemistry. It is very important for the production of fine chemicals and pharmaceuticals<sup>2</sup>. Among the first reactions that have been performed under heterogeneous catalysis are the hydrogenations and, in general, the redox processes which are extensively used in synthetic organic chemistry. Acid-base heterogeneous catalysis has been successively developed by exploiting the physicochemical properties of zeolites<sup>3</sup>, clays<sup>4</sup> and metal oxides<sup>5</sup>. These solid catalysts form the basis of some new industrial processes, which have been developed to replace traditional problematic synthetic methods<sup>6</sup>.

The electrophilic nature of the carbonyl group is a dominant feature of its extensive chemistry. One of the major challenges in the many multiuse synthesis is the protection of carbonyl group from nucleophilic attack until its electrophilic properties can be exploited. The protection of aldehydes and ketones has been served by

a relatively small repertoire of protecting groups. Of these, acetals, thioacetals, oxathiolanes, 1,1-diacetates, and nitrogenous derivatives have proven to be the most useful.

### **Acetalization reaction**

The acetalization of aldehydes and ketones are reactions of synthetic interest in organic chemistry. They are found to be highly effective for the synthesis of enantiomerically pure compounds<sup>7-8</sup> that find practical application in the fields of synthetic carbohydrates<sup>9</sup>, steroids<sup>10</sup>, pharmaceuticals and fragrance<sup>11</sup> and polymer chemistry<sup>12</sup>. Various kinds of acids are well known to catalyse these reactions in homogeneous and heterogeneous phases<sup>13</sup>. However, the major problem associated with these reactions is that dimethyl acetal is formed using trimethyl orthoformate instead of the more appropriate methanol. In the typical methanol/HCl system, the strong acidity of the latter often produces by-products<sup>14</sup>.

Transition metal complexes have been used as effective catalysts for acetalization reactions. Gorla and Venanzi observed for the first time the possibility of using cationic, solvento complexes of Rh (III), Pd (II) and Pt (II) as catalysts for the acetalization of a variety of aldehydes and ketones<sup>15</sup>. They identified the basic requirement for achieving high catalytic activity as the presence of a minimum of 2 positive charges on the complex to ensure sufficient Lewis acidity. Cataldo et al. reported the first unambiguous example of the use of noble metals as possible catalysts for this reaction by testing a variety of diphosphine cationic complexes of palladium and platinum<sup>16</sup>.

Recently, solid acid catalysts such as silica gel, alumina<sup>17</sup>, zeolite<sup>18</sup>, resins<sup>19</sup>, clays<sup>20</sup> and hydrous zirconium oxide<sup>21</sup> have been reported to be active for acetalization. The acetalization of carbonyl compounds with methanol was investigated by Uemura et al. in the presence of cation-exchanged montmorillonite ( $M^{n+}$ -Mont;  $M^{n+} = Ce^{3+}$ ,  $Zr^{4+}$ ,  $Fe^{3+}$ ,  $Al^{3+}$ ,  $Zn^{2+}$ ,  $H^+$ , and  $Na^+$ ). Of these,  $Ce^{3+}$ -mont has been identified as an

effective catalyst for substrate selective acetalization.  $\text{Ce}^{3+}$ -mont has the proper acidity and drying ability which drives the equilibrium of the reaction to the acetal side with complete conversion of the carbonyl compounds.  $\text{Ce}^{3+}$  cation acts as a Lewis acid site and activates the carbonyl group by coordination in the order of 1 KJ / mol<sup>20</sup>. In the presence of ethylene glycol, natural kaolinitic clay is a convenient catalyst for the chemoselective protection of a variety of aliphatic, aromatic, heteroaromatic, and  $\alpha$ ,  $\beta$ -unsaturated aldehydes, while ketones failed to undergo deprotection<sup>22</sup>.

Climent et al. compared the catalytic activity of Y and beta zeolites as well as mesoporous and amorphous silica-alumina for the preparation of dimethylacetals of aldehydes using reaction with trimethyl orthoformate<sup>23</sup>. It has been found that with small size aldehydes, zeolites are intrinsically more active than the mesoporous materials. However, when using reactants with molecular size larger than 7 Å, geometric constraints do not allow their diffusion inside the pores, and thus only the external surface area of these materials becomes available to the reactants. In these circumstances, the large pores of MCM-41 make this material more adequate for carrying out the acetalization reactions.

Sulphated metal oxides are also proven to be good catalysts for these types of reaction. Arata et al. reported that mesoporous sulphated metal oxides such as sulphated oxides of  $\text{ZrO}_2$ ,  $\text{TiO}_2$ ,  $\text{Fe}_2\text{O}_3$ ,  $\text{SnO}_2$ ,  $\text{Al}_2\text{O}_3$ ,  $\text{HfO}_2$ , and  $\text{SiO}_2$  can effectively catalyse the reaction between carbonyl compounds and trimethylorthoformate producing dimethylacetals at room temperature<sup>24</sup>. Highly acidic sulphated zirconia has been proposed for the synthesis of acetals from aldehydes and ketones with 2, 2-dimethyl-1, 3-propanediol with the removal of water<sup>25</sup>. The same reaction has been successfully tested with yttria-zirconia in chloroform at room temperature<sup>26</sup>.

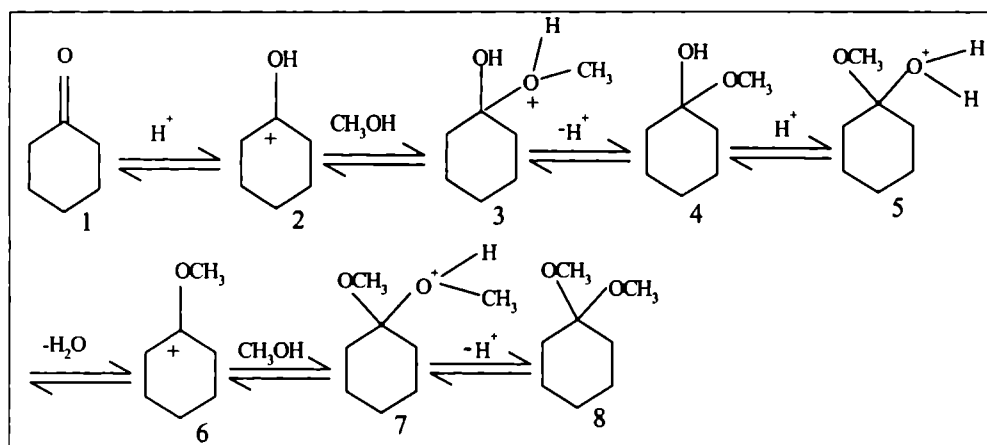
The 1, 2-diacetals can act as an efficient selective protecting groups for the protection of diequatorial 1, 2 diol units in carbohydrates<sup>27-28</sup>. Cyclohexane-1, 2-diacetal (CDA) protection of monosaccharide units offers rapid access to important building blocks for oligosaccharide synthesis<sup>29-30</sup>. Ley et al. reported the preparation,

structure, derivatisation and NMR data of cyclohexane 1, 2-diacetal protected carbohydrates<sup>31-32</sup>.

### **De -acetalization reaction (Hydrolysis of dimethyl acetal)**

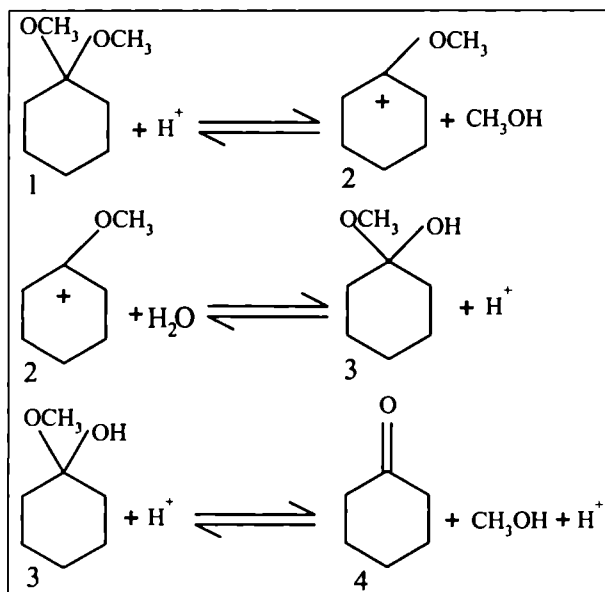
The regeneration of carbonyl compounds from their acetals is generally performed under acidic conditions. For deacetalization, different heterogeneous catalysts have been proposed. Commercially available montmorillonite K-10 clay is being effectively utilized for the easy cleavage of acetals<sup>33-34</sup>. Na-Y zeolite promote the cleavage of acetals in presence of nitrobenzene at room temperature<sup>18</sup>. The water molecules that remain adsorbed in the zeolite after thermal activation are active during the hydrolytic cleavage. When no external water is added to the system, progress of the reaction depends on the water that remains absorbed in the zeolite. Mordenite has also been utilized for the cleavage of acetals. The results show that a wide range of acetals, including saturated,  $\alpha$ ,  $\beta$ - unsaturated, aliphatic, aromatic, and heteroaromatic compounds, can be cleaved under these conditions<sup>35</sup>. Metal oxides such as sulphated  $ZrO_2$ ,  $TiO_2$ ,  $Fe_2O_3$ ,  $SnO_2$ ,  $Al_2O_3$ ,  $HfO_2$  and  $SiO_2$  are also found to catalyse the hydrolysis of dimethyl acetal, regenerating the parent carbonyl compounds. These solid acids not only provide an excellent synthetic route for the manufacture dimethyl acetals of large molecular size but also act as versatile catalysts in protecting and deprotecting carbonyl groups during organic synthesis<sup>36</sup>. The general mechanism of the acetalization reaction is shown in Scheme 1.

As clear from the mechanism a number of equilibrium steps are involved in the reaction. In the first step, the carbonyl compound takes up an  $H^+$  from the catalyst surface leading to the formation of hemiacetal (structure 4). Hemiacetal, not being detected, must be undergoing further protonation leading to dimethoxy cyclohexane (structure 8)<sup>37-38</sup>.



Scheme 1

Mechanism of acetalization of cyclohexanone using methanol



Scheme 2.

Mechanism of the hydrolysis of dimethoxy cyclohexane.

A three-step mechanism is generally accepted for the acid catalysed hydrolysis of dimethoxy cyclohexane<sup>36, 38-39</sup>. The mechanism is depicted in Scheme 2, in which protonation of dimethyl acetal takes place at first to form the oxocarbenium ion (structure 2). The oxocarbenium ion then undergoes hydrolysis to form the hemiacetal (structure 3). Hemiacetal further protonates resulting in the formation of cyclohexanone (structure 4).

In the present work, the acetalization of cyclohexanone and the hydrolysis of the corresponding dimethyl acetal using transition metal (W, Mo & Cr) doped ceria systems and their sulphated analogues has been performed. The reaction always yielded 1,1 dimethoxy cyclohexane as the exclusive product. The results of hydrolysis indicate that pure ceria does not have the capacity to hydrolyse dimethyl acetal. In the case of molybdenum and chromium doped systems a complete reversal to cyclohexanone is observed. However, tungsten incorporated systems show less activity.

#### **4.2 Protection reaction (Acetalization of cyclohexanone)**

The liquid- phase acetalization reaction was conducted at room temperature by mixing cyclohexanone and methanol in the particular molar ratio. The experimental procedure is given in section 2.6 of Chapter 2.

#### **4.3 Effect of reaction variables**

Since the reaction conditions play an important role in deciding the catalytic activity, an attempt has been made to optimise the reaction variables such as reaction temperature, reaction time, catalyst concentration and the molar ratio of cyclohexanone to methanol. The optimisation process is performed using 0.25 g of SC catalyst.

### I. Effect of Temperature

The dependence of cyclohexanone conversion on the reaction temperature is studied in the range of room temperature and 100 °C with 1:10 molar ratio of cyclohexanone to methanol. The results are given in Figure 4.1.

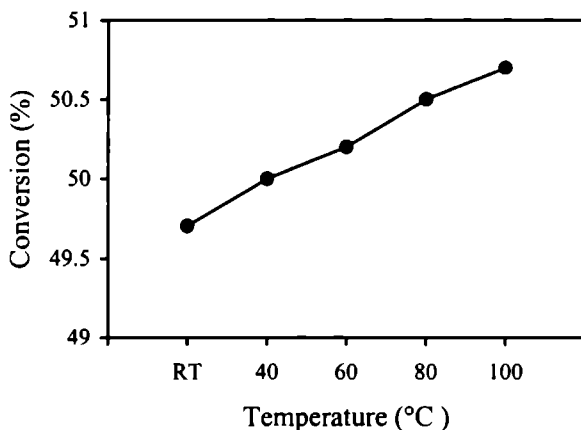


Figure 4.1

Influence of temperature on cyclohexanone conversion.

Catalyst-0.25 g SC, time-1 h, molar ratio of cyclohexanone to methanol-1:10

From the Figure 4.1 it is clear that a very small increase in the percentage conversion is observed by raising the reaction temperature from room temperature to 100 °C. At room temperature the conversion is 49.7% and it reaches to 50.7% at 100 °C. It is also observed that at all temperatures dimethyl acetal is the sole product. It is clear from the mechanism of the reaction that acetalization reaction is an equilibrium reaction. Here temperature does not have much influence in determining the catalytic activity.

### II. Effect of reaction time

To show the influence of reaction time upon the conversion of cyclohexanone,

reaction was carried out continuously for 20 hrs, at room temperature, with cyclohexanone to methanol molar ratio 1:10. The results are shown in Figure 4.2.

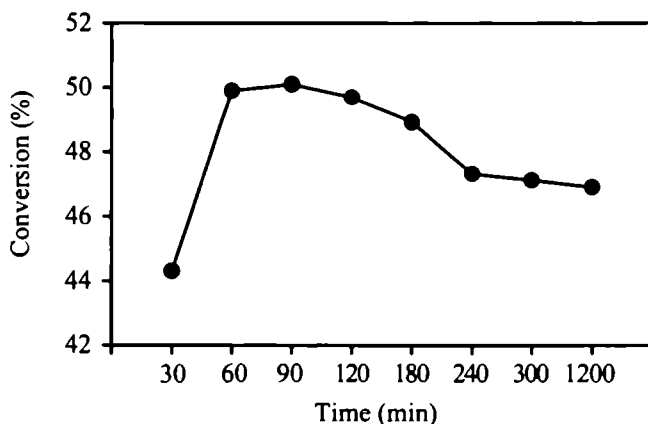


Figure 4.2

Influence of reaction time on cyclohexanone conversion.

Catalyst-0.25 g SC, temperature-RT, molar ratio of cyclohexanone to methanol-1:10.

Figure 4.2 shows that during the initial stages of the reaction the percentage conversion increases, and approaches equilibrium within 60 minutes, with a conversion of 49.9%. The conversion remains constant for the next 30 minutes. After that, a small decrease in conversion is noticed with time.

The decrease in the catalytic activity may be due to the larger absorption and lower diffusion rates of the bulky reaction products on the catalyst surface. Climent et al. compared the deactivation of zeolite H-Y and MCM - 41, in the acetalization of heptanal, 2-phenylpropanal and larger aldehydes like diphenylacetaldehyde<sup>23</sup>. While zeolites are intrinsically more active catalysts than mesoporous MCM-41, they deactivate more rapidly than mesoporous materials as the products will get adsorbed by the catalyst resulting in the blocking of the pores or active sites leading to a loss of catalytic activity.

### III. Effect of cyclohexanone to methanol molar ratio

To investigate the effect of molar ratio of cyclohexanone to methanol on the conversion of cyclohexanone, a set of experiments were performed with different molar ratios of cyclohexanone and methanol at room temperature for 30 minutes. The ratios are changed by keeping the amount of cyclohexanone a constant. Figure 4.3 shows the effect of molar ratio on the conversion.

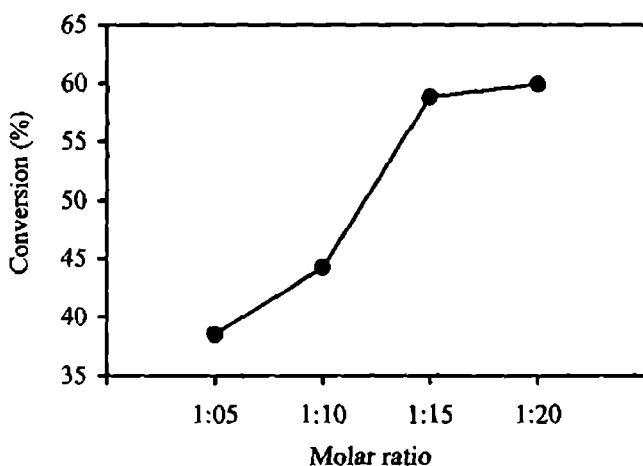


Figure 4.3

The influence of molar ratio on cyclohexanone conversion.

Catalyst-0.25 g SC, temperature-RT, time-30 minutes.

The molar ratio seems to play a major role in deciding the catalytic activity. With an increase in the concentration of methanol in the reaction mixture, the percentage conversion increases, as seen in Figure 4.3. The conversion increases from 44.3 to 58.8% upon changing the molar ratio from 1:10 to 1:15. A small increase in conversion is noticed by increasing the molar ratio further. Increase in methanol concentration results in increase in solvation effects, leading to increased product formation.

#### IV. Effect of catalyst concentration

In heterogeneous catalysis, the amount of catalyst plays an important role in determining the rate of the reaction. To study this, reactions were carried out at room temperature for 30 minutes, by taking different amounts of catalyst. In all the cases, the molar ratio of cyclohexanone to methanol was kept as 1:15. Figure 4.4 shows the effect of catalyst concentration on the reaction.

Figure 4.4 shows that the conversion of cyclohexanone is negligible in the absence of the catalyst. As the amount of catalyst increases to 0.15 g, the percentage conversion increases from 3.6 to 50.8%. The conversion further increases with increase in the catalyst concentration.

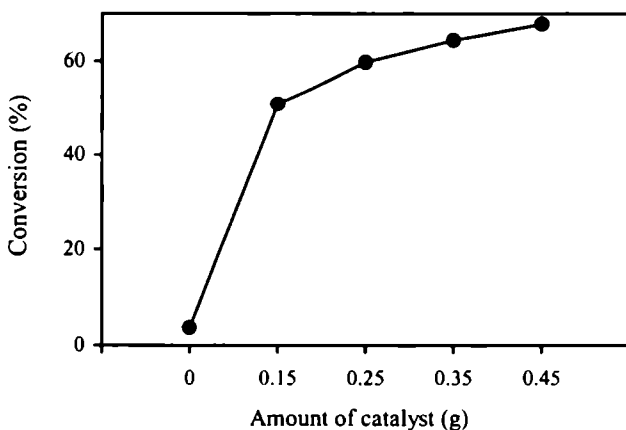


Figure 4.4

Influence of catalyst concentration on cyclohexanone conversion

Temperature-RT, time-30 minutes, cyclohexanone to methanol molar ratio-1:15.

The results indicate that the amount of catalyst has a positive role in determining the conversion. The product yield is found to be proportional to the amount of catalyst establishing that the reaction proceeds through a heterogeneous pathway.

### V. Effect of metal leaching

Metal leaching studies give an idea about the nature of the reaction. For this, the solid catalyst was removed from the reaction mixture by filtration and subsequently the catalytic activity of the filtrate is tested. The reactions are carried out at room temperature for 30 minutes, keeping the molar ratio of cyclohexanone to methanol as 1:15. The results obtained are presented in Table 4.1. The filtrate is further subjected to qualitative analysis for testing the presence of leached metal ions.

Table 4.1

Influence of metal leaching in acetalization of cyclohexanone with methanol.

Time (min)	Conversion (%)	Selectivity (%)
30	64.5	100
30*	65.2	100
60*	65.8	100

Catalyst-0.35 g SC, temperature-RT, cyclohexanone to methanol molar ratio 1:15.

\* After filtration.

According to Table 4.1, the conversion of cyclohexanone at the time of filtration is 64.5%. After the removal of the catalyst, though the reaction is continued for one more hour, no noticeable change in conversion is observed. From these results it is clear that metal ions are not leached out from the catalyst surface during the reaction. This points to the true heterogeneous nature of the reaction.

#### 4.4 Catalytic Activity of different catalyst systems

A comparative evaluation of the catalytic activity of various ceria catalysts is presented here. All the reactions are performed at room temperature with 1:15 molar ratio of cyclohexanone to methanol for 30 minutes. The amount of catalyst in all cases is kept as 0.25 g.

### a) Tungsten incorporated systems

Table 4.2 shows the catalytic activities of various tungsten modified catalysts together with its sulphated analogues for the acetalization reaction. An attempt is made to correlate the catalytic activity with acid amount. Figure 4.5 shows the influence of acidity on the conversion of cyclohexanone.

From the Table 4.2, it is evident that pure  $\text{CeO}_2$  gives very low conversion under specified reaction conditions. However, modified systems show better activity towards the reaction. In all the cases dimethyl acetal is the exclusive product. The sulphated systems show comparatively higher activity. Among the simple supported systems, the conversion gradually increases as the tungsten loading increases to 10%, and thereafter decreases. In the case of sulphated systems, maximum activity is shown by  $\text{CSW}_5$  system, where the conversion is 61.9%.

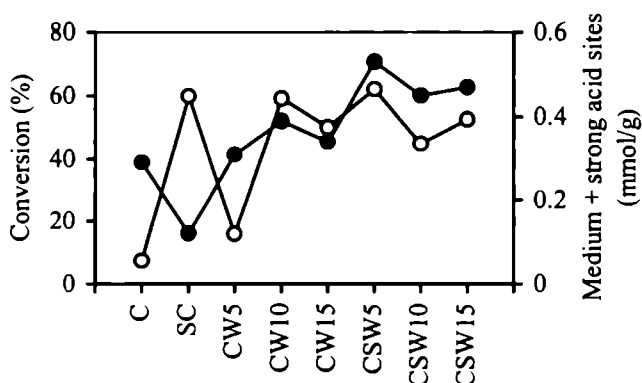
Table 4.2

Activity of tungsten incorporated systems in the acetalization of cyclohexanone

Catalytic systems	Conversion (%)	Selectivity (%)
Blank	3.6	100
C	7.4	100
SC	59.8	100
$\text{CW}_5$	15.8	100
$\text{CW}_{10}$	59.1	100
$\text{CW}_{15}$	50.0	100
$\text{CSW}_5$	61.9	100
$\text{CSW}_{10}$	44.7	100
$\text{CSW}_{15}$	52.6	100

Amount of Catalyst-0.25 g, temperature-RT, time -30 minutes,  
molar ratio of cyclohexanone to methanol-1:15.

Since acetalization is an acid catalysed reaction, the difference in activity among the systems can be due to the difference in the acidity among them. Figure 4.5 reveals that percentage conversion for different systems is in agreement with the sum of medium and strong acid sites as measured by the ammonia TPD studies. Among the simple supported systems,  $CW_{10}$  has the highest medium+strong acid sites, which in turn gives the maximum conversion. In the case of sulphated systems,  $CSW_5$  gives the maximum conversion in accordance to number of acid sites. The blank run performed indicates negligible conversion in the absence of the catalyst.



-●- Amount of medium + strong acid sites -○- Conversion ( % )

Figure 4.5

Catalytic activity correlated with the sum of medium and strong acid sites obtained from ammonia TPD.

In the case of metal oxides, medium +strong acid sites are found to play an important role in determining the catalytic efficiency. Lin et al. compared the catalytic activity of sulphated  $Fe_2O_3$  and  $TiO_2$ , and observed that the less acidic sulphated  $Fe_2O_3$  was as active as the more acidic sulphated  $TiO_2$  towards this reaction<sup>36</sup>. This can be explained based on the fact that the sum of the number of medium strong and strong acid sites is about the same in both the catalysts.

### b) Molybdenum incorporated systems

The results obtained for acetalization reaction over molybdenum incorporated pure and sulphated ceria systems are shown in the Table 4.3. Pure and sulphated ceria are also screened for comparing the catalytic activity. The variation of conversion with acid amount is presented in Figure 4.6.

Table 4.3

Activity of molybdenum incorporated systems in the acetalization of cyclohexanone.

Catalytic systems	Conversion (%)	Selectivity (%)
C	7.4	100
SC	59.8	100
CM <sub>5</sub>	70.2	100
CM <sub>10</sub>	58.5	100
CM <sub>15</sub>	62.3	100
CSM <sub>5</sub>	67.0	100
CSM <sub>10</sub>	59.1	100
CSM <sub>15</sub>	72.7	100

Amount of Catalyst-0.25 g, temperature-RT, time-30minutes,  
molar ratio of cyclohexanone to methanol-1:15.

From Table 4.3, it is noticeable that all the molybdenum doped systems show remarkable activity in the reaction. Among the molybdenum supported ceria systems, CM<sub>5</sub> shows the maximum conversion of 70.2%. However, as the percentage of molybdenum is increased further the conversion decreases for the CM<sub>10</sub> system and then increases in the case of CM<sub>15</sub> system. The same trend is seen in the case of sulphated systems also.

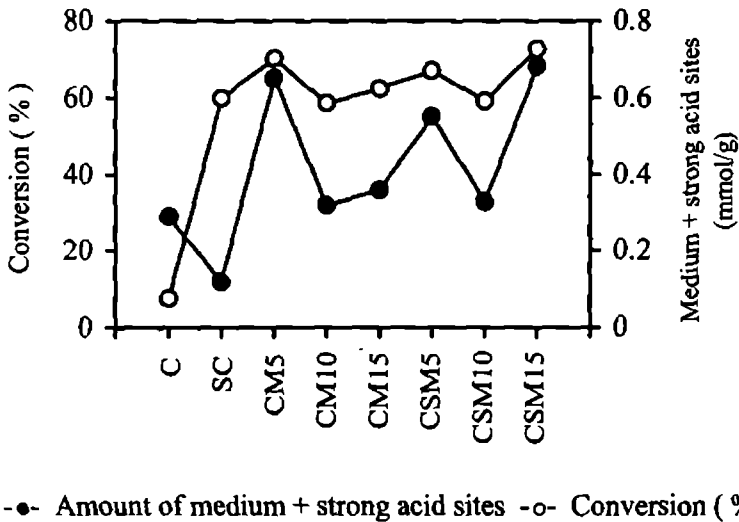


Figure 4.6

Catalytic activity correlated with the sum of medium and strong acid sites obtained from ammonia TPD.

Figure 4.6 illustrates that among the simple supported systems, the number of medium+strong acid sites are higher for  $CM_5$  system. In accordance with this acidity value,  $CM_5$  shows the maximum conversion. In the case of sulphated systems, the one with maximum molybdenum loading exhibits the highest conversion.

### c) Chromium incorporated systems

The catalytic efficiencies of chromium incorporated systems as well as their sulphate modified series in the acetalization reaction are given in Table 4.4. The changes in acidity value obtained by ammonia TPD method with chromium loading in the case of chromium-doped systems are presented in Figure 4.7.

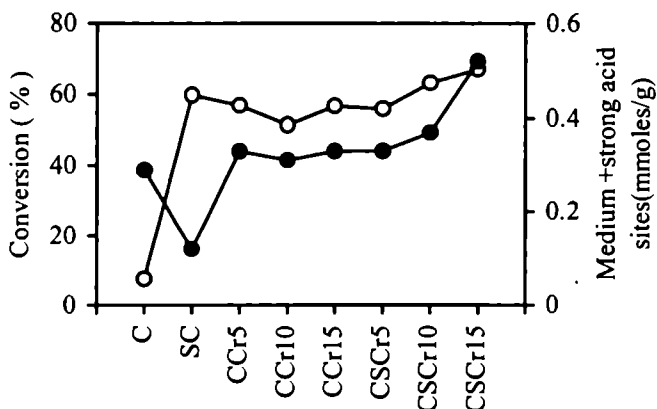
Table 4.4  
Activity of chromium incorporated systems in the  
acetalization of cyclohexanone

Catalytic systems	Conversion (%)	Selectivity (%)
C	7.4	100
SC	59.8	100
CCr <sub>5</sub>	56.9	100
CCr <sub>10</sub>	51.5	100
CCr <sub>15</sub>	56.7	100
CSCr <sub>5</sub>	55.9	100
CSCr <sub>10</sub>	63.2	100
CSCr <sub>15</sub>	67.1	100

Amount of Catalyst-0.25 g, temperature-RT, time-30 minutes, molar ratio of cyclohexanone to methanol-1:15.

The results presented in Table 4.4 shows the percentage conversion to be almost the same for CCr<sub>5</sub> & CCr<sub>15</sub> systems. Among the sulphated analogues as the chromium loading increases the percentage conversion also increases. In all the cases dimethyl acetal is the exclusive product.

From Figure 4.7, it is evident that the conversion is in agreement with the amount of medium and strong acid sites. In the case of simple supported systems, CCr<sub>5</sub> and CCr<sub>15</sub> have almost the same amount of medium and strong acid sites which gives the same percentage conversion. Among the sulphate modified systems, as the chromium loading increases, an increase in the amount of medium and strong acid sites is observed. This in turn paves the way for the increase in percentage conversion.



-●- Amount of medium + strong acid sites -○- Conversion (%)

Figure 4.7

Catalytic activity correlated with the sum of medium and strong acid sites determined from ammonia TPD.

#### 4.5 De-protection reaction (Hydrolysis of dimethoxy cyclohexane)

Hydrolysis of dimethoxy cyclohexane was performed at room temperature in the presence of trace amount of water. The experimental procedure is given in section 2.6 of Chapter 2.

#### 4.6 Catalytic activity of different catalytic systems

##### a) Tungsten incorporated systems

Table 4.5 shows the conversion of dimethoxy cyclohexane in the hydrolysis reaction over tungsten-modified systems. Conversion in the case of pure and sulphated ceria is also reported to have a comparison.

Table 4.5 clearly indicates that pure ceria is less effective for the reversal of dimethoxy cyclohexane to cyclohexanone. In the case of modified systems, 100% conversion is observed for all the tungsten modified systems except for  $CW_5$  &  $CW_{10}$ . In all the cases cyclohexanone is the exclusive product.

Table 4.5  
Activity of tungsten incorporated systems in the hydrolysis of dimethoxy cyclohexane.

Catalytic systems	Conversion (%)	Selectivity (%)
C	2.00	100
SC	100	100
CW <sub>5</sub>	80.0	100
CW <sub>10</sub>	81.9	100
CW <sub>15</sub>	100	100
CSW <sub>5</sub>	100	100
CSW <sub>10</sub>	100	100
CSW <sub>15</sub>	100	100

Amount of Catalyst-0.25 g, temperature-RT, time-1 h, molar ratio of cyclohexanone to methanol-1:15.

#### b) Molybdenum incorporated systems

Table 4.6 shows the catalytic performance of molybdenum-doped systems towards the hydrolysis of dimethoxy cyclohexane.

As evident from Table 4.6, molybdenum incorporated pure ceria systems as well as its sulphated derivatives are capable of complete transformation of dimethoxy cyclohexane to cyclohexanone. These systems have proven as effective catalysts for the deprotection reaction.

Table 4.6  
Activity of molybdenum incorporated systems in the hydrolysis of  
dimethoxy cyclohexane.

Catalytic systems	Conversion ( % )	Selectivity ( % )
C	2.00	100
SC	100	100
CM <sub>5</sub>	100	100
CM <sub>10</sub>	100	100
CM <sub>15</sub>	100	100
CSM <sub>5</sub>	100	100
CSM <sub>10</sub>	100	100
CSM <sub>15</sub>	100	100

Amount of Catalyst-0.25 g, temperature-RT, time-1 h, molar ratio of  
cyclohexanone to methanol-1:15.

### c) Chromium incorporated systems

Table 4.7 presents the results of the hydrolysis of dimethoxy cyclohexane over different chromium incorporated pure ceria systems and its sulphated analogues.

Chromium systems also give 100% conversion of dimethyl acetal, proving that they are highly effective in the de-protection reaction.

Table 4.7

Activity of chromium incorporated systems in the hydrolysis of dimethoxy cyclohexane.

Catalytic systems	Conversion (%)	Selectivity (%)
C	2.00	100
SC	100	100
CCr <sub>5</sub>	99.4	100
CCr <sub>10</sub>	99.8	100
CCr <sub>15</sub>	100	100
CSCr <sub>5</sub>	100	100
CSCr <sub>10</sub>	100	100
CSCr <sub>15</sub>	100	100

Amount of Catalyst-0.25 g, temperature-RT, time-1 h, molar ratio of cyclohexanone to methanol-1:15.

#### 4.7 Conclusions

The summary of the results of the various studies is presented below:

- \* Transition metal (W, Mo and Cr) incorporated pure ceria and its sulphated analogues effectively catalyse the acetalization of cyclohexanone with methanol.
- \* The reaction always yields dimethoxy cyclohexane as the sole product.
- \* The amount of medium and strong acid sites plays an imperative role in determining the catalytic activity.
- \* Reaction variables such as temperature of the reaction, reaction time, cyclohexanone to methanol molar ratio, and catalyst concentration are indispensable factors influencing the catalytic activity of the systems.

- \* Metal leaching studies prove the true heterogeneous nature of the reaction.
- \* The catalytic systems are capable of hydrolysing the dimethoxy cyclohexane in the presence of trace amounts of water.
- \* The catalytic systems are in general versatile in protecting and deprotecting carbonyl groups during organic synthesis.

## REFERENCES

1. P. A. Wender, S. T. Handy and D. L. Wright, *Chem. Ind.*, (1997) 765.
2. R. A. Sheldon and H. van Bekkum, "Fine Chemicals through Heterogeneous Catalysis", Wiley, Weinheim, 2001.
3. S. E. Sen, S. M. Smith and K. A. Sullivan, *Tetrahedron.*, 55 (1999) 12657.
4. M. Balogh and P. Laszlo, *Organic Chemistry Using Clays*, Springer-Verlag, New York, 1993.
5. G. W. Kabalka and R. M. Pagni, *Tetrahedron.*, 53 (1997) 7999.
6. T. W. Bastock and J. H. Clark, In *Speciality Chemicals*, B. Pearson, Ed., Elsevier, London, 1992.
7. A. Mori and H. Yamamoto, *J. Org. Chem.*, 50 (1985) 5444.
8. K. Narasaka, M. Inoue, T. Yamada, J. Sugimori and N. Iwasawa, *Chem. Lett.*, (1987) 2409.
9. D. M. Clode, *Chem. Rev.*, 79 (1979) 491.
10. J. R. Bull, J. Floor and G. J. Kruger, *J. Chem. Res. Synop.*, (1979) 224.
11. K. Bruns, J. Conracl and A. Steigel, *Tetrahedron.*, 35 (1979) 2523.
12. A. J. Elliot, in *1,3- Doioxolane Polymers in Comprehensive Heterocyclic Polymers*, A. J. Elliot, Ed., Pergamon Press, Oxford, U.K. Vol.6, 1984.
13. T. W. Greene and P. G. M. Wuts, *Protective Groups in Organic Synthesis*, 2<sup>nd</sup> Ed., New York, John Wiley & Sons, 1991.
14. Y. Tanaka, N. Sawamura and M. Iwamoto, *Tetrahedron Lett.*, 39 (1998) 9457.

15. F. Gorla and L. M Venanzi, *Helv. Chim. Acta.*, 73 (1990) 690.
16. M. Cataldo, E. Nieddu, R. Gavagnin, F. Pinna and G. Strukul, *J. Mol. Catal. A.*, 142 (1999) 305.
17. Y. Kamitori, M. Hojo, R. Masuda and T. Yoshida, *Tetrahedron Lett.*, 26 (1985) 4767.
18. A. Corma, M. J. Climent, H. Garcia and J. Primo, *Appl. Catal. A. Gen.*, 59 (1990) 333.
19. G. A. Olah, S. C. Narang, D. Meidar and G. F. Salem, *Synthesis.*, (1981) 282.
20. J. Tateiwa, H. Horiuchi and S. Uemura, *J. Org. Chem.*, 60 (1995) 4039.
21. M. Shibagki, K. Takahashi, H. Kuno and H. Matsushita, *Bull. Chem. Soc. Jpn.*, 63 (1990) 1258.
22. D. Ponde, H. B. Borate, A. Sudalai, T. Ravindranathan and V. H. Desphande, *Tetrahedron Lett.*, 37 (1996) 4605.
23. M. J. Climent, A. Corma, S. Iborra, M. C. Navarro and J. Primo, *J. Catal.*, 161 (1996) 783.
24. K. Arata, *Appl. Catal. A. Gen.*, 146 (1996) 3.
25. A. Sarkar, O. S. Yemul, B. P. Bandgar, N. B. Gaikwad and P. P. Wadgaonkar, *Org. Prep. Proceed. Int.*, 28 (1996) 613.
26. G. C. G. Pals, A. Keshavaraja, K. Saravanan and P. Kumar, *J. Chem. Res. (S)*, (1996) 426.
27. P. Grice, S. V. Ley, J. Pietruszka, H. W. M. Priepe, *Angew. Chem. Int. Ed. Engl.*, 35 (1996) 197.
28. S.V. Ley, R. Downham, P. J. Edwards, J. E. Innes and M. Woods, *Contmp. Org. Synth.*, 2 (1995) 365.
29. S.V. Ley and H. W. M. Priepe, *Angew. Chem. Int. Ed. Engl.*, 33 (1994) 2292.
30. S.V. Ley, H. W. M. Priepe and S. L. Warriner, *Angew. Chem. Int. Ed.*

*Engl.*, 33 (1994) 2290.

31. P. Grice, S. V. Ley, J. Pietruszka, H. W. M. Priepe and S. L. Warriner, *J. Chem. Soc., Perkin Trans. 1* (1997) 351.
32. P. Grice, S. V. Ley, J. Pietruszka, H. W. M. Priepe and E. P. E. Walther, *Synlett.*, (1995) 781.
33. T. S. Li and S. H. Li, *Synth. Commun.*, 27 (1997) 2299.
34. E. C. L. Gautier, A. E. Graham, A. McKillop, A. P. Standen and R. J. K. Taylor, *Tetrahedron Lett.*, 38 (1997) 1881.
35. M. N. Rao, P. Kumar, A. P. Singh and R. S. Reddy, *Synth. Commun.*, 22 (1992) 1299.
36. C. H. Lin, S. D. Lin, Y. H. Yang and T. P. Lin, *Catal. Lett.*, 73 (2001).
37. J. March, "Advanced Organic Chemistry- Reactions, Mechanism and Structure"- John Wiley & Sons, Ed.4 (1992) 889.
38. T. H. Fife, *Acc. Chem. Res.* 5 (1972) 264.
39. E. H. Cordes and H. G. Bull, *Chem. Rev.*, 74 (1974) 581.

\*\*\*\*\*

### *Oxidative Dehydrogenation of Ethylbenzene*

#### **Abstract**

---

*The oxydehydrogenation of hydrocarbons is currently of increasing importance because of energetic and thermodynamic reasons. It offers a potentially attractive means for the production of alkenes. In the present chapter the catalytic activity of transition metal promoted ceria systems and its sulphated counterparts towards the oxidative dehydrogenation of ethylbenzene is described. The reaction parameters such as air flow, temperature of the reaction, feed rate of the reactant and time on stream were optimised to obtain better conversion and product selectivity. An attempt has been made to correlate the catalytic activity of different systems with the amount of medium acid sites obtained from ammonia TPD. The results suggest that reaction parameters play a decisive role in determining the activity and selectivity of the reaction. Good agreement can be established between the catalytic activity and strength of medium acid sites.*

---

## 5.1 Introduction

The catalytic dehydrogenation of ethylbenzene is of industrial importance in the manufacture of styrene as it is extensively used as an intermediate for the manufacture of polystyrene and numerous thermoplastics. About three million tons of styrene is produced annually in Japan alone. Styrene is commercially manufactured by the catalytic dehydrogenation of ethylbenzene over iron oxide promoted by alkali metal ions<sup>1-3</sup>. Since this direct dehydrogenation is limited by thermodynamic equilibrium, high reactor temperatures (> 600 °C) are required and typical conversions are low. Also, the high temperatures required for favourable conversion bring about severe cracking in the more complex alkyl benzenes.

The oxydehydrogenation reaction is a potential alternative for the manufacture of styrene at lower temperatures without thermodynamic restrictions on the yield<sup>4</sup>. Various catalysts have been reported as efficient catalysts for the oxidative dehydrogenation of ethylbenzene<sup>5-6</sup>. Vrieland reported a wide variety of metal pyrophosphate catalysts, which are very active and selective in the oxidative dehydrogenation of ethylbenzene and suggested that the actual catalytic surface is a carbonaceous layer formed on the surface of the pyrophosphates<sup>7</sup>. Catalysts based on phosphates of nickel, zirconium, aluminium, cerium and calcium have also been reported as active catalysts in oxydehydrogenation reactions<sup>8-9</sup>. Turco et al. investigated the catalytic properties of zirconium- tin mixed phosphates and observed that mixed zirconium- tin phosphates give much higher ethylbenzene conversion with respect to pure Zr and Sn phosphates, the selectivity to styrene being likewise high. They concluded that surface acidity of medium-high strength plays a relevant role in the reaction through the formation of a catalytically active coke<sup>10</sup>. According to Alkhozov et al. the important factor is not only the acidity but also the kind of carbonaceous deposit on these acid sites<sup>11</sup>. Various aluminas initially showed widely different activities but eventually reached a common state, which they suggest is a surface with carbonaceous residue. There is convincing evidence that carbon by itself is active for this reaction. Allen et

al. showed that typical carbons give good activity and selectivity for this reaction; but the activity was found to decrease with time<sup>12</sup>.

Seoane and Cortes investigated the production of styrene by oxidative dehydrogenation of ethylbenzene with molecular oxygen over nickel and tungsten mixed oxides supported on alumina. They suggested that the reaction proceeds through a series of consecutive oxidation steps, each intermediate adsorbed species being able either to desorb to the gas phase or react further on the surface of the catalyst<sup>13</sup>. Ferrites, a subgroup of spinels is highly active for the oxydehydrogenation reactions<sup>14</sup>. The catalytic effectiveness of ferrites for many such reactions arises because of the ease with which iron can exchange its oxidation state between 2 and 3. Rare earth oxides especially CeO<sub>2</sub> is used as a component in new catalyst reformulations for the oxidative dehydrogenation of paraffins and ethylbenzene<sup>15</sup>. Jyothi et al. investigated the catalytic activity of rare earth promoted sulphated tin oxide in the oxidative dehydrogenation of ethylbenzene and concluded that sulphated tin oxide displayed better oxidation activity compared to non sulphated analogues<sup>16</sup>.

This chapter presents an exhaustive investigation on vapour-phase oxidative dehydrogenation of ethylbenzene over tungsten, molybdenum and chromium incorporated pure ceria and its sulphated analogues. All the catalytic systems show considerable activity towards the reaction with high selectivity towards styrene.

## **5.2 Oxidative dehydrogenation of ethylbenzene**

The oxidative dehydrogenation of ethylbenzene over the modified ceria catalysts was done in vapour-phase and the experimental procedure adopted is given in section 2.6 of Chapter 2. The influence of temperature, flow rate, air flow and time on stream were investigated in detail to optimise the reaction conditions. The reactions were done in the presence of air. Gas chromatographic analysis showed styrene as the major product along with benzene, toluene and carbon oxides as the minor products.

A blank run (without catalyst) was carried out at 500 °C, which indicated negligible conversion.

### 5.3 Process optimisation

The reaction conditions were found to have an imperative role in determining the catalytic activity and selectivity towards different products. So to have the highest performance of the catalysts, the reaction conditions such as temperature, flow rate, air flow and time on stream are optimised.

#### I. Effect of air flow

In order to study the influence of air flow upon ethylbenzene conversion and styrene selectivity, a series of experiments were performed in the absence and varying amounts of oxygen. The reactions were carried out using 0.5 g of CSM<sub>5</sub> catalyst at a temperature of 450 °C for 2 h. In all studies ethylbenzene flow was maintained as 4 mL/h. The results are given in Table 5.1

Table 5.1

Effect of airflow in oxidative dehydrogenation of ethylbenzene

Air flow rate (mL/min)	Ethylbenzene conversion (%)	Selectivity (%)			
		Benzene	Toluene	C-oxides	Styrene
0	4.6	6.8	8.9	1.2	83.1
5	10.3	2.5	5.9	1.7	89.9
10	16.8	2.3	4.0	3.4	90.4
15	20.2	2.1	3.8	4.5	89.6

Catalyst-0.5 g CSM<sub>5</sub>, temperature-450 °C,  
time on stream –2 h, flow rate-4 mL/h

Results presented in Table 5.1 indicate that in the absence of air flow very little conversion of ethylbenzene is noticed. With an increase in the concentration of oxygen from 5 to 15 mL/min the percentage conversion increase rapidly from 10.3 to

20.2%. At the same time styrene selectivity increases at first and shows a small decrease at 15 mL/min. Styrene selectivity of 90.4% is noticed at airflow of 10 mL/min.

The presence of oxygen is found to enhance the catalytic activity towards oxidative dehydrogenation of ethylbenzene. This enhancement in the presence of oxygen is due to the fact that the additional air supply re-oxidises the reduced catalyst thereby providing the oxygen needed for hydrogen abstraction. The increased availability of oxygen is found to enhance the formation of C-oxides.

## II. Effect of temperature

To have an understanding of the influence of temperature on the catalytic activity, a set of reactions were performed in the temperature range from 350 to 550 °C. The airflow rate and ethylbenzene flow rate were maintained at 15 mL/min and 4 mL/h. The activity and selectivity pattern obtained is presented in Table 5.2.

Table 5.2

Effect of reaction temperature in oxidative dehydrogenation of ethylbenzene

Temperature (°C)	Ethylbenzene conversion (%)	Selectivity (%)			
		Benzene	Toluene	C-oxides	Styrene
350	9.2	0.9	2.9	23.0	73.2
400	15.6	1.8	3.5	14.8	79.9
450	20.2	2.1	3.8	4.5	89.6
500	31.8	3.2	10.1	1.9	84.8
550	34.6	4.4	15.4	1.7	78.5

Catalyst-0.5 g CSM<sub>5</sub>, time on stream -2 h, air flow-15 mL/min,  
flow rate-4 mL/h

Table 5.2 shows that as the temperature of the reaction increases an appreciable increase in the conversion of ethylbenzene is observed. A rise in temperature from 350 to 550 °C results in an increase of conversion from 9.2 to 34.6%. However, styrene selectivity increases first in the temperature range 350-450 °C and thereafter it decreases. Maximum styrene selectivity is observed at 450 °C, where ethylbenzene conversion is about 20.2%. As the temperature is increased further to 550 °C, the styrene selectivity falls from 84.8 to 78.5%, with simultaneous enhancement in the selectivity of toluene and benzene. The selectivity to C-oxides is found to decrease with rise in temperature.

Turco et al. investigated the influence of reaction temperature in the oxidative dehydrogenation of ethylbenzene over zirconium-tin mixed phosphates and found that with an increase of temperature from 400 to 500 °C, ethylbenzene conversion increases from 16 to 64%<sup>10</sup>. It was reported in the case of sulphated tin oxide modified with CeO<sub>2</sub>, that as temperature increases from 450 to 500 °C an increase in ethylbenzene conversion occurs, but the selectivity to styrene increase at first and then decreases. The selectivity to C-oxides decreases in this case also<sup>16</sup>. Bokade et al. studied the oxidative dehydrogenation of ethylbenzene over Cu<sub>1-x</sub>Co<sub>x</sub>Fe<sub>2</sub>O<sub>4</sub> and observed that styrene selectivity increased first in the temperature range of 375 to 425 °C and thereafter decreased because of the increased rate of side reactions like disproportionation and dealkylation reaction at high temperatures<sup>14</sup>. In the present case, since an increase in temperature from 500 to 550 °C, results in a decrease of styrene selectivity, 500 °C is taken as the optimum reaction temperature of the reaction.

### **III. Effect of flow rate**

For studying the effect of flow rate on ethylbenzene conversion and product selectivity, five flow rates (3, 4, 5, 6 and 7 mL/h) were selected. The reaction tem-

perature was kept as 500 °C while airflow was maintained as 15 mL/min. The results obtained are depicted in Figure 5.1.

Figure 5.1 shows that the percentage conversion of ethylbenzene is maximum at lower flow rates. As the flow rate is increased from 3 to 7 mL/h, the conversion of ethylbenzene decreases from 33.2 to 14.4%. Regarding the styrene selectivity, with an increase in flow rate from 3 to 5 mL/h, selectivity was found to increase from 76.7 to 90.9%. Thereafter selectivity decreases with flow rate. Toluene selectivity was found to decrease with an increase in feed rate.

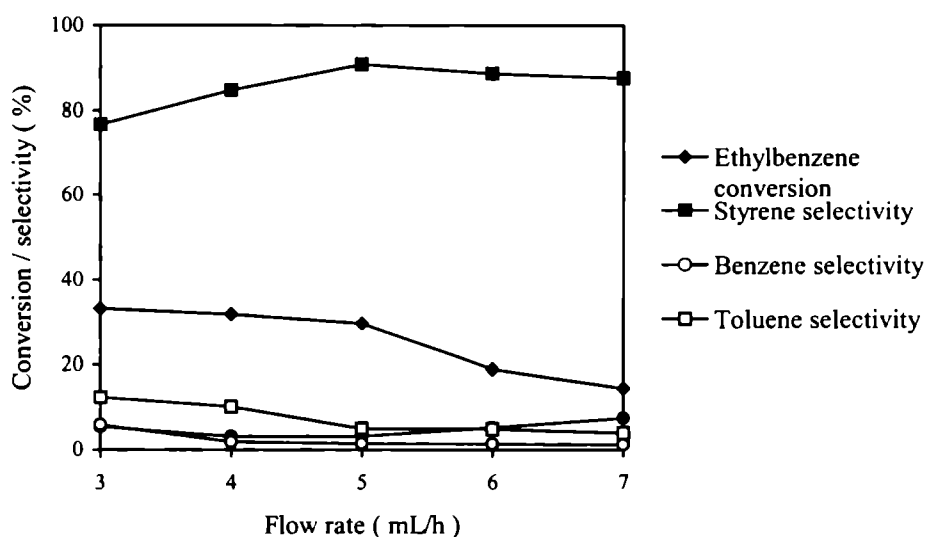


Figure 5.1

Effect of flow rate in oxidative dehydrogenation of ethylbenzene

Catalyst-0.5 g CSM<sub>3</sub>, temperature-500 °C, time on stream -2 h,

air flow-15 mL/min

The decrease in conversion with increase in flow rate may be due to the decreased contact time of the reactants with the catalyst surface. The residence time of the reactants at the catalyst surface is an important parameter in determining the formation of the products. At higher feed rates, the reactants will not get enough time

to get adsorbed on the catalyst surface, which eventually leads to decrease in conversion. Similar trend is reported by Vrieland in the case of oxydehydrogenation of ethylbenzene to styrene over cerium pyrophosphate, where a decrease in flow rate (increase in reactant concentration) increases ethylbenzene conversion from 67.2 to 73.2%<sup>7</sup>.

#### 1V. Effect of time on stream

To study the nature of deactivation of the catalytic systems, the reaction was carried out continuously for 6 hours at 500 °C. The flow rate of ethylbenzene and air flow rate were kept as 5 mL/h and 15 mL/min respectively. The reaction mixture was collected at every hours and the results are depicted in Figure 5.2.

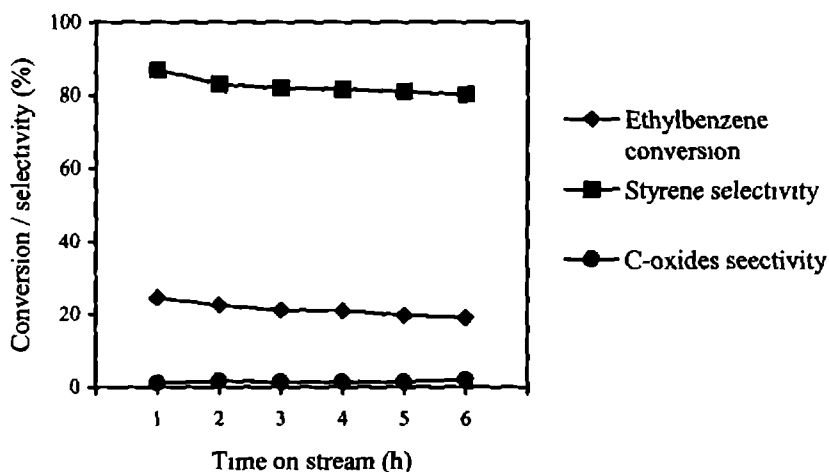


Figure 5.2

Effect of time on stream in oxidative dehydrogenation of ethylbenzene

Catalyst-0.5 g CSW<sub>3</sub>, temperature-500 °C, flow rate-5 mL/h, air flow-15 mL/min

The results presented in Figure 5.2 show that even though there is a small drop in catalytic activity for the second hour, in subsequent hours the activity is nearly constant. Same trend is seen regarding styrene selectivity also. The maximum conversion obtained is 24.5%, where the styrene selectivity is 86.9%.

Deactivation studies establish that the catalytic system possess reasonable stability even after 6 h of reaction run. The decrease in activity during the initial stages of the reaction is due to the reduction of the metal ions present on the catalyst surface. These ions are further reoxidized by the external supply of air thus providing long term catalytic stability to the systems.

#### 5.4 Catalytic activity of different systems

A comparative evaluation of the catalytic activity of different catalytic systems for the oxidative dehydrogenation of ethylbenzene is described here. All the reactions were done at a reaction temperature of 500 °C for 2 hrs, while the air flow rate and feed rate were kept as 15 mL/ min and 5 mL/h respectively.

##### a) Tungsten incorporated systems

The results obtained for oxidative dehydrogenation over tungsten modified ceria series are given in Table 5.3. Pure as well as sulphated ceria are also scanned for catalytic activity to have a comparison. Since surface acidity plays an important role in the oxydehydrogenation of ethylbenzene, an attempt is made to correlate the catalytic activity with acid amount; the results are presented in Figure 5.3.

It can be inferred from Table 5.3 that though sulphate modification of pure ceria result in a reduction of catalytic activity, tungsten incorporation of the sulphated ceria enhanced the catalytic efficiency towards oxidative dehydrogenation of ethylbenzene. Among the simple supported systems, maximum conversion is observed in the case of CW<sub>10</sub> system. Similar is the case with sulphated systems also. The selectivity pattern obtained for styrene shows a gradual decrease with tungsten loading, in simple systems. In sulphated systems, styrene selectivity at first increases upto CSW<sub>10</sub> system and then decreases.

Table 5.3  
Oxidative dehydrogenation activity of tungsten doped systems

Catalytic Systems	Conversion (%)	Selectivity (%)			
		Benzene	Toluene	Styrene	C-oxides
C	26.2	3.4	6.2	89.0	1.4
SC	18.6	3.9	7.1	87.1	1.9
CW <sub>5</sub>	23.3	2.8	11.2	85.6	0.5
CW <sub>10</sub>	28.6	5.7	9.5	83.1	1.7
CW <sub>15</sub>	21.5	6.3	9.6	81.2	2.9
CSW <sub>5</sub>	32.4	6.2	9.2	82.9	1.7
CSW <sub>10</sub>	35.5	3.9	6.4	88.7	1.1
CSW <sub>15</sub>	29.4	6.2	8.9	83.9	1.0

Amount of catalyst-0.5 g, temperature-500 °C, flow rate-5 mL/h,  
time on stream - 2 h, air flow-15 mL/min

Figure 5.3 illustrates that acid amount plays a decisive role in the oxidative dehydrogenation of ethylbenzene. The catalytic activity of the systems is in good agreement with the amount of medium acid sites obtained from ammonia TPD. Among the tungsten supported pure systems, maximum activity is shown by CW<sub>10</sub> system in accordance with number of medium acid sites. Similarly CSW<sub>10</sub> has maximum number of medium acid sites among sulphated systems, which in turn gives maximum conversion.

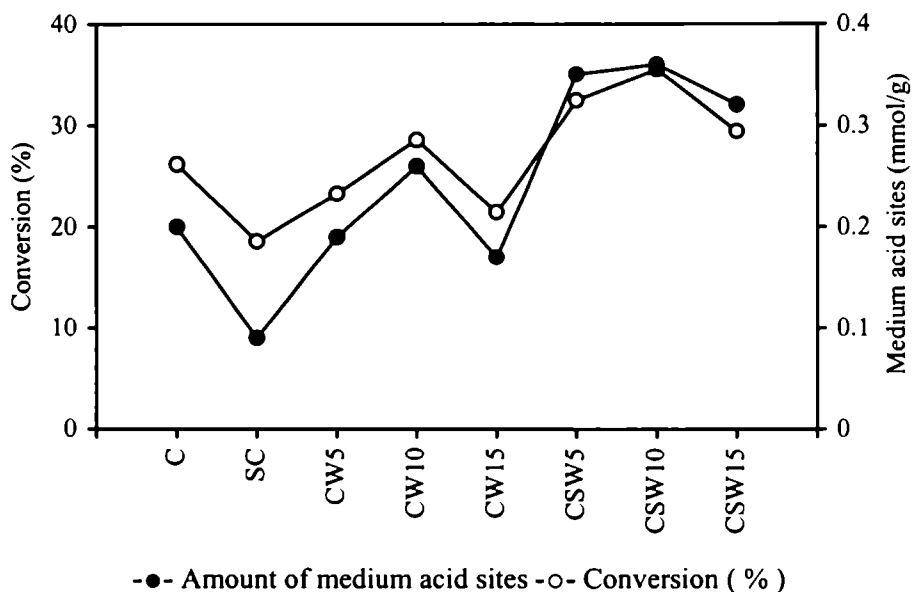


Figure 5.3

Catalytic activity correlated with the amount of medium acid sites  
obtained from ammonia TPD.

From the literature there are evidence that surface acid amount plays a direct<sup>17-18</sup> or an indirect<sup>19</sup> role in the oxidative dehydrogenation of ethylbenzene. Tagawa et al. studied silica alumina, tin oxides, and phosphates and concluded that moderate acid strength is the key factor<sup>20</sup>. Removal of strong acid sites by addition of sodium acetate improved the selectivity to styrene but excessive sodium deactivated the catalyst. A similar conclusion was reached by Fiedorow et al. with alumina where small amounts of sodium ion did not affect activity even though strong acid sites would have been removed<sup>17</sup>. Echigoya et al. found that introducing acidity into silica by addition of either magnesium or zirconium correlated well with oxydehydrogenation activity<sup>21</sup>. Pyridine in the feed, which would adsorb on strong acid sites at these temperatures, did not affect the oxidation reaction.

**b) Molybdenum incorporated systems**

The catalytic efficiencies of molybdenum supported catalysts in oxidative dehydrogenation of ethylbenzene are given in Table 5.4. The correlation between ethylbenzene conversion and surface acidity is presented in Figure 5.4.

Table 5.4

Oxidative dehydrogenation activity of molybdenum doped systems

Catalytic Systems	Conversion (%)	Selectivity (%)			
		Benzene	Toluene	Styrene	C-oxides
C	26.2	3.4	6.2	89.0	1.4
SC	18.6	3.9	7.1	87.1	1.9
CM <sub>5</sub>	37.5	2.0	3.7	92.7	1.6
CM <sub>10</sub>	23.8	2.1	4.5	87.6	5.9
CM <sub>15</sub>	26.5	2.2	4.2	91.5	2.1
CSM <sub>5</sub>	28.9	3.2	5.4	90.9	0.5
CSM <sub>10</sub>	26.6	1.6	3.1	94.1	1.2
CSM <sub>15</sub>	30.6	1.1	2.3	92.6	4.0

Amount of Catalyst-0.5 g, temperature-500 °C, flow rate-5 mL/h,  
time on stream - 2 h, air flow-15 mL/min

From Table 5.4, it is clear that the molybdenum doped systems show remarkable styrene selectivity in oxidative dehydrogenation reaction compared to pure systems. An exception is seen in the case of CM<sub>10</sub> system, where styrene selectivity is lower than pure ceria. In all the cases styrene is formed as the major product with small amounts of benzene, toluene and carbon oxides. Among molybdenum supported systems maximum activity is shown by CM<sub>5</sub> system, where as CSM<sub>15</sub> gives maximum conversion among sulphated systems.

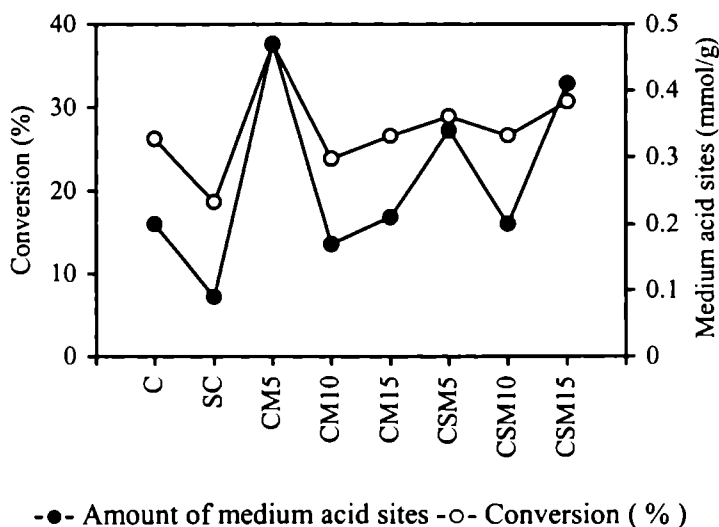


Figure 5.4

Catalytic activity correlated with the amount of medium acid sites obtained from ammonia TPD.

The activity of molybdenum modified systems is found to be in accordance with amount of medium acid sites as clear from the Figure 5.4.  $CM_5$  and  $CSM_{15}$  possess maximum number of medium acid sites among pure and sulphated systems. These systems are more active towards the reaction based on their acidity value.

Kania et al. studied the catalytic activity of  $Fe_2O_3$ ,  $Cr_2O_3$ , NiO,  $MoO_3$  and MgO modified  $\gamma$ - alumina in the oxidative dehydrogenation of ethylbenzene. They observed that nickel oxide-alumina and molybdena-alumina catalysts are characterised by an increase in activity for the oxidative dehydrogenation reaction in comparison with  $\gamma$ - alumina. This enhancement in the catalytic activity is ascribed to the increase in the amount of acid centres of moderate or weaker strength, though a decrease is noticed for the strong sites<sup>22</sup>.

### c) Chromium incorporated systems

The results obtained for the oxidative dehydrogenation of ethylbenzene over chromium incorporated systems are depicted in Table 5.5. The influence of acidity on the activity of the catalysts is shown in Figure 5.5.

Table 5.5

Oxidative dehydrogenation activity of chromium doped systems

Catalytic Systems	Conversion (%)	Selectivity (%)			
		Benzene	Toluene	Styrene	C-oxides
C	26.2	3.4	6.2	89.0	1.4
SC	18.6	3.9	7.1	87.1	1.9
CCr <sub>5</sub>	23.2	4.9	7.8	85.5	1.9
CCr <sub>10</sub>	22.6	5.6	7.8	83.2	3.3
CCr <sub>15</sub>	23.5	3.8	6.2	89.4	0.6
CSCr <sub>5</sub>	23.6	7.2	9.4	82.9	0.4
CSCr <sub>10</sub>	27.8	5.7	8.4	85.5	0.5
CSCr <sub>15</sub>	33.5	3.7	6.0	88.9	1.4

Amount of Catalyst-0.5 g, temperature-500 °C, flow rate-5 mL/h,  
time on stream - 2 h, air flow-15 mL/min

Table 5.5 indicates that chromium doping of pure ceria decreased ethylbenzene conversion and styrene selectivity to a certain extent. In the sulphated systems, at higher chromium loading, an increase in ethylbenzene conversion is observed, with a small reduction in styrene selectivity.

Figure 5.5 clearly shows the one to one correlation between catalytic activity and the amount of moderate acid sites obtained from TPD of ammonia. CSCr<sub>15</sub> gives maximum conversion, which is in agreement with number of medium acid sites.

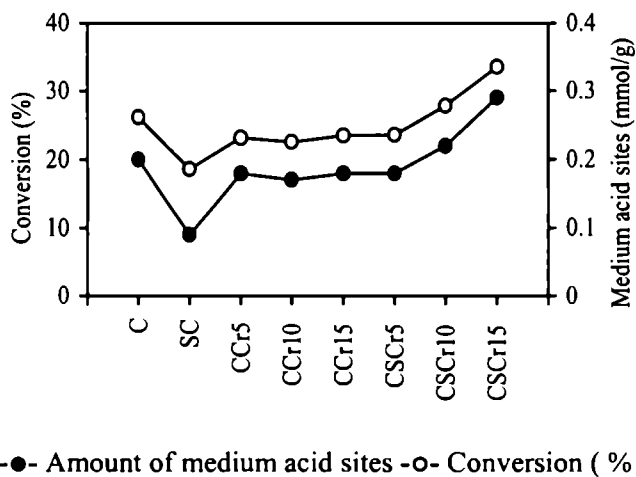
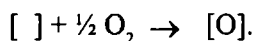
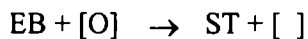


Figure 5.5

Catalytic activity correlated with the amount of medium acid sites obtained from ammonia TPD.

### 5.5 Mechanism of the reaction

In the oxidative dehydrogenation of ethylbenzene, one of the most probable mechanism is one which involves the abstraction of hydrogen from ethylbenzene by lattice oxygen on the surface to form styrene through a  $\pi$  allyl intermediate and re-oxidation of the catalyst by gas phase oxygen. This mechanism is known as Mars-van Krevelen mechanism<sup>23-24</sup>. A condition for the operation of this mechanism is that the catalyst contains metal ion with variable valencies, notably transition metal ion able to cope with the varying degree of surface oxidation<sup>25</sup>. A  $\pi$  allyl mechanism is generally accepted in the oxidation of olefins. The following sequences involve the redox cycle of adsorbed styrene and the catalyst surface as suggested by Hanuza and co-workers<sup>26</sup>.



where [ ] is the anion vacancy and [O] is the lattice oxygen.

Schattler and De Boer have reported that the rate determining step of propylene oxidation is the dissociative adsorption of propylene by a cleavage of the C-H bond in the methyl group of propylene in  $^{14}\text{C}$  tracer studies<sup>27</sup>. Moreover the competitive reaction of ethylbenzene with other aromatic hydrocarbons over  $\text{SnO}_2\text{-P}_2\text{O}_5$  catalysts suggest that ethylbenzene is adsorbed by the abstraction of  $\alpha\text{-H}$  on the catalyst<sup>28</sup>.

Wang et al. proposed a reaction mechanism based on the acid-base properties of a series of Cu-Co ferrites<sup>29</sup>. According to this mechanism, the dehydrogenation of the ethylbenzene over these oxides proceeds by the acid-base bifunctional mechanism, in which  $\alpha\text{-H}$  of ethylbenzene attacks the acid site of the catalyst, and simultaneously the  $\beta\text{-H}$  attacks the basic site of the catalyst. The partial positive charge on the  $\alpha\text{-C}$  of transition state could be stabilized by the aromatic ring. They proved that the balance of acid-base property is very important for an efficient ethylbenzene dehydrogenation.

Alkhazov et al. assumed that in the oxidative dehydrogenation of ethylbenzene over modified aluminas, ethylbenzene is adsorbed first on acid centers of the catalyst surface<sup>30</sup>. They claimed that the reaction pathway depends on the strength of adsorption; stronger the adsorption the greater is the ethylbenzene conversion (including the formation of carbon oxides). In this process, base centres on the catalyst surface also play an important role, as they activate the oxygen from the gas phase, which takes part in this reaction. Oxygen activated on strong base centres at higher temperatures has been found to be responsible for the total oxidation of hydrocarbons. Therefore, such a catalyst which has acid and base centres of moderate or weaker strength on its surface is the most suitable for the oxidative dehydrogenation of ethylbenzene. The moderate and weak acid sites of alumina are responsible for the formation of styrene as suggested by Fiedorow et al.<sup>17</sup>. According to Bagnasco et al. surface acid site of medium-high strength play a significant role in the oxidative dehydrogenation of ethylbenzene<sup>31</sup>. Hagemeyer et al. claimed a redox process involving the dehydro-

genation of ethylbenzene by contact with a catalyst containing a reducible metal oxide ( $\text{Bi}_2\text{O}_3$ ,  $\text{CeO}_2$  and  $\text{Cr}_2\text{O}_3$ ) in the absence of oxygen and simultaneous reduction of the catalyst, followed by oxidation of reduced catalyst with an oxidising agent<sup>32</sup>.

A plausible mechanism for the oxidative dehydrogenation of ethylbenzene is given in Figure 5.6. The first step of the mechanism involves the coordination of ethylbenzene to the acid site and the basic group adjacent to the acid site abstracts the  $\alpha$ -hydrogen from the coordinated ethyl benzene to give a stable adsorbed species represented by the structures (2&3). The OH group thus formed over the catalyst surface then abstracts the  $\beta$ -hydrogen and the subsequent desorption of water activates the molecular oxygen. The reversibly adsorbed oxygen is converted to  $\text{O}^-$  species over the catalyst surface, which regenerates the active site.

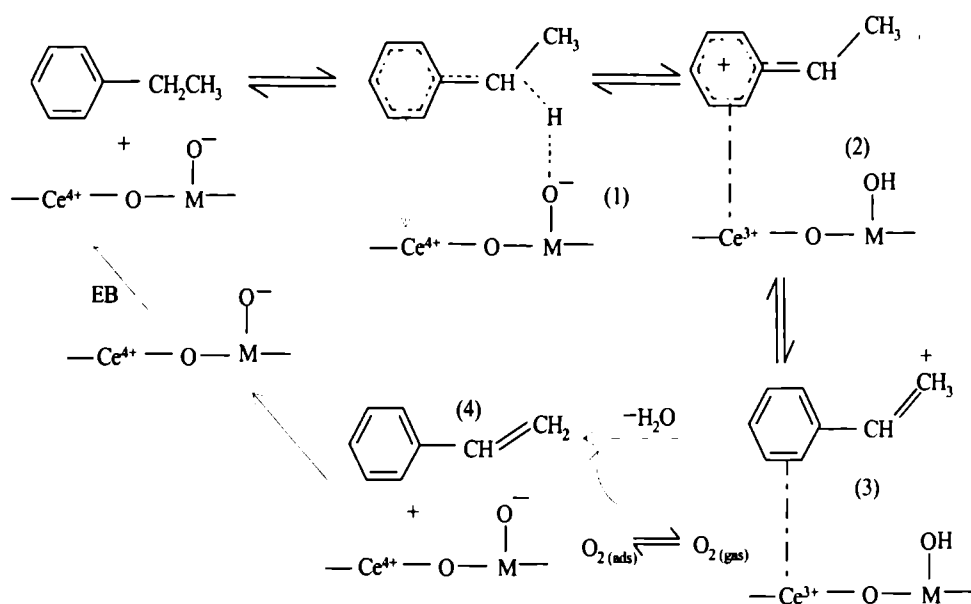


Figure 5.6

A possible mechanism for the oxydehydrogenation of ethylbenzene over ceria systems.

## 5.6 Conclusions

- \* Supported ceria catalysts are found to exhibit high activity and selectivity in the oxidative dehydrogenation of ethylbenzene.
- \* Reaction always yielded styrene as the predominant product along with benzene, toluene and C-oxides as the minor products.
- \* The catalytic activity is significantly influenced by the reaction parameters such as temperature of the reaction, feed rate, air flow rate and reaction time.
- \* Surface acidity, especially the medium acid sites, play an important role in determining the catalytic activity.

## REFERENCES

1. E. H. Lee, *Catal. Rev.*, 8 (1973) 285.
2. B. Delmon, P. A. Jacobs and G. Poncelet, *Preparation of Catalysts II* (Elsevier, Amsterdam, 1979) pp.293.
3. D. E. Stobbe, F. R. Van Buren, M. S. Hoogenraad, A. J. van Dillen and J. W. Geus, *J. Chem. Soc. Faraday Trans.*, 87 (1991) 1639.
4. L. E. Cadus, L. A. Arrua, O. F. Gorriz and J. B. Rivarola, *Ind. Eng. Chem. Res.*, 27 (1988) 2241.
5. Y. Yang, J. F. Yu, T. H. Wu and J. Z. Sun, *Chin. J. Catal.*, 18 (1997) 126.
6. B. Gryzbowska-Swierskosz, *Appl. Catal. A. Gen.*, 157 (1997) 409.
7. G. E. Vrieland, *J. Catal.*, 111 (1988) 1.
8. G. F. Crum and S. J. Paton, U. S. Patent. 4, 291, 184 (1981).
9. G. F. Crum and S. J. Paton, U. S. Patent.4, 291, 183 (1981).
10. G. Bagnasco, P. Ciambelli, M. Turco, A. La Ginstra and P. Patrono, *Appl. Catal. A. Gen.*, 68 (1991) 69.
11. T. G. Alkhazov, A. E. Lisovskii, M. G. Safarov, A. M. Dadesheva, V. B. Lapin, N. A. Kurbanov, Sh. A. Feizullaeva, Yu. A. Ismailov and T. Kh. Gulakhmedova, *React. Kinet. Catal. Lett.*, 12 (1979) 189.

12. R. H. Allen, T. Jr. Alfrey and L. D. Yats, U. S. Patent 3, 487, 564 (1970).
13. Cortes and J. L. Seoane, *J. Catal.*, 34 (1974) 7.
14. T. Mathew, S. Malwadkar, S. Pai, N. Sharanappa, C. P. Sebastian, C.V.V. Satyanarayana, and V.V. Bokade, *Catal. Lett.*, 91 (2003).
15. R. X. Valenzuela, G. Bueno, V. C. Corberan, Y. Xu and C. Chen, *Catal. Today.*, 61 (2000) 43.
16. T. M. Jyothi, K. Sreekumar, M. B. Talwar, A. A. Belhekar, B. S. Rao and S. Sugunan, *Bull. Chem. Soc. Jpn.*, 73 (2000) 1.
17. R. Fiedorow, W. Przystako, M. Sopa and I. G. Dalla Lana, *J. Catal.*, 68 (1981) 33.
18. T. Tagawa, T. Hattori and Y. Murakami, *J. Catal.*, 75 (1982) 56.
19. P. Galli, A. La Ginestra, P. Patrono, M. A. Massucci, C. Ferragina, P. Ciambelli and G. Bagnasco, Italian Pat. N. 21587 A/86 (1986).
20. T. Tagawa, T. Hattori, Y. Murakami, K. Iwayama, Y. Ishida and H. Uchida, *Appl. Catal. A. Gen.*, 2 (1982) 67.
21. E. Echigoya, H. Sano and M. Tanaka, "Eighth international Congress on Catalysis, Berlin.1984", Vol.5, P.623. Dechema, Frankfurt-am-Main, 1984.
22. W. Kania and K. Jurczyk, *Appl. Catal. A. Gen.*, 61 (1990) 35.
23. P. Mars and D. W. van der Krevelen, *Chem. Eng. Sci.*, 8 (1954) 41.
24. Maltha, T. L. F. Favre, H. F. Kist, A. P. Zuur and V. Ponce, *J. Catal.*, 149 (1994) 364.
25. S. Meijers, T. P. Pruys van der Hoeven, V. Ponce, J. P. Jacobs and H. H. Brongersma, *J. Catal.*, 161 (1996) 459.
26. J. Hanuza and B. Jezowska-Trzebiatowska, *J. Mol. Catal.*, 4 (1978) 271.
27. W. W. H. Sachtler and W. H. De Boer, in "Proceedings, 3<sup>rd</sup> International Congress on Catalysis, Amsterdam, 1964," Amsterdam, North-Holand, 1965, p. 252.
28. Y. Murakami, I. Iwayama, H. Uchida, T. Hattori and T. Tagawa, *J. Catal.*,

71 (1981) 257.

29. Wang, W-F. Chang, R-J. Shiau, J-C. Wu and C-S. Chung, *J. Catal.*, 83 (1983) 438.
30. T. G. Alkhazov, A. E. Lisovski, M. Safarov and A. M. Dadasheva, *Kinet. Catal.*, 13 (1972) 509.
31. G. Bagnasco, P. Ciambelli, M. Turco, A. La Ginestra and P. Partono, *Appl. Catal. A. Gen.*, 68 (1991) 69.
32. A. Hagemeyer, W. J. Poeoel, W. Buechele, O. Hofstadt, A. Deimling and W. Hoffman, German Patent, DE 4422770 (1996).

\*\*\*\*\*

### *Beckmann Rearrangements*

#### **Abstract**

---

*The catalytic efficiency of the supported ceria catalysts in the gas-phase Beckmann rearrangement of salicylaldoxime and cinnamaldoxime has been presented in this chapter. The effect of various reaction parameters like temperature of the reaction, feed rate, time on stream etc. are investigated in detail to have better performance of the catalysts. The catalysts are found to be efficient for the preparation of benzoxazole by the Beckmann rearrangement of salicylaldoxime, and isoquinoline by the rearrangement of cinnamaldoxime. Surface acid amount of the catalytic systems was found to play a decisive role in determining the activity and selectivity in the reaction.*

---

## SECTION 1

### BECKMANN REARRANGEMENT OF SALICYLALDOXIME

#### 6.1 Introduction

Benzoxazoles are of great interest as they have a number of optical applications such as photoluminescents, whitening agents and laser dyes<sup>1-3</sup>. They are also used as intermediates for organic synthesis and therapeutic materials<sup>4-5</sup>. They are usually synthesized by the condensation of 2-aminophenols with benzaldehyde or benzoic acid derivatives, followed by intramolecular cyclization<sup>6-7</sup>. Recently Hiratani et al. demonstrated a novel synthetic method for the preparation of 2-substituted bis(benzoxazole) derivatives from 1, 3-bis(phenyloxy)-2-methylene propanes having carbamoyl groups at the o-position of the phenyl group via tandem Claisen rearrangement. These bis(benzoxazoles) are applicable to thermo-induced fluorescence materials<sup>8</sup>.

2-(Hydroxyphen-2'-yl) benzoxazole and its derivatives have been studied due to their interesting spectroscopic and photophysical properties<sup>9-10</sup>. This molecule shows fluorescent emission with a large Stokes shift that originates from an intermolecular proton-transfer reaction in the electronic excited state (ESIPT)<sup>11</sup>. This phenomenon has widespread implications in the action of many lasing dyes, photostabilizers and in biology<sup>12</sup>. Within the ensemble of bezoxazole type dyes, one important molecule is 2, 5-bis(benzoxazol-2'-yl)-4-methoxyphenol due to its great photostability and very high quantum yield in fluorescence emission. This molecule exhibits dual luminescence, even in aprotic solvents<sup>13</sup>.

Serotonin (5-hydroxytryptamine, 5-HT) mediates a wide range of pharmacological effects in the central and peripheral nervous systems<sup>14</sup>. Among the seven classes of 5-HT receptor subtypes (5-HT<sub>1</sub>-5-HT<sub>7</sub>), particular attention has been focused on the 5-HT<sub>3</sub> receptor in medicinal chemistry. The 5-HT<sub>3</sub> receptor antagonists prevent the nausea and vomiting that commonly occur during cytotoxic cancer chemotherapy

and/or radiation therapy. Yamada et al. prepared a series of benzoxazoles with a nitrogen-containing heterocyclic substituent at the 2-position and evaluated for 5-HT<sub>3</sub> partial agonist activity on isolated guinea pig ileum<sup>15</sup>. It was found that the nature of the substituent at the 5-position of the benzoxazole ring affected the potency for the 5-HT<sub>3</sub> receptor, and the 5-chloro derivatives showed increased potency. 5-Chloro-7-methyl-2-(4-methyl-1-homopiperaziny) benzoxazole exhibited a high binding affinity in the same range as that of the 5-HT<sub>3</sub> antagonist granisetron, and its intrinsic activity was 12% of that of 5-HT. Compounds of this type are expected to be effective for the treatment of irritable bowel syndrome (IBS) without the side effect of constipation.

Aromatic polybenzoxazoles have excellent mechanical and thermal properties. These polymers can be spun into ultrahigh-strength fibers and are capable of being used in the area of conventional and molecular composites<sup>16-20</sup>. Synthesis of aromatic polybenzoxazoles is generally achieved by two different synthetic methods. One is a one-step method using poly(phosphoric acid) (PPA), phosphorous pentoxide/methane sulphonic acid (PPMA) or trimethylsilyl polyphosphate (PPSE) /o-dichlorobenzene as the reaction medium based on bis-(o-aminophenols) and aromatic diacids<sup>21-23</sup>. The other one is a two-step method, a poly(o-hydroxyamide) which is initially synthesized by condensation of an aromatic diacid chloride with bis(o-aminophenol), then thermally cyclized with loss of water in the bulk state or in solution to the final aromatic benzoxazole polymer<sup>24-26</sup>. In fact, mononuclear o-aminophenols used as monomers for polybenzoxazoles, are readily oxidized. This determines their use as trimethylsilyl derivatives or hydrochlorides. It is also reported that aramides, containing a cyano, nitro or halogen group ortho to the amide nitrogen can be converted thermally at high temperatures to benzoxazole polymers via intramolecular aromatic nucleophilic displacement reaction by the amide oxygen<sup>27-28</sup>. More recently, Mathias demonstrated a successful thermal conversion of hydroxy-containing polyimides to polybenzoxazoles with loss of carbondioxide<sup>29</sup>. Although

aromatic polybenzoxazoles have long been of interest for their excellent properties, low solubility and difficult processability limited these materials as choices for new material development. Efforts in the synthesis of processable polybenzoxazoles led to fluorinated monomers and copolymers via preformed benzoxazole linkages<sup>30-31</sup>.

In the presented study an attempt is made to prepare benzoxazole by the Beckmann rearrangement of salicylaldehyde over different transition metal (W, Mo & Cr) incorporated pure ceria and its sulphated derivatives. Not much literature is available on the use of solid acids in these types of reaction.

Since Beckmann rearrangement is an acid catalyzed reaction, an attempt is also made to correlate the acid structural properties with the catalytic activity. The reaction conditions such as temperature of the reaction, feed rate, time on stream etc. are optimized to have better performance of the catalytic systems. The results of the study reveal that the catalytic systems prepared can act as versatile catalysts for the Beckmann rearrangement of salicylaldehyde with high selectivity towards benzoxazole.

## **6.2 Beckmann rearrangement of salicylaldehyde**

The vapour phase Beckmann rearrangement of salicylaldehyde was carried out in a conventional fixed bed reactor and the experimental procedure is given in section 2.6 of Chapter 2. The reaction products were identified by the gas chromatographic analysis of the reaction mixture by comparing with the authentic samples. Further confirmation was done by the gas chromatography-mass spectrum analysis. Among the various products formed, benzoxazole was found as the major product. The catalytic activity was expressed as the percentage conversion of salicylaldehyde and the selectivity for a particular product is expressed as the amount of that product divided by the total amount of products, multiplied by 100.

### 6.3 Process optimisation

The reaction conditions such as temperature of reaction, flow rate, time on stream etc. were studied to optimise the conversion of salicylaldoxime and the selectivity towards benzoxazole. The results are presented below.

#### I. Effect of temperature

The conversion of salicylaldoxime and selectivity to different products at different temperatures is shown in Table 6.1 and Figure 6.1. The reaction temperature was varied from 150 to 300 °C, and the reactions were performed over the representative sample CM<sub>15</sub> with a flow rate of 4 mL/h.

Table 6.1  
Influence of reaction temperature on salicylaldoxime  
conversion and product selectivity

Temperature (°C)	Conversion (%)	Selectivity (%)			
		Phenol	Nitrile	Salicylaldehyde	Benzoxazole
150	93.1	-	2.6	42.3	55.1
200	98.7	-	3.8	13.1	83.2
250	100	58.9	4.3	10.2	26.6
300	100	82.6	4.7	-	12.7

Catalyst-0.5 g CM<sub>15</sub>, flow rate-4 mL/h, time on stream-2 h

The results presented in Table 6.1 reveal that the oxime conversion increases with increase in temperature. Above 200 °C, complete conversion of salicylaldoxime is observed. The selectivity towards benzoxazole reaches a maximum at 200 °C, and decreases at higher temperatures, while there is an increase in the phenol selectivity with temperature. The selectivity for salicylaldehyde has found to decrease with temperature.

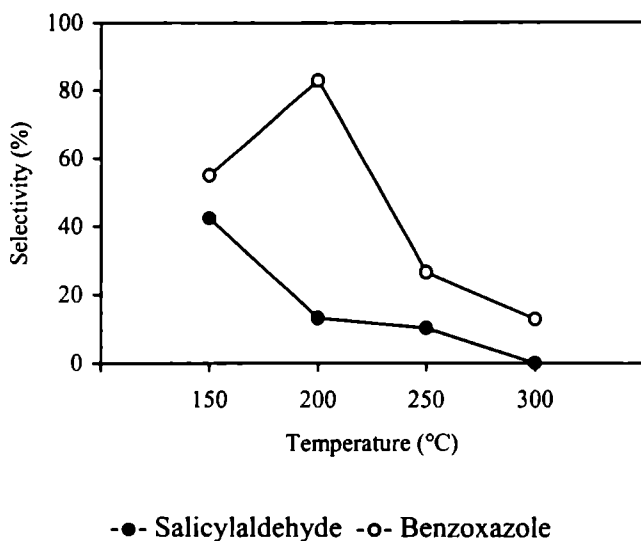


Figure 6.1

Influence of temperature on product selectivity

Catalyst-0.5 g  $CM_{15}$ , flow rate-4 mL/h, time on stream -2 h

Temperature was found to have a promotional effect in the conversion of salicylaldoxime. Above 200 °C, though there is complete conversion of oxime, a lower selectivity for benzoxazole is observed. Higher temperature was found to facilitate the decarboxylation process, thereby yielding phenol as the major product.

## II. Effect of flow rate

The influence of flow rate on the conversion of salicylaldoxime and selectivity of the products over  $CM_{15}$  catalyst is shown in Table 6.2 and Figure 6.2. The reaction temperature was kept as 200 °C and the flow rates were varied from 3 to 6 mL/h.

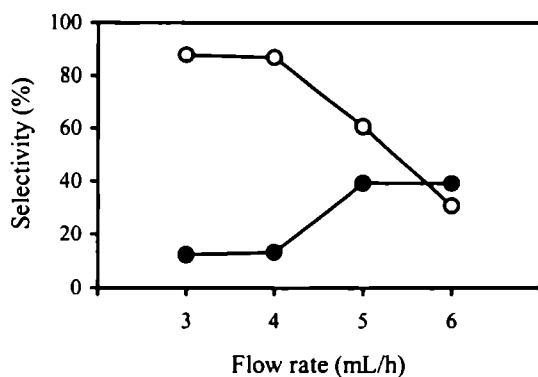
Table 6.2

Influence of flow rate on salicylaldehyde conversion and product selectivity

Flow rate (mL/h)	Conversion (%)	Selectivity (%)			
		Phenol	Nitrile	Salicylaldehyde	Benzoxazole
3	99.9	-	0.1	12.4	87.5
4	98.7	-	0.2	13.1	86.8
5	99.7	10.0	0.4	29.4	60.6
6	99.9	30.2	0.6	39.1	30.7

Catalyst-0.5 g  $CM_{15}$ , reaction temperature-200 °C, time on stream -2 h

It can be seen from Table 6.2 that there is no change in the conversion upon increasing the flow rate from 3 to 6 mL/h. The selectivity of benzoxazole remains almost the same for the flow rates 3 & 4 mL/h. Higher flow rates were found to decrease the benzoxazole selectivity. A gradual increase is observed regarding the selectivity of salicylaldehyde with flow rate. Formation of phenol is noticed at 5 and 6 mL/h. At all flow rates a negligible amount of nitrile is also formed.



-●- Salicylaldehyde -○- Benzoxazole

Figure 6.2

Influence of flow rate on product selectivity

Catalyst-0.5 g  $CM_{15}$ , reaction temperature-200 °C, time on stream -2 h

Results presented in the Table 6.2 and Figure 6.2 show that flow rate does not have much influence in determining the rate of this reaction. But the selectivity towards various products was strongly influenced by the feed rate. Higher flow rates were found to result in the formation of appreciable amount of phenol.

### III. Effect of time on stream

A set of experiments were carried out to evaluate the stability of the systems with reaction time. In order to test the deactivation of the prepared systems, we have carried out the reaction continuously for 8 hours at 200 °C and the reaction mixture was analysed at intervals of one hour. The flow rate was maintained at 4 mL/h and the reaction was carried out over the representative sample CM<sub>15</sub>. The results are presented in Figure 6.3.

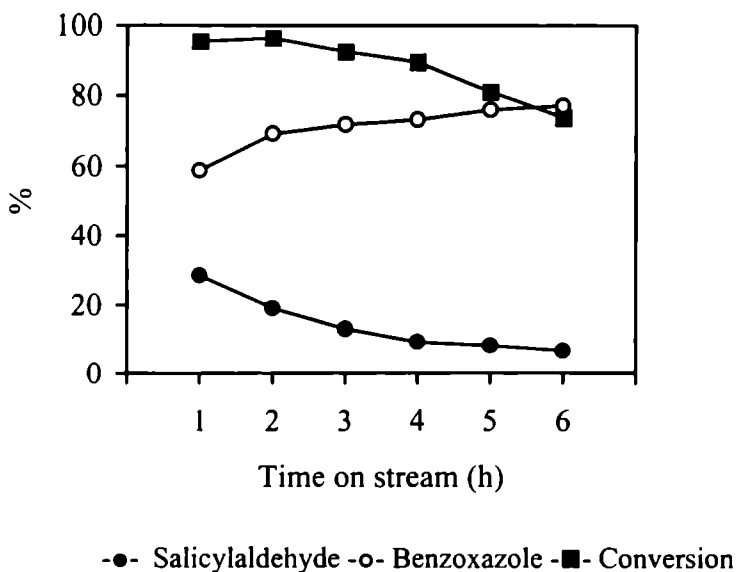


Figure 6.3

Influence of time on stream on product selectivity and conversion  
Catalyst-0.5 g CM<sub>15</sub>, reaction temperature-200 °C, flow rate-4 mL/h

The results presented in Figure 6.3 show that the reactivity of the catalyst systems decreases with time on stream, while the selectivity to benzoxazole goes on increasing. Though in the second hour there is a small increase in the conversion of oxime on subsequent hours the catalytic activity declines with time. The benzoxazole selectivity increases from 58.7 to 77.1% as the reaction time is increased to 6 hours. At the same time the selectivity to salicylaldehyde shows a continuous decrease with time. The reduction in catalytic activity with time may be due to the strong adsorption of basic products and reactants in the acid sites.

#### 6.4 Activity of different catalytic systems

A comparison of the catalytic activity of modified ceria catalysts in the vapour phase Beckmann rearrangement is discussed in the following section. All the reactions were done at a temperature of 200 °C for 2 hrs at a flow rate of 4 mL/h. An attempt has been made to correlate the acid structural properties with catalytic activity.

##### a) Tungsten incorporated systems

Table 6.3 presents the catalytic activity of various tungsten oxide incorporated ceria catalysts together with sulphated analogues for the vapour-phase Beckmann rearrangement of salicylaldoxime.

From Table 6.3, it is perceptible that among the simple supported systems, the catalytic activity is almost similar for  $CW_{10}$  and  $CW_{15}$  system. Moreover all the sulphated systems exhibit 100% conversion towards the reaction. Although there is not much change in the catalytic activity among the systems, the selectivity to different products varies considerably. The formation of phenol is observed only in the low loaded samples. With regard to benzoxazole selectivity,  $CSW_{10}$  gives the highest selectivity and it amounts to 77.6%. Pure ceria exhibits very low selectivity towards benzoxazole. However, salicylaldehyde selectivity is the highest in this case. Figure 6.4 illustrates the dependence of benzoxazole selectivity with the amount of weak plus medium acid sites present in the catalytic systems.

Table 6.3  
Catalytic activity of tungsten incorporated ceria systems

Catalytic systems	Conversion (%)	Selectivity (%)			
		Phenol	Nitrile	Salicyl-aldehyde	Benz-oxazole
C	91.5	1.7	2.1	94.8	1.3
SC	94.8	-	9.9	25.2	64.9
CW <sub>5</sub>	92.7	8.2	11.1	27.8	52.9
CW <sub>10</sub>	96.7	5.9	15.2	30.3	48.6
CW <sub>15</sub>	95.1	-	9.4	31.9	58.7
CSW <sub>5</sub>	100	5.4	14.3	20.4	60.1
CSW <sub>10</sub>	100	1.5	10.2	12.1	77.6
CSW <sub>15</sub>	100	-	9.1	20.7	70.2

Catalyst-0.5 g, reaction temperature-200 °C, time on stream -2 h, flow rate-4 mL/h.

Comparing the acidity pattern and the benzoxazole selectivity presented in Figure 6.4, it is clear that the weak plus medium acid sites play an important role in determining the benzoxazole selectivity. In the case of pure ceria very little formation of benzoxazole is noticed, whereas almost all the modified systems show selectivities greater than 50%. In the case of modified systems CSW<sub>10</sub> gives the highest selectivity towards benzoxazole, in accordance with the amount of weak plus medium acid sites and it amounts to 77.6%.

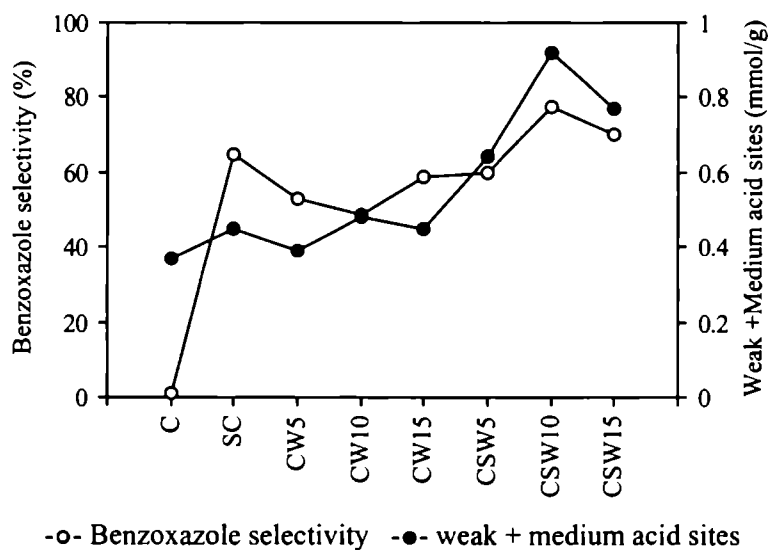


Figure 6.4

Correlation of amount of weak plus medium acid sites from TPD measurements with benzoxazole selectivity

### b) Molybdenum incorporated systems

The results obtained for molybdena doped ceria systems and their sulphated analogues in the Beckmann rearrangement of salicylaldehyde is presented in Table 6.4. The influence of surface acidity in determining the selectivity towards benzoxazole is shown in Figure 6.5.

Table 6.4 shows that in the case of molybdenum doped systems also, there is not much change in the percentage conversion with rise in molybdenum concentration, but there is significant change in the selectivity to different products. In the case of simple supported systems, the selectivity to benzoxazole at first decreases with increase in molybdena loading and then an increase is observed for the  $CM_{15}$  system. Similar trend is seen in the case of sulphated systems also.  $CM_{10}$  and  $CSM_{10}$  possess the maximum selectivity to salicylaldehyde in the case of molybdenum incorporated simple and sulphated series.

Table 6.4  
Catalytic activity of molybdenum incorporated ceria systems

Catalytic systems	Conversion (%)	Selectivity (%)			
		Phenol	Nitrile	Salicyl-aldehyde	Benzoxazole
C	91.5	1.7	2.1	94.8	1.3
SC	94.8	-	9.9	25.2	64.9
CM <sub>5</sub>	98.9	-	13.4	15.2	71.4
CM <sub>10</sub>	95.2	-	10.5	24.2	65.2
CM <sub>15</sub>	96.3	-	11.7	19.1	69.3
CSM <sub>5</sub>	97.2	1.6	11.5	12.8	74.1
CSM <sub>10</sub>	95.6	1.2	15.9	25.2	57.6
CSM <sub>15</sub>	100	0.7	9.8	8.1	81.4

Catalyst-0.5 g, reaction temperature-200 °C, time on stream-2 h, flow rate-4 mL/h.

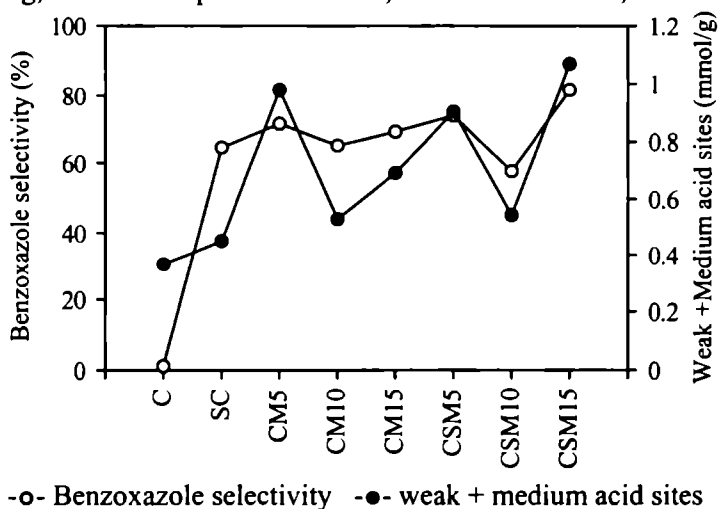


Figure 6.5

Correlation of amount of weak plus medium acid sites from TPD measurements with benzoxazole selectivity

Figure 6.5 clearly shows that the variation of benzoxazole selectivity is in accordance with the amount of weak plus medium acid sites obtained from ammonia TPD method. The amount of weak plus medium acid sites possessed by the catalysts was found to decrease at first with increase in molybdenum loading and thereafter increases. The selectivity to benzoxazole also follows the same pattern.

### c) Chromium incorporated systems

Table 6.5 represents the results of reactions carried out over chromia incorporated ceria systems under optimised conditions. The correlation between the benzoxazole selectivity and the amount of weak plus medium acid sites is shown in Figure 6.6.

Table 6.5  
Catalytic activity of chromium incorporated ceria systems

Catalytic systems	Conversion (%)	Selectivity (%)			
		Phenol	Nitrile	Salicyl-aldehyde	Benz-oxazole
C	91.5	1.7	2.1	94.8	1.3
SC	94.8	-	9.9	25.2	64.9
CCr <sub>5</sub>	100	0.8	13.7	14.2	71.3
CCr <sub>10</sub>	96.1	1.2	10.5	40.1	48.2
CCr <sub>15</sub>	97.0	3.0	11.1	38.1	47.8
CSCr <sub>5</sub>	97.8	1.1	12.3	34.0	52.6
CSCr <sub>10</sub>	100	2.8	12.9	31.2	53.1
CSCr <sub>15</sub>	100	2.2	14.2	12.9	70.7

Catalyst-0.5 g, reaction temperature-200 °C, time on stream-2 h, flow rate-4 mL/h.

In the case of chromium incorporated sulphated systems, complete conversion of salicylaldehyde is observed for the high loaded sulphated samples ( $\text{CSCr}_{10}$  &  $\text{CSCr}_{15}$ ), but in the case of simple systems  $\text{CCr}_5$  gives the complete conversion. The selectivity to benzoxazole was found to decrease with increase in chromium loading in simple systems, whereas in the case of sulphated systems the selectivity varies in a reverse order. The formation of phenol is observed in all the cases.

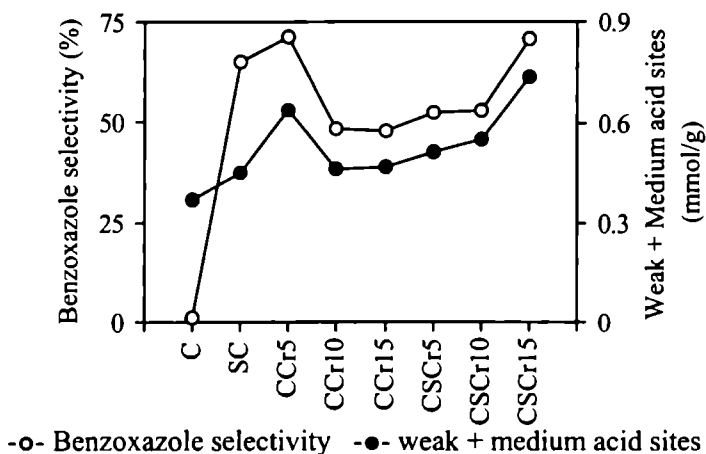


Figure 6.6

Correlation of amount of weak plus medium acid sites from TPD measurements with benzoxazole selectivity

Figure 6.6 clearly points to the active participation of the weak plus medium acid sites in determining the benzoxazole selectivity. The amount of weak plus medium acid sites possessed by the systems  $\text{CCr}_5$  and  $\text{CSCr}_{15}$  is found to be almost the same. In accordance with their acidity value these systems are found to give almost similar benzoxazole selectivity. Similar is the case with  $\text{CCr}_{10}$ - $\text{CCr}_{15}$  and  $\text{CSCr}_5$ - $\text{CSCr}_{10}$  systems also.

## 6.5 Conclusions

- \* Transition metal (W, Mo & Cr) promoted ceria systems and their sulphated analogues are proved to be efficient catalysts in the vapour-phase Beckmann

rearrangement of salicylaldoxime.

- \* The reaction yielded salicylaldehyde and benzoxazoles as the major products while phenol and nitriles are formed as minor products.
- \* The reaction conditions such as temperature of the reaction, flow rate and time on stream have profound influence in determining the selectivity towards various products.
- \* Surface acidity, especially the weak plus medium acid sites play a significant role in the formation of benzoxazole.

## SECTION 2

### BECKMANN REARRANGEMENT OF CINNAMALDOXIME

#### 6.6 Introduction

Alkaloids are well known as biologically active substances. Many of them have been reported to possess antiviral, antimicrobial and immunomodulating activities. Alkaloids are also demonstrated to be potent antitumor agents. Vinca alkaloids are an important class of currently used anticancer drugs, applied in the combination therapy of leukemia and solid tumors. Other alkaloids are in different stages of pre-clinical and clinical trials. Isoquinoline is the main heterocyclic ring for a class of alkaloids, that have medicinal and toxic properties. Isoquinoline alkaloids such as protopine, hernandezine and thalfoe-tidine are found to have cytotoxic activity on tumor cell lines.

Repair and maintenance of chromosomes are, in part, controlled by the addition and removal of polymers of ADP-ribose to the DNA-binding proteins involved<sup>1</sup>. ADP-ribose units are added by poly(ADP-ribose) polymerase (PARP) and removed by poly(ADP-ribose)glycohydrolase (PARG). The involvement of poly (ADP-ribosyl)ation in a wide range of physiological and pathophysiological processes renders it a useful target to study biological systems and for therapeutic intervention

strategies. Pathophysiological effects are mediated through over activity of the isoform PARP-1, which depletes stores of nicotinamide adenine dinucleotide (NAD<sup>+</sup>), the PARP substrate, leading to cell death. 5-substituted isoquinoline-1-ones are potent inhibitors of PARP with potential therapeutic applications in several diseases, including cancer, myocardial infarction, diabetes, stroke, rheumatoid arthritis, haemorrhagic shock, and retroviral infections<sup>2-8</sup>. As a regulatory enzyme, PARP has beneficial roles in health and detrimental roles in disease and, therefore, inhibitors need to be targeted selectively to diseased tissues.

Bischler-Napieralski cyclization is one of the best routes for the synthesis of isoquinoline. In this reaction a  $\beta$ -phenethylamide is made to undergo cyclodehydration to a 3, 4-dihydroisoquinoline by heating with condensing agents such as phosphorous pentoxide or anhydrous zinc chloride at high temperature or phosphoryl chloride, phosphorous pentachloride at lower temperatures. Dehydrogenation to the isoquinoline may be effected by heating the dihydro compound with sulphur or selenium, or catalytically with palladium black<sup>9-11</sup>. However these catalysts are highly corrosive and some of them are hygroscopic nature, which makes their handling very difficult. In the present work we have synthesized isoquinoline by the vapour phase Beckmann rearrangement of cinnamaldoxime.

### **6.7 Beckmann rearrangement of cinnamaldoxime**

The vapour-phase Beckmann rearrangement of cinnamaldoxime was carried out in a conventional fixed bed reactor and the experimental procedure is given in section 2.6 of Chapter 2. The reaction yielded cinnamionitrile and isoquinoline as the major products. Among the various side products formed, only cinnamaldehyde was estimated, while all the remaining minor products were grouped under 'side products'. The catalytic activity was expressed as the percentage conversion of cinnamaldoxime. The influence of reaction conditions such as temperature of the reaction, flow rate and time on stream were also investigated in detail.

## 6.8 Process optimisation

Reactions were performed under atmospheric pressure in presence of  $N_2$  to have inert atmosphere. The results of optimization of the reaction conditions are given below.

### I. Effect of temperature

The influence of reaction temperature on the total conversion and selectivity to different products is presented in Table 6.6. The reaction temperature was varied from 150 to 300 °C and the reactions were done over the representative sample  $CM_{15}$ .

Table 6.6  
Influence of reaction temperature on cinnamaldoxime conversion  
and product selectivity

Temperature (°C)	Conversion (%)	Selectivity (%)			
		Cinnamo- nitrile	Cinnamal- dehyde	Isoquinoline	Side products
150	95.6	38.4	1.2	59.6	0.8
200	99.8	52.4	0.3	46.1	1.2
250	100	58.2	-	39.5	2.3
300	100	63.8	-	32.3	3.9

Catalyst-0.5 g  $CM_{15}$ , flow rate-4 mL/h, time on stream -2 h

Results presented in Table 6.6 indicates that as the temperature of the reaction increases, there is enhancement in the conversion of cinnamaldoxime and 100% conversion is observed at temperatures above 200 °C. This increase in percentage conversion is at the cost of selectivity to isoquinoline which is only 32.3% at 300 °C.

## II. Effect of feed rate

The feed rate of the reactants were found to alter the catalytic activity to a great extent. To show this, a series of reactions were carried out at different flow rates (3-6 mL/h) over the representative sample  $CM_{15}$  and the results are presented in Table 6.7.

Table 6.7

Influence of flow rate on cinnamaldoxime conversion and product selectivity

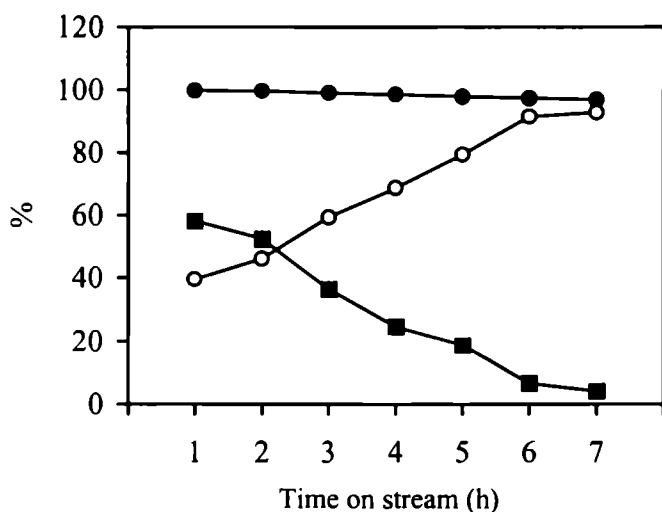
Flow rate (mL/h)	Conversion (%)	Selectivity (%)			
		Cinnamo- nitrile	Cinnamal- dehyde	Isoquinoline	Side products
3	100	58.6	0.1	38.7	0.8
4	99.8	52.4	0.3	46.1	1.2
5	95.2	48.5	1.7	43.9	5.8
6	90.9	47.3	5.8	39.6	7.2

Catalyst-0.5 g  $CM_{15}$ , reaction temperature-200 °C, time on stream -2 h

As can be observed from the Table 6.7, the conversion decreases from 100 to 90.9% as the flow rate is increased from 3 to 6 mL/h. At the same time selectivity of isoquinoline show an initial increase at 4 mL/h (46.1%) and then decreases continuously. The flow rates of the reactants were found to alter the contact time of the reactants and higher flow rates lead to a reduction in catalytic activity. However the trend in which the selectivity to isoquinoline varies suggests that the 4 mL/h is the optimum feed rate for the reactants for the formation of the desired product.

### III. Effect of time on stream

In order to find the effect of reaction time on the conversion of cinnamldoxime and selectivity for isoquinoline, reaction was carried out for 7 hours, and the products were analyzed at every hour. The results of the deactivation study are depicted in Figure 6.7.



-●- Conversion -○- Isoquinoline selectivity -■- Cinnamaldehyde selectivity

Figure 6.7

Influence of time on stream on product selectivity and conversion

Catalyst-0.5 g  $CM_{15}$ , reaction temperature-200 °C, flow rate-4 mL/h

The results presented in Figure 6.7 indicate that the reactivity of the catalytic systems decreases slightly after seven hours of reaction run. But the selectivity to cinnamionitrile and isoquinoline varies significantly with time. Isoquinoline selectivity was found to increase with time at the expense of selectivity to cinnamaldehyde. Deactivation studies point to the fact that the catalytic systems possess reasonable stability even after seven hours of reaction. The small decrease in activity may be due to the adsorption of basic reactants and products in the acid sites.

### 6.9 Performance of different catalyst systems

A comparative evaluation of the catalytic activity of various ceria catalysts in the vapour-phase Beckmann rearrangement of cinnamaldoxime is presented in this section. Under optimized conditions of reaction temperature 200 °C and flow rate 4 mL/h, all the prepared systems were tested for activity over a reaction time of 2 hrs. An attempt has been made to correlate the surface acidity and the catalyst efficiency.

#### a) Tungsten incorporated systems

Table 6.8 shows the catalytic activities of various tungsten incorporated ceria systems together with its sulphated analogues for the vapour phase Beckmann rearrangement of cinnamaldoxime.

Table 6.8  
Catalytic activity of tungsten incorporated systems

Catalyst	Conversion (%)	Selectivity (%)			
		Cinnamo-nitrile	Cinnamal-dehyde	Isoquinoline	Side products
C	89.6	54.5	3.5	42.0	-
SC	96.5	71.7	3.1	25.2	-
CW <sub>5</sub>	92.3	63.3	0.5	35.9	0.3
CW <sub>10</sub>	100	50.1	0.7	48.8	0.4
CW <sub>15</sub>	96.5	59.0	1.0	39.2	0.8
CSW <sub>5</sub>	99.6	43.1	0.5	55.2	1.2
CSW <sub>10</sub>	100	31.5	0.7	66.9	0.9
CSW <sub>15</sub>	99.9	45.8	0.4	52.4	1.4

Catalyst-0.5 g, reaction temperature-200 °C, time on stream-2 h, flow rate-4 mL/h

From Table 6.8, it is clear that pure ceria has the lowest catalytic activity among the different systems. Almost cent percentage activity is shown by the tungsten doped systems. But the selectivity to cinnamionitrile and isoquinoline changes significantly among the systems. Maximum selectivity to isoquinoline is obtained for the  $CSW_{10}$  system, where it amounts to 66.9%. All the sulphated samples show higher selectivity to isoquinoline than the simple supported systems. The influence of surface acidity in the formation of isoquinoline is depicted in Figure 6.8.

Figure 6.8 clearly shows that weak plus medium strength acid sites influence the formation of isoquinoline.  $CW_{10}$  and  $CSW_{10}$  possess the highest amount of weak plus medium acid sites among the simple supported and sulphated series respectively, which in turn gives the highest selectivity to isoquinoline among the corresponding systems. A comparison of the number of weak plus medium acid sites of tungsten incorporated simple and sulphated systems points to the fact that tungsten incorporated sulphated systems possess more number of weak plus medium acid sites than the simple systems. In a similar way selectivity to isoquinoline is higher for the tungsten incorporated sulphated systems.

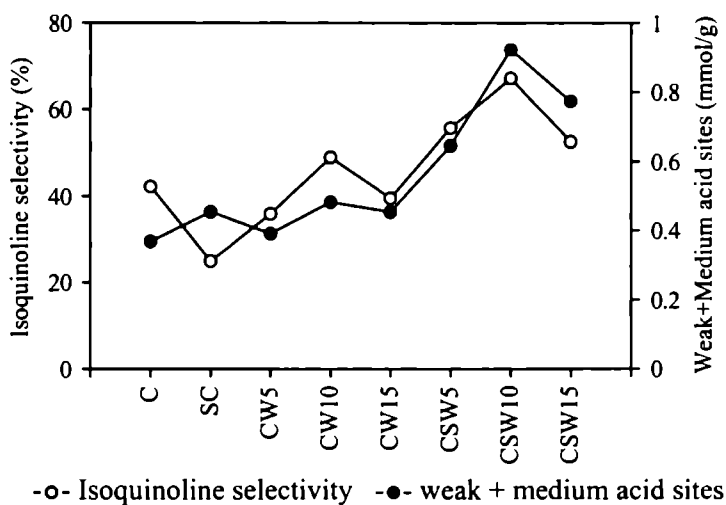


Figure 6.8

Correlation of amount of weak plus medium acid sites from TPD measurements with isoquinoline selectivity

**b) Molybdenum incorporated systems**

The catalytic activity of different molybdenum modified ceria catalysts and its sulphated analogues is presented in Table 6.9.

Table 6.9

Catalytic activity of molybdenum incorporated systems

Catalyst	Conversion (%)	Selectivity (%)			
		cinnamo-nitrile	cinnamal-dehyde	isoquinoline	side products
C	89.6	54.5	3.5	42.0	-
SC	96.5	71.7	3.1	25.2	-
CM <sub>5</sub>	100	34.9	0.2	64.8	0.1
CM <sub>10</sub>	97.8	59.2	0.1	40.4	0.3
CM <sub>15</sub>	99.8	52.4	0.3	46.1	1.2
CSM <sub>5</sub>	100	45.8	0.2	53.1	0.9
CSM <sub>10</sub>	98.1	55.1	0.5	43.3	1.1
CSM <sub>15</sub>	100	34.4	1.2	60.7	3.7

Catalyst-0.5 g, reaction temperature-200 °C, time on stream-2 h, flow rate-4 mL/h

The results show that incorporation of molybdenum into pure cerium oxide enhances the catalytic activity towards the reaction. High catalytic activity is exhibited by all systems. The selectivity towards various products varies considerably with change in molybdenum concentration. Systems with 10 wt% molybdenum give highest selectivity to cinnamonnitrile whereas, reverse trend is observed in the case of isoquinoline selectivity. In all the cases negligible amounts of cinnamaldehyde is also formed. The dependence of isoquinoline selectivity on the amount of weak plus medium acid sites are shown in Figure 6.9.

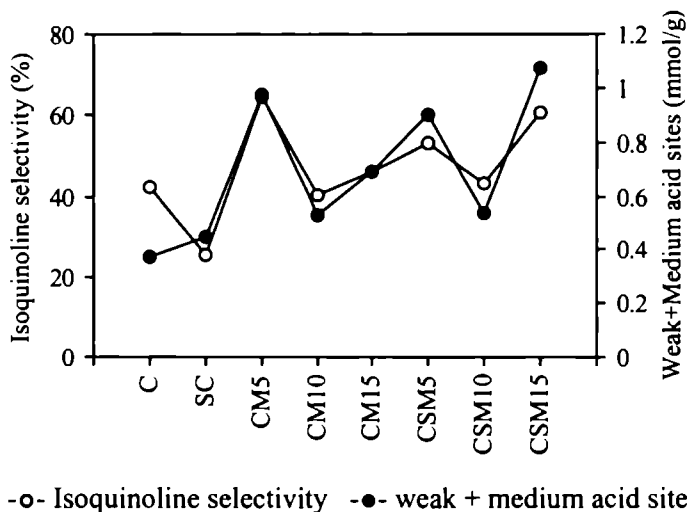


Figure 6.9

Correlation of amount of weak plus medium acid sites from TPD measurements with isoquinoline selectivity

There is good agreement between the amount of weak plus medium acid sites and selectivity to isoquinoline. As clear from the Figure 6.9 among the different systems, CM<sub>5</sub> possess highest number of weak plus medium acid sites as obtained from TPD of ammonia. It gives 64.8% of isoquinoline.

### c) Chromium incorporated systems

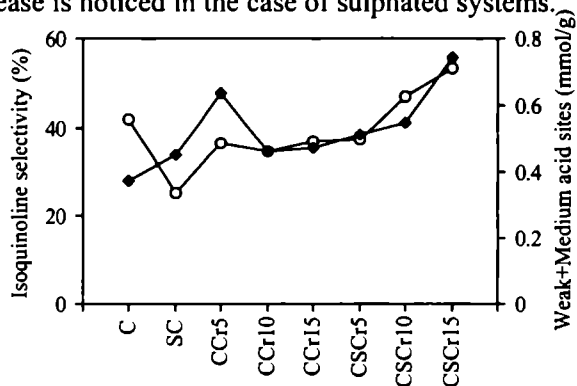
The results obtained for chromium doped systems are presented in Table 6.10. A one-to-one comparison between the selectivity to isoquinoline and the amount of weak plus medium acid sites is presented in Figure 6.10.

Table 6.10  
Catalytic activity of chromium incorporated systems

Catalyst	Conversion (%)	Selectivity (%)			
		Cinnam-nitrile	Cinnamal-dehyde	Isoquinoline	Side products
C	89.6	54.5	3.5	42.0	-
SC	96.5	71.7	3.1	25.2	-
CCr <sub>5</sub>	98.7	61.2	1.4	36.5	0.9
CCr <sub>10</sub>	96.9	53.0	8.2	34.4	4.4
CCr <sub>15</sub>	97.8	55.6	2.5	36.7	5.2
CSCr <sub>5</sub>	98.0	57.6	3.9	37.3	1.2
CSCr <sub>10</sub>	98.2	48.8	2.9	46.9	1.4
CSCr <sub>15</sub>	99.8	42.5	1.4	53.3	2.8

Catalyst-0.5 g, reaction temperature-200 °C, time on stream-2 h, flow rate-4 mL/h

Table 6.10 shows that chromium incorporated sulphated systems give higher selectivity to isoquinoline than the simple doped systems. This is in accordance with the amount of weak plus medium acid sites possessed by them, which is clear from Figure 6.10. The selectivity to cinnamonnitrile decreases as the chromium loading is increased from 5 to 10 wt%, and then increases for the CCr<sub>15</sub> system, whereas, a continuous decrease is noticed in the case of sulphated systems.



-○- Isoquinoline selectivity -●- weak + medium acid sites

Figure 6.10

Correlation of amount of weak plus medium acid sites from TPD measurements with isoquinoline selectivity

## 6.10 Conclusions

- \* Supported ceria catalysts afford high activity and selectivity in the vapour-phase Beckmann rearrangement of cinnamaldoxime.
- \* Isoquinoline and cinnamionitrile are formed as the major products during the reaction with small amounts of cinnamaldehyde.
- \* The catalytic behavior is influenced by the reaction parameters like reaction temperature, feed rate and time on stream significantly. Deactivation studies suggest small reduction in catalytic activity, pointing to the stability of the catalytic systems with time.
- \* Surface acidity of the catalysts, especially the number of weak plus edium acid sites, influences the formation of isoquinoline.

## REFERENCES

### SECTION 1

1. U. Claussen and H. Harnisch, *Eur. Pat. Appl.*, 25 (1981) 136.
2. S. Stendby, *Surfactant Sci. Ser.*, 5 (1981) 729.
3. A. Reser, L. J. Leyshon, D. Saunders, M. V. Mijovic, A. Bright and J. Bogie, *J. Am. Chem. Soc.*, 94 (1972) 2414.
4. J. Roussilhe, E. Fargin, A. Lopez, B. Despax and N. Pailous, *J. Org. Chem.*, 48 (1983) 3736.
5. I. N. Houpis, A. Molina, J. Lynch, R. A. Reamer, R. P. Volante and P. J. Reider, *J. Org. Chem.*, 58 (1993) 3176.
6. R. D. Desali, R. F. Hunter and A. R. K. Khakidi, *J. Chem. Soc.*, (1934) 1186.
7. R. J. Perry, *J. Org. Chem.*, 57 (1992) 2883.
8. E. Koyama, G. Yang and K. Hiratani, *Tetrahedron Lett.*, 41 (2000) 8111.
9. M. F. Rodriguez Prieto, B. Nickel, K.H. Grellmann and A. Mordzinski, *Chem. Phys. Lett.*, 146 (1988) 387.
10. A. Mordzinski, *Chem. Phys. Lett.*, 150 (1988) 254.
11. A. Mordzinski and W. Kühnle, *J. Phys. Chem.*, 90 (1986) 1455.

12. K. Das, N. Sarkar, A. K. Ghosh, D. Majumdar, N. D. Nath and K. Bhattacharyya, *J. Phys. Chem.*, 98 (1994) 9126.
13. A. Mordzinski, A. Grabowska, W. Kuhnle and A. Krowczynski, *Chem. Phys. Lett.*, 101 (1983) 291.
14. G. J. Kilpatrick, K.T. Bunce and M. B. Tyers, *5-HT<sub>3</sub> Receptors. Med. Chem. Res. Rev.*, 10 (1990) 441.
15. Y. Sato, M. Yamada, S. Yoshida, T. Soneda, M. Ishikawa, T. Nizato, K. Suzuki, and F. Konno, *J. Med. Chem.*, 41 (1998) 3015.
16. C. Arnold Jr, *J. Polym. Sci. Macromol. Rev.*, 14 (1979) 265.
17. P. E. Cassidy, *Thermally Stable Polymers*: Marcel Dekker: New York, 1980.
18. J. F. Wolfe and F. E. Arnold, *Macromolecules.*, 14 (1981) 909.
19. E. W. Choe and S. N. Kim, *Macromolecules.*, 14 (1981) 920.
20. A. W. Chow, S. P. Bitler, P. E. Penwell, J. J. Osborne and J. R. Wolfe, *Macromolecules.*, 22 (1989) 3514.
21. D. M. Dotrong, M. H. Evers and R. C. Moore, *J. Am. Chem. Soc. Prepn.*, 31(2) (1990) 675.
22. M. Ueda, H. Sugita and M. Sato, *J. Polym. Sci. Polym. Chem. Ed.*, 24 (1986) 1019.
23. P. A. Relghardt, *Polym. Commun.*, 31 (1990) 453.
24. T. Kubota and R. Nakanishi, *J. Polym. Sci. Part B.*, 2 (1964) 655.
25. W. W. Moyer, C. Cole and T. Anyos, *J. Polym. Sci. Part A.*, 3 (1965) 2107.
26. P. M. Hergenrother, W. Wrasidlo and H. H. Levine, *Am. Chem. Soc. Prepn.*, 5 (1964) 153.
27. S. Kim, E. M. Pearce and T. K. Kwei, *Polym. Adv. Technol.*, 1 (1990) 49.
28. S. S. Kim and E. M. Pearce, *Makromol. Chem. Suppl.*, 15 (1989) 187.
29. G. I. Tullos, J. M. Powers, S. J. Jeskev and I. J. Mathias, *Macromolecules.*, 32 (1999) 3598.
30. J. G. Hilborn, J. W. Labadie and J. L. Hedrick, *Macromolecules.*, 20

(1990) 2854.

31. H. R. Kricheldorf and S. A. Thomsen, *J. Polym. Sci. Polym. Chem.*, 17 (1991) 1751.
32. O. Kiyoshi and M. Akira, *J. Catal.*, 46 (1977) 71.
33. H. L. Frisch, L. Hyuang and W. Zeng, *J. Memb. Sc.*, 170 (2000) 35.

## SECTION 2

1. S. Smith, *Trends Biochem. Sci.*, 26(2001) 174.
2. C. Y. Watson, W. J. D. Wish and M. D. Threadgill, *Bioorg. Med. Chem.*, 6 (1998) 721.
3. A. W. White, R. Almasy, A. H. Calvert, N. J. Curtin, R. J. Griffin, Z. Hosaomsky, K. Maegley, D. R. Newell, S. Srinivasan and B. T. Golding, *J. Med. Chem.*, 43 (2000) 4084.
4. C. Thiemermann, J. Bowes, F. P. Myint and J. R. Vane, *Proc. Natl. Acad. Sci. U.S.A.* 94 (1997) 679.
5. F. G. Soriano, L. Virag, P. Jagtap, E. Szabo, J. G. Mabley, L. Liaudet, A. Marton, D. D. Hoyt, K. G. K. Murthy, A. L. Salzman, G. J. Southan and C. Szabo, *Nat. Med. (N. Y.)* 7 (2001) 108.
6. G. E. Abdelkarim, K. Gertz, C. Harms, J. Katchanov, U. Dirnagl, C. Szabo and M. Endres, *Int. J. Mol. Med.*, 7 (2001) 255.
7. R. W. Pero, B. Axelsson, D. Siemann, D. Chaplin and G. Dougherty, *Mol. Cell. Biochem.*, 193 (1999) 119.
8. M. C. McDonald, H. M. Filipe, J. A. Wright, M. Abderlrahman, M. D. Threadgill, A. S. Thompson and C. Thiemermann, *Br. J. Pharmacol.*, 130 (2000) 843.
9. I. L. Finar, *Organic Chemistry I* ELBS Co. Ltd. 1964.
10. W. M. Whaley and T. R. Givindachari, *Organic Reactions VI* (New York, 1951), p. 74.
11. E. P. Styngach and A. A. Semenov, *Khim. Geterotsikl. Soedin.*, 7 (1971) 621.

12. D. Bdaleton and H. G. Foley, *J. Org. Chem.*, 38 (1973) 4200.
13. H. L. Frisch, L. Hyuang and W. Zeng, *J. Memb. Sc.*, 170 (2000) 35.
14. A. Lalitha, K. Pitchumani, P. Kannan and C. Srinivasan, *Tetrahedron.*, 54 (1998) 15667.
15. K. Masanobu, T. Haruhiko, K. Yasunao and O. Shigero, *Chem. Lett.*, 10 (1997) 997.
16. O. Kiyoshi, M. Junichi and M. Akira, *J. Chem. Soc. Faraday Trans.*, 1, 77 (1981) 569.
17. O. Kiyoshi, O. Ryuji and M. Akira, *J. Catal.*, 50 (1977) 379.
18. O. Kiyoshi and M. Akira, *J. Catal.*, 46 (1977) 71.

\*\*\*\*\*

### *Methyl Tert-Butyl Ether Synthesis*

#### **Abstract**

---

*Pollution from motor vehicles is responsible in industrialised nations for ozone forming smog, hazardous carbon monoxide pollution, and other toxic air pollutants. Methyl tert-butyl ether (MTBE) is widely used as an oxygenate for gasoline not only to enhance the octane number but also to make motor vehicle fuel burn more cleanly, replacing toxic additives like lead. Also the synthesis of MTBE offers interesting insights into etherification reactions in general. In the present chapter the catalytic efficiency of transition metal (W, Mo & Cr) modified ceria systems and their sulphated analogues in the gas- phase MTBE synthesis is presented. The effect of various reaction parameters like reaction temperature, flow rate, duration of reaction and methanol to tertiary butanol molar ratio are investigated in detail. The difference in the catalytic activity of the systems has been related to the difference in the surface acidity among them. The performance of the catalytic systems points to its potential in the MTBE technology.*

---

## 7.1 Introduction

Due to strong environmental concerns about fuel emissions, the use of metal octane enhancers such as tetra-ethyl lead (TEL), tetra-methyl lead (TML), and methyl cyclopentadienyl manganese tricarbonyl (MMT) in gasoline has been phased out in many countries<sup>1-3</sup>. The concept of reformulated gasoline (RFG) was introduced in the United States to reduce hazardous emissions<sup>4-5</sup>. The addition of fuel oxygenates to gasoline for increased octane number, higher engine efficiency, and reduction of the polluting components in exhaust gases (such as CO, hydrocarbons, and polynuclear aromatics) has been one of the results of adoption of RFG. Among many potential oxygenated compounds, methyl-tert butyl ether (MTBE) has been widely utilized as a gasoline additive because of its good antiknocking properties, outstanding physical properties such as volatility, miscibility in gasoline, and help in the reduction of hazardous emissions<sup>6</sup>. It also acts as a volume extender, by adding volume to the gasoline pool and by reducing the severity of the naphtha reforming and related conversion operations. MTBE has highly favourable performance qualities from the refiner's perspective, including low sulphur content, acceptable blending vapour pressure, high miscibility in gasoline, moderate boiling point, and stability in storage. Additionally, MTBE's cost, compared to those of other high-octane components, made it the economical choice in the refinery market place.

MTBE was first manufactured commercially in the early 1970s in Europe by Chemische Werke Huls in West Germany and by ANIC in Italy<sup>7</sup>. The current commercial MTBE synthesis is a liquid-phase reaction of methanol and isobutene over sulphonated ion-exchange resins at low temperatures (30-100 °C) and moderately high pressures (usually upto 2.0 Mpa). Although the resin catalysts are very active, they have some major drawbacks such as thermal fragility, sensitivity to methanol-to-isobutene ratios, and corrosive problems<sup>8-10</sup>. In addition, the deactivated resin catalyst cannot be regenerated and must be properly disposed under current environmental regulations<sup>11</sup>. Another problem concerning MTBE production from isobutene is

that the source of isobutene is limited to catalytic cracking and steam cracking fractions of petroleum refining.

Commercially, MTBE is produced from tert-butyl alcohol (TBA), a chemical produced as a by-product in a number of reaction processes such as the Halcon process (propylene oxide synthesis), where 3.5 kg of tertiarybutanol is produced per kg of propylene oxide<sup>12</sup>. There are two ways to produce MTBE from TBA, an indirect and a direct method. In the indirect method, TBA is dehydrated to isobutene in the first reactor, followed by reaction of isobutene with methanol to produce MTBE in the second reactor<sup>13</sup>. In the direct method, MTBE is produced by reacting TBA directly with methanol in one reactor in the presence of an acid catalyst in which water is also formed as a by-product.

Inorganic solid acid catalysts such as microporous zeolites<sup>14-15</sup>, heteropoly acids (HPA's)<sup>16-18</sup> and inorganic oxides such as Nb<sub>2</sub>O<sub>5</sub>, TiO<sub>2</sub>, ZrO<sub>2</sub>, SiO<sub>2</sub><sup>19</sup> are now considered to be potential alternative catalysts for MTBE synthesis and other etherification reactions.

Zeolites have been investigated as efficient catalysts for MTBE formation. A number of papers have been published focusing on the application of zeolites such as H-Y, H-omega, H- mordenite, H-ZSM-5 and H-beta as alternative catalysts for the synthesis of MTBE<sup>20-22</sup>. Collignon et al. studied MTBE synthesis on a series of zeolites H-Beta with Si/Al ratios ranging from 13 to 194 and found that these materials are significantly more active than all other zeolite types employed. Over zeolites H-Beta with a Si/Al ratio of 25.7, a maximum MTBE yield of ca 50% was obtained at 333 K. This high catalytic activity was explained by a contribution of the large external surface of the zeolites H-Beta used as catalysts<sup>23</sup>. Investigating the MTBE synthesis on zeolites H-ZSM-5 and H-Y, Kogelbauer et al. observed an increase in the MTBE formation rate and a suppression of by-products after pre adsorption of methanol molecules. This is a hint to the important role of adsorbate complexes formed by adsorption of methanol molecules for the activity of zeolites in MTBE synthesis<sup>24</sup>.

In the early 1990s, worldwide MTBE production exhibited the highest growth rate of all the commodity chemicals<sup>25-28</sup>. Further improvements on fuel quality had been expected to make the trend continue beyond 2000. However, concern has been expressed about MTBE as a health hazard. It is currently being banned in California to prevent contamination of ground water<sup>29-30</sup>. The possible alternatives to MTBE are ethanol, ethyl-tert butyl ether (ETBE), Tert-amyl methyl ether (TAME), and Tert-butyl alcohol (TBA). It is reported that more than 85% of reformulated gasoline uses MTBE vs. 8% ethanol. However, these alternatives are less favourable. Gasoline blends have been reported to drastically increase hydrocarbon emissions over MTBE blends<sup>31</sup>. Moreover, substantially increased use of ethanol as a gasoline additive is likely to result in sharply higher prices for consumers<sup>32</sup>. Although MTBE may be produced in lesser amounts in the future, its synthesis still offers interesting insights into etherification reactions in general. Thus, it can be thought as a model reaction for understanding the potential use of novel solid acid catalysts for the synthesis of ethers. The synthesis of other ethers will undoubtedly increase as the search intensifies for a replacement of MTBE as a gasoline additive.

In the present work, we have investigated the possibility of using transition metal (W, Mo & Cr) incorporated pure ceria and its sulphated analogues for the vapour phase MTBE synthesis from methanol and tertiary butyl alcohol (TBA). The reaction variables such as temperature of the reaction, time on stream, molar ratio of methanol to tertiary butanol and flow rate were optimised to have maximum conversion. Since, the general mechanism of the reaction suggests that etherification takes place via the intermediate formation of the corresponding tertiary carbocation followed by the nucleophilic attack of the methanol molecules<sup>33-35</sup>, it is assumed that an enhancement of surface acidity will favour the processes. So, an attempt is also made to correlate the catalytic efficiency of the systems with the surface acidity.

## **7.2 Methyl tertiary butyl ether synthesis**

The vapour phase MTBE synthesis from methanol and tert-butyl alcohol

was carried out in a conventional fixed bed reactor and the experimental procedure is given in section 2.6 of Chapter 2. The product identification was done by the gas chromatographic analysis of the liquid reaction mixture. It was then confirmed by the gaschromatography-mass spectrometer technique. The reaction always yielded MTBE as the major product. The percentage conversion is calculated on the basis of tert-butanol converted into the product.

### 7.3 Process optimisation

MTBE synthesis was carried out under atmospheric pressure in the presence of nitrogen. The optimisation process was done with 0.5 g of CSW<sub>15</sub> catalyst. A detailed investigation on the process optimisation is discussed below.

#### I. Effect of temperature

Figure 7.1 illustrates the relationship between the conversion of tert-butanol and the reaction temperature in MTBE synthesis over modified ceria systems in the temperature range of 100 to 200 °C. The reactions were carried out at a molar ratio of methanol to tert-butanol of 10:1, and the flow rate was kept as 4 mL/h.

From Figure 7.1, it is clear that the reaction is sensitive to slight changes in temperature. A notable increase in tert-butanol conversion is observed in the temperature range 100-150 °C followed by a decay at higher reaction temperatures. The conversion of tertiarybutanol reaches a maximum at 150 °C and it amounts to 52.2%.

The reduction in catalytic activity at higher temperatures can be ascribed to the formation of the co product isobutene either through tert-butanol dehydration or MTBE product de-etherification<sup>36</sup>. Isobutene thus formed will then be lost from the reflux apparatus. Based on thermodynamic equilibrium, the higher temperatures will largely promote side reactions over acid catalysts to produce other hydrocarbons or oxygenates, leading to a linear reduction in the conversion to MTBE with increasing temperatures<sup>37</sup>.

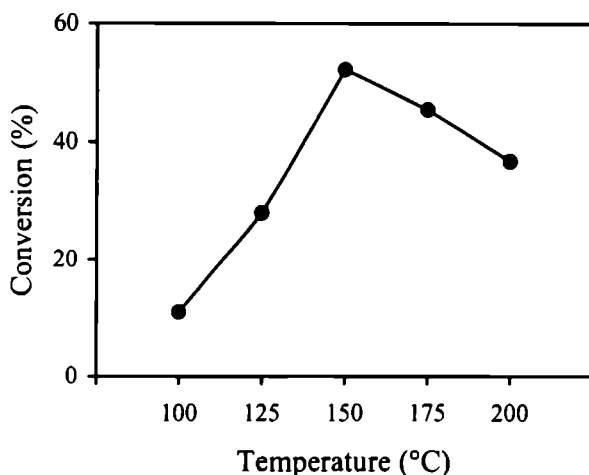


Figure 7.1

The effect of temperature on conversion in MTBE synthesis.

Catalyst – 0.5 g CSW<sub>15</sub>, molar ratio of methanol to tert-butanol-10:1.

TOS- 2 h, flow rate-4 mL/h

The descending portion of the curve at higher temperatures corresponds to the shift in equilibrium towards a lower yield of MTBE. This type of bell shaped curve is reported in the case of HPW/MCM-41 also, where the HPW/MCM-41 catalysts showed good activity at temperatures close to 100 °C, which make them comparable to that of commercial Amberlyst-15 and thereafter reduction in conversion with rise in temperature was noticed<sup>32</sup>. The effect of temperature on the MTBE synthesis conversion over zeolites has been widely studied which showed that for zeolites such as H-Y and H-ZSM-5, the percentage conversion increased with temperatures below 90 °C, after that it decreases and approaches equilibrium at higher temperatures<sup>38-42</sup>. The above literature points to the fact that for each catalyst there is an optimal temperature range at which the highest conversion can be obtained. In the present case this optimal temperature is at 150 °C.

## II. Effect of flow rate

In the case of gas phase reactions flow rate is an important parameter that has influence on the reactivity. The flow rate alters the contact time of the reactants and products on the catalyst surface. For studying the effect of flow rate on tertiary butanol conversion, four flow rates (3, 4, 5 and 6 mL/ h) were selected. The reactions were done at a temperature of 150 °C for 2 hrs. The results obtained are shown in Figure 7.2.

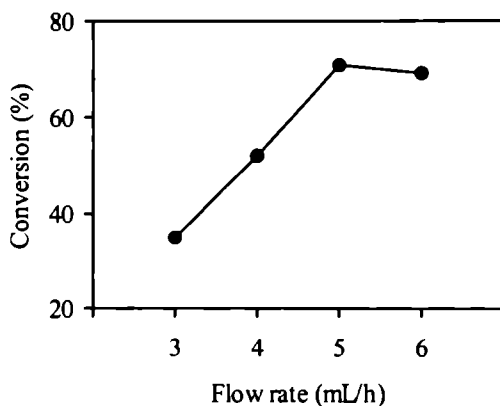


Figure 7.2

Influence flow rate in MTBE synthesis.

Catalyst -0.5 g CSW<sub>15</sub>, temperature-150 °C, tert-butanol to methanol  
molar ratio- 1:10, TOS-2 h

The results presented in Figure 7.2 indicate that as the flow rate changes from 3 to 5 mL/h, the conversion of tert-butanol increases from 34.9 to 70.7%. Above 5 mL/h, an increase in flow rate decreases the conversion. Brandao et al. investigated the gas phase synthesis of MTBE from methanol and tert-butanol over microporous niobium silicate AM-11 and found that an increase of WHSV has no significant effect on the selectivity for MTBE, whereas the conversion of tertiary butanol decreased markedly. They concluded that longer residence time favoured the yield of MTBE<sup>43</sup>. In the present case also the residence time of the reactants was found to play a decisive role in determining the catalytic activity. At higher flow rates, since

the residence time for the reactants on the catalyst surface is smaller, reduction in the catalytic activity is observed.

### III. Effect of molar ratio

To understand the influence of reactant concentration in determining the catalytic activity, a series of experiments were conducted at a reaction temperature of 150°C with flow rate of 5 mL/h. Figure 7.3 depicts conversion levels of tert-butanol with various methanol/tert-butanol molar ratios.

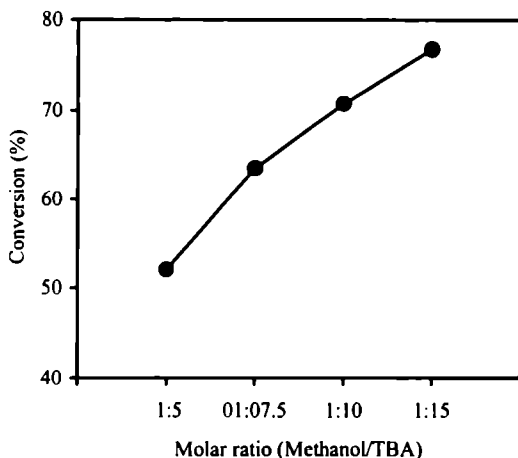


Figure 7.3

Influence of methanol to tertiary butanol molar ratio in MTBE synthesis.

Catalyst – 0.5 g CSW<sub>15</sub>, temperature-150 °C, flow rate-5 mL/h, TOS- 2 h

Methanol to tert-butanol molar ratio is found to exert a positive influence on MTBE formation. As the molar ratio is increased from 1:5 to 1:15, the percentage conversion increase from 52.0 to 76.8%. In all the cases MTBE is formed as the exclusive product. An increase in the concentration of methanol results in an increase in the number of molecules, which in turn results in an increase in the number of effective collisions. Another reason for the increased conversion is the fact that

the excess methanol suppresses the formation and secondary reaction of isobutene and thus promotes the conversion and selective formation of MTBE<sup>43</sup>.

#### IV. Effect of time on stream

In order to evaluate the stability of the catalytic systems with reaction time, reaction was carried out continuously for 8 hours at 150 °C and the reaction mixture was analyzed at intervals of one hour. The activity profile obtained for CSW<sub>13</sub> system as a function of time on stream is given in Figure 7.4.

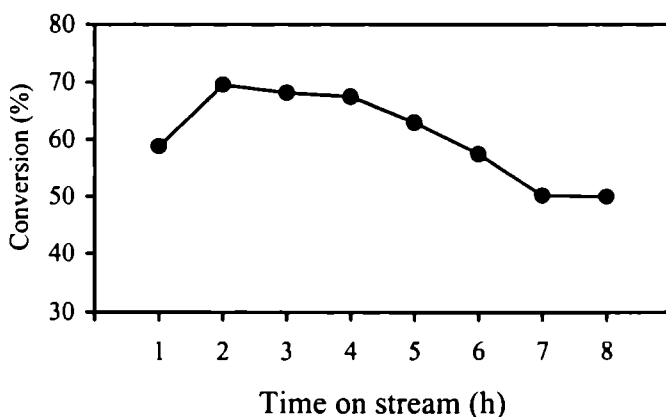


Figure 7.4

Influence of time on stream in MTBE synthesis

Catalyst-1 g CSW<sub>13</sub>, temperature-150 °C, molar ratio of methanol to tert- butanol-10:1, flow rate-5 mL/h

Figure 7.4 clearly indicates that the reactivity of the catalyst systems increases during the first two hours and remains almost the same up to the fourth hour. Thereafter considerable decrease was noticed, and only 50% conversion was observed after eight hours of reaction. Xia et al. studied the time on stream activity of various mesoporous catalysts like HPW/MCM-41, NaAlMCM-41, HAlMCM-41 and H<sub>2</sub>SO<sub>4</sub>/

MCM-41 in which the reactions were carried out at the respective optimal reaction temperatures<sup>37</sup>. They observed that with an increase in time on stream to 110 h and with the exception of H<sub>2</sub>SO<sub>4</sub>/MCM-41, the selective conversion of tertiary butanol to MTBE hardly changes, showing the excellent stability of these catalysts. This is attributed to the relatively small diffusion hindrance over mesoporous catalysts, in which the adsorption-desorption processes readily occur, decelerating the deactivation of the catalysts by coking. The reduction in catalytic activity in the case of H<sub>2</sub>SO<sub>4</sub>/MCM-41 catalyst was ascribed to the leaching of mobile H<sub>2</sub>SO<sub>4</sub> molecules in the gas-liquid stream. The results of present study show that the catalytic system possesses reasonable activity for four hours of reaction run only. The qualitative analysis of the product mixture doesn't show the presence of sulphate ions, which argues against the probability of sulphate leaching. Further the reduction of activity with time may be due to the poisoning of the catalyst by coking or the readsorption of the products on the catalyst surface.

#### **7.4 Catalytic efficiency of different systems**

The catalytic activity of three series (W, Mo & Cr doped) of modified ceria catalysts along with their sulphated derivatives is presented in this section. All the reactions were done at a reaction temperature of 150 °C with a methanol to tert - butanol molar ratio of 15:1 and the flow rate was kept as 5 mL/h. Because of the acid catalysed nature of the reaction, the increase in the percentage conversion is correlated with the increase in the surface acidity of the systems as determined by ammonia TPD method.

##### **a) Tungsten incorporated systems**

A series of experiments were performed to evaluate the catalytic activity of tungsten modified samples. The results are depicted in Table 7.1. The correlation between the percentage conversion and the total acidity of the systems obtained from ammonia TPD method is given in Figure 7.5.

Table 7.1

Activity of tungsten incorporated systems in the MTBE synthesis

Catalytic systems	Conversion (%)	Selectivity (%)
C	24.2	100
SC	31.4	100
CW <sub>5</sub>	39.7	100
CW <sub>10</sub>	56.5	100
CW <sub>15</sub>	58.0	100
CSW <sub>5</sub>	76.8	100
CSW <sub>10</sub>	80.1	100
CSW <sub>15</sub>	77.3	100

Amount of Catalyst-0.5 g, temperature-150 °C, time on stream -2 h, molar ratio of methanol to tert-butanol-15:1, flow rate-5 mL/h

From Table 7.1, it is evident that pure ceria gives the lowest conversion under the specified reaction conditions. Enhancement in catalytic activity was observed with modification. Comparing the catalytic activity of simple as well as sulphated systems, it was observed that sulphate modification has a positive influence on the catalytic activity of supported systems towards the reaction. Among the sulphated systems maximum activity is shown by CSW<sub>10</sub> system, and it amounts to 80.1%.

From the Figure 7.5, it is clear that total acidity is lowest for pure ceria which in turn gives the lowest conversion. As the tungsten loading increases the total acidity of the systems was found to increase. This paved way for their higher conversion. Among the sulphated systems, CSW<sub>10</sub> possess maximum number of acid sites, which gives the highest conversion.

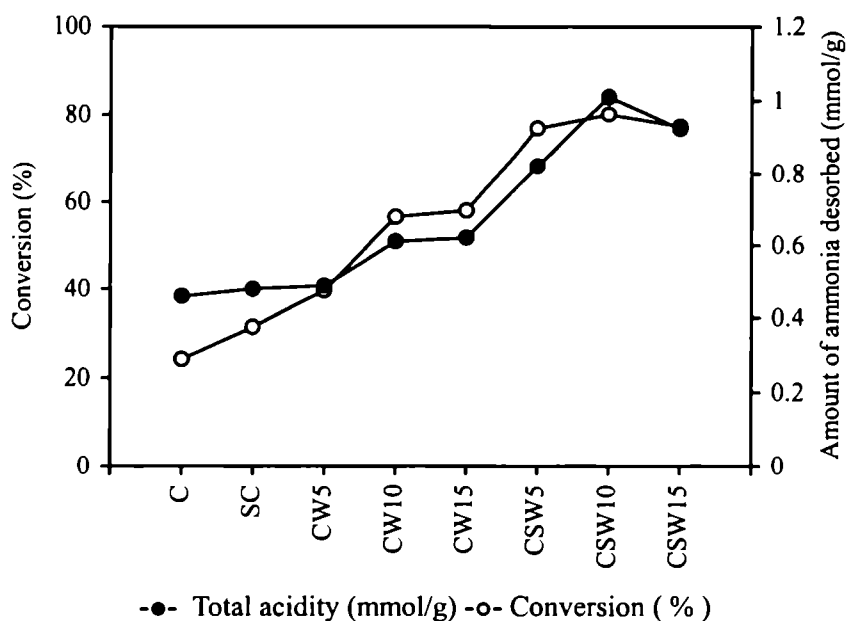


Figure 7.5

Catalytic activity correlated with the total acidity obtained from ammonia TPD.

The catalytic activity of different systems is found to be in accordance with the surface acidity possessed by them. Xia et al. studied the catalytic activity of MCM-41 supported 12-tungstophosphoric acid (HPW) catalysts with various HPW loading for the gas-phase synthesis of MTBE. They observed that the surface acidity of HPW/MCM-41 catalysts was enhanced stepwise by increasing the HPW loading. In agreement to the acidity values the catalytic activity of the systems also increased with HPW loading<sup>37</sup>.

### b) Molybdenum incorporated systems

The catalytic efficiencies of molybdenum incorporated ceria systems as well as their sulphate modified series in MTBE synthesis are presented in Table 7.2. The tert-butanol conversion is correlated with total acidity as obtained from ammonia TPD ( Figure 7.6 )

Table 7.2

Activity of molybdenum incorporated systems in the MTBE synthesis

Catalytic systems	Conversion (%)	Selectivity (%)
C	24.2	100
SC	31.4	100
CM <sub>5</sub>	75.6	100
CM <sub>10</sub>	42.1	100
CM <sub>15</sub>	49.7	100
CSM <sub>5</sub>	56.4	100
CSM <sub>10</sub>	36.3	100
CSM <sub>15</sub>	78.6	100

Amount of Catalyst-0.5 g, temperature-150 °C, time on stream -2 h, molar ratio of methanol to tert-butanol-15:1, flow rate-5 mL/h

From Table 7.2, it is clear that ceria in the pure form is less active in the MTBE synthesis than the supported catalysts. In the case of molybdenum impregnated systems, a sharp decrease in percentage conversion is observed as we move from CM<sub>5</sub> to CM<sub>10</sub> system, although a slight increase is noticed for CM<sub>15</sub> system. Among the sulphated series, maximum activity is shown CSM<sub>15</sub> system.

Figure 7.6 illustrates that the activity pattern in the case of molybdenum doped systems is in agreement with surface acidity values obtained from TPD of ammonia. Among the molybdenum systems surface acidity is the highest for CSM<sub>15</sub> system. Since the activity is related to the surface acidity, this system gives the maximum conversion. According to Xia, Hidajat and Kawi, who studied the catalytic activity of various mesoporous catalysts like HPW (50%)/MCM-41, H<sub>2</sub>SO<sub>4</sub>/MCM-41, HAIMCM-41, NaAIMCM-41 and SiMCM-41, the catalytic activity towards MTBE synthesis corresponds to the surface acidity possessed by them. The relative

concentrations of the total acid sites in these mesoporous catalysts is in the decreasing order HPW (50%)/MCM-41 > H<sub>2</sub>SO<sub>4</sub>/MCM-41 > HAlMCM-41 > NaAlMCM-41 >> Si-MCM-41. The activity of these catalysts was found to increase in the same order, thus pointing to the involvement of total number of acid sites in MTBE synthesis<sup>37</sup>.

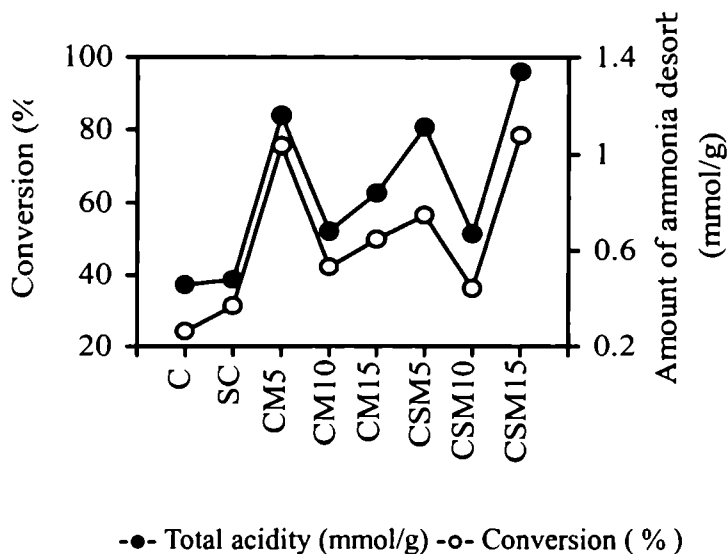


Figure 7.6

Catalytic activity correlated with the total acidity obtained from ammonia TPD.

### c) Chromium incorporated systems

To study the catalytic efficiencies of chromium doped ceria and sulphated ceria systems, a set of reactions were performed under optimised reaction conditions. The results are presented in Table 7.3. The difference in catalytic activity among the systems is correlated with the difference in surface acidity possessed by these catalysts, as depicted in Figure 7.7.

Table 7.3

Activity of chromium incorporated systems in the MTBE synthesis

Catalytic systems	Conversion (%)	Selectivity (%)
C	24.2	100
SC	31.4	100
CCr <sub>5</sub>	39.7	100
CCr <sub>10</sub>	33.4	100
CCr <sub>15</sub>	34.2	100
CSCr <sub>5</sub>	35.8	100
CSCr <sub>10</sub>	38.4	100
CSCr <sub>15</sub>	41.4	100

Amount of Catalyst-0.5 g, temperature-150 °C, time on stream -2 h,  
molar ratio of methanol to tert-butanol-15:1, flow rate-5 mL/h

From Table 7.3, it is noticeable that all the systems show remarkable activity towards the reaction. Among the chromium doped systems, as the percentage of chromium increases, the catalytic activity decreases from CCr<sub>5</sub> to CCr<sub>10</sub>, and a small increase is noticed for CCr<sub>15</sub>. An enhancement in catalytic activity is observed for sulphated as well as chromium incorporated ceria systems. Among the chromium incorporated sulphated systems highest percentage conversion is given by CSCr<sub>15</sub>, which amounts to 41.4%.

From Figure 7.7, the total acidity of the supported systems is found to decrease as the percentage of chromium is increased from 5 to 10, there after a small increase is noticed. As far as sulphated systems are considered, a gradual increase in surface acidity is seen with modification. The catalytic activity of the systems was found to be in agreement with the surface acidity.

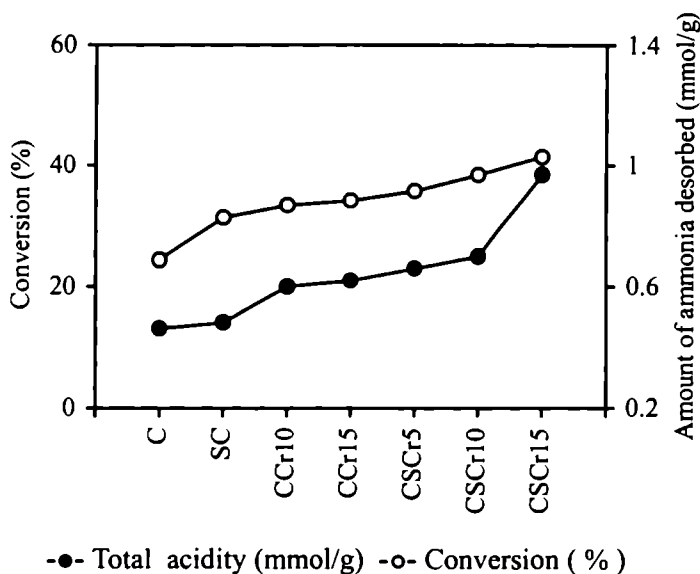


Figure 7.7

Catalytic activity correlated with the total acidity obtained from ammonia TPD

### 7.5 Conclusions

The following are the key points derived from this study:

- \* Transition metal promoted (W, Mo & Cr) ceria systems and their sulphated analogues are found to catalyse the vapour phase methyl tertiary butyl ether synthesis with considerable activity.
- \* The reaction gives 100% selectivity to methyl tertiary butyl ether over all the systems.
- \* Study about the reaction parameters such as temperature of the reaction, reaction time, methanol to tertiary butanol molar ratio and flow rate suggest that these parameters play an important role in determining the catalytic activity and each has a specific value for maximum conversion.
- \* The agreement between the catalytic activity and the surface acidity points to the fact that the difference in catalytic activity among the systems can be related to the difference in the surface acidity possessed by them.

## REFERENCES

1. J. E. Peeples, The Clean Air Act: A brave New World for Fuel Reformulation. Fuel Reformulation, 1991, 1, 27.
2. F. L. Potter, Clean Air Act History Marked by Battle, Compromise. Fuel Reformulation, 1991, 1, 22.
3. C. Subramaniam and S. Bhatia, *Canadian J. Chem. Eng.*, 65 (1987) 613.
4. W. J. Piel and R. X. Thomas, *Hydrocarbon Processing.*, 69 (1990) 68.
5. D. Seddon, *Catal. Today.*, 15 (1992) 1.
6. G. H. Unzelman, *Fuel Reformulation.*, 1(1991) 50.
7. Z. Ziyang, K. Hidajat and A. K. Ray, *J. Catal.*, 200 (2001) 209.
8. T. Takesono and Y. Fujiwara, US Patent 4, 182, 913, 1980.
9. L. V. Mao, R. R. Carli, H. Ahlafi and V. Ragaini, *Catal. Lett.*, 6 (1990) 321.
10. P. Chu and G. H. Kuhl, *Ind. Eng. Chem. Res.*, 26 (1987) 365.
11. A Study of the Acid-Catalyzed Synthesis of MTBE on Inorganic Solid Acids, Ph.D. Dissertation, University of Pittsburgh, 1995.
12. P. Wiseman, *Petrochemicals*, UMIST series in Science and Technology (Ellis Horwood, Chichester, 1986).
13. A. Ali and S. Bhatia, *J. Chem. Eng.*, 44 (1990) 97.
14. T. Horwath, M. Seiler and M. Hunger, *Appl. Catal. A. Gen.*, 197 (2000) 227.
15. M. Hunger, T. Horvath and J. Weitkamp, *Microporous and Mesoporous Mater.*, 22 (1998) 357.
16. J. S. Kim, J. M. Kim, G. Seo, N. C. Park and S. Niiyama, *Appl. Catal. A. Gen.*, 37 (1988) 45.
17. J. M. Adams, K. Martin, R. W. McCabe and S. Murray, *Clays Clay Miner.*, 34 (1986) 597.
18. M. E. Quiroga, N. S. Figoli and U. A. Sedran, *J. Chem. Eng.*, 67 (1997) 199.
19. S. Okazaki and N. Wada, *Catal. Today.*, 16 (1993) 349
20. A. Kogelbauer, M. Öcal, A. A. Nikolopoulos, J.G. Goodwin Jr and G. Marcelin,

- J. Catal.*, 148 (1994) 157.
21. A. M. Kazi, J. G. Goodwin Jr, G. Marcelin and R. Oukaci, *Ind. Eng. Chem. Res.* 34 (1995) 718.
  22. A. A. Nikolopoulos, A. Kogelbauer, J. G. Goodwin Jr and G. Marcelin, *J. Catal.*, 158 (1996) 76.
  23. F. Collignon, M. Mariani, S. Moreno, M. Remy and G. Poncelet, *J. Catal.*, 166 (1997) 53.
  24. A. Kogelbauer, M. Öcal, A. A. Nikolopoulos, J. G. Goodwin Jr and G. Marcelin, *J. Catal.* 152 (1995) 122.
  25. S. J. Ainsworth, *Chem. Eng. News.*, 1991, 69 (23) 13.
  26. M. S. Reisch, *Chem. Eng. News.*, 1992, 70 (15) 16.
  27. G. J. Hutchings, C. P. Nicolaidis and M. S. Scurrrell, *Catal. Today.*, 15 (1992) 23.
  28. E. M. Kirschner, *Chem. Eng. News.*, 1996, 74 (15) 16.
  29. J. E. Reuter, B.C. Allen, R.C. Richards, J. F. Pankow, C. R Goldman, R. L. Scholl and J. S. Seyfried, *Environ. Sci. Technol.*, 32 (1998) 3666.
  30. New Study Reaffirms Low MTBE Toxicity. *Chem. Eng. News.*, 2001, (25) 22.
  31. T. Chang, Controversy Over MTBE in Gasoline Rages on Oil Gas J. 97 (1999) 51.
  32. M. McCoy, *Chem. Eng. News.*, 1999, 77 (31) 5.
  33. C. P. Nicolaidis, C. J. Stotijn, E.R.A. van der Veen and M. S. Visser, *Appl. Catal. A. Gen.*, 103 (1993) 223.
  34. G. J. Hutchings, C.P. Nicolaidis, and M. S. Scurrrell, *Catal. Today.*, 15 (1992) 23.
  35. R. Le Van Mao, T. S. Le, M. Fairbairn, A. Muntasar, S. Xiao, and G. Denes, *Appl. Catal. A. Gen.*, 185 (1999) 41.
  36. J. F. Knifton and J. C. Edwards, *Appl. Catal. A. Gen.*, 183 (1999) 1.
  37. Q. H. Xia, K. Hidjat, and S. Kawi, *J. Catal.*, 209 (2002) 433.

38. A. A. Nikolopoulos, A. Kogelbauer, J. G. Goodwin and G. Marcelin, *Appl. Catal. A. Gen.*, 119 (1994) 69.
39. A. Kogelbauer, A. A. Nikolopoulos, J. G. Goodwin and G. Marcelin, *Study in Surf. Sci. and Catal.*, 84 (1994) 1685.
40. A. A. Nikolopoulos, R. Oukaci, J. G. Goodwin and G. Marcelin, *Catal. Lett.*, 27 (1994) 149.
41. A. Kogelbauer, M. Ocal, A. A. Nikolopoulos, J. G. Goodwin and G. Marcelin, *J. Catal.*, 148 (1994) 157.
42. F. Collignon, M. Mariani, S. Moreno, M. Remy and G. Poncelet, *J. Catal.*, 166 (1997) 53.
43. P. Brandao, A. Philippou, J. Rocha and M. W. Anderson, *Catal. Lett.*, 73 (2001) 59.

\*\*\*\*\*

### *Summary And Conclusions*

#### **Abstract**

---

*The importance of environmentally friendly catalysts in the modern age forms the basis of the present research work. The major objectives of the present work consists of (a) the preparation of cerium oxide with enhanced textural and structural properties and to modify it by transition metals and sulphate ions in an attempt to increase the surface acidity as well as electronic properties of pure ceria (b) characterization of the modified catalysts and determination of surface acidity (c) measurement of the catalytic activity of the prepared systems towards industrially important reactions like acetalization of cyclohexanone and the hydrolysis of the dimethyl acetal, MTBE synthesis, oxidative dehydrogenation of ethylbenzene and Beckmann rearrangement of oximes. This chapter deals with the summary of the results of the present work and also the scope for further research in this field.*

---

## 8.1 Introduction

Since the conventional hydroxide method used for the preparation of ceria yields samples with low surface area and thermal stability, a new method called pseudo-template method is adopted to prepare High Surface Area (HSA)  $\text{CeO}_2$ . This method exploits the interaction of hydrous cerium oxide with a cationic surfactant under basic conditions to promote exchange reaction with hydroxy surface groups. In an attempt to enhance the surface acidity and electronic properties of cerium oxide we have modified it with transition metals like tungsten, molybdenum, chromium and also with sulphate ions. Since the knowledge about the structure and composition of the surface is critical in explaining the reactivity and selectivity of a solid catalyst a systematic investigation of the physico-chemical properties of the prepared systems was carried out. The catalytic activity of the supported metal oxides and their sulphated counterparts have also been measured in several reactions of industrial relevance. The characterization and catalytic activity results were compared with that of pure cerium oxide. The thesis is dedicated to several aspects of supported ceria catalysts giving emphasis to its preparation, characterization results and catalytic performance towards industrially important reactions. The chapter-wise summary of the thesis is given below.

## 8.2 Summary

Chapter 1 gives a brief literature review on metal oxides, supported and sulphated metal oxides. The importance of cerium oxide in the current environmental aspect is discussed in detail. This chapter also includes literature survey on reactions such as acetalization and de-acetalization reaction, oxidative dehydrogenation reaction, MTBE synthesis and Beckman rearrangements. Since much attention is given to the surface acid amount of the catalytic systems, different methods for its measurement are also discussed.

Chapter 2 focuses on the materials used for the present work and the techniques employed for characterizing the catalytic systems. The preparation method

adopted in the present study is described in detail. The experimental procedures used for the evaluation of catalytic activity are also presented in this chapter.

Chapter 3 describes the results of physico-chemical characterization of the prepared catalytic systems. The catalytic systems were characterized by surface area and pore volume measurements, X-ray diffraction analysis and Infra red spectroscopy. Thermal stability of the samples was revealed by Thermogravimetric analysis, and elemental composition of the prepared systems was obtained from Energy dispersive X-ray analysis. Scanning electron microscopy was used to know the surface topography of the catalysts and, the metal ion coordination was obtained from UV-vis diffuse reflectance spectroscopy. Surface acidic properties of the prepared systems were examined by temperature programmed desorption of ammonia, perylene adsorption studies, TGA of adsorbed 2, 6 - dimethyl pyridine and also by catalytic test reactions like cumene cracking and cyclohexanol decomposition reaction.

Chapter 4 discusses the application of the catalytic systems towards acetalization and de-acetalization reaction. Since protection and deprotection reactions play a significant role in organic synthesis, this reaction seems to have great relevance. The acetalization of cyclohexanone was carried out using methanol. The influence of reaction parameters such as temperature of the reaction, reaction time and cyclohexanone to methanol molar ratio on the catalytic activity was subjected to investigation. Metal leaching studies are also performed to have an idea about the nature of the reaction. Attempt has been made to correlate the catalytic activity with the surface acidic properties of the catalytic systems.

Chapter 5 illustrates the catalytic activity of the systems towards oxidative dehydrogenation of ethylbenzene. The catalytic activity and selectivity of all the systems were measured under optimised reaction conditions such as temperature of the reaction, air flow, time on stream and flow rate of ethylbenzene. The variation of catalytic activity among the systems was correlated with difference in the surface acid amount possessed by them.

Chapter 6 describes the activity measurements of the catalytic systems for the vapour phase Beckmann rearrangement of salicylaldoxime and cinnamaldoxime. Here also the reaction conditions are optimized to have better activity and selectivity. The influence of surface acid amount in determining the percentage conversion and selectivity to different products are also taken into consideration.

Chapter 7 narrates the performance of the catalytic systems in the vapour phase MTBE synthesis from methanol and tertiary butanol. Since etherification reaction is an acid catalyzed reaction, attempt to correlate the catalytic activity with surface acid amount is also made. The reaction conditions are optimised before measuring the performance of different catalytic systems.

Chapter 8 presents the summary, important conclusions and future prospects of the present work.

### **8.3 Conclusions**

The major conclusions that can be drawn from the present research work are the following.

- \* Pseudo-template method is found to be an efficient method for the preparation of cerium oxide with high surface area. Although modification with transition metal and sulphate ions decrease the surface area, there is enhancement in the physico-chemical characteristics and surface properties compared to simple systems.
- \* The XRD patterns of the prepared systems reveal characteristic fluorite phase of ceria which remained intact after modification. No characteristic peaks of incorporated metal oxides are seen in the XRD patterns of modified samples, pointing to the fact that the incorporated metal oxides are highly dispersed on the surface of the support and also their concentration is below the corresponding dispersion capacity.
- \* Decrease of surface area and pore volume upon modification suggests

that the incorporated metal ions are occupying the surface vacant sites of the support, and pore blockage is responsible for the reduction in surface area.

- \* SEM pictures of the samples show agglomeration of the particles upon modification with transition metals and sulphate ions. Agglomeration of the particles leads to increase in the crystallite size values, which is clear from the crystallite size values calculated using Scherer equation.
- \* IR bands show characteristic absorptions of ceria, transition metal oxides and sulphated species. The presence of tetra coordinated  $Ce^{4+}$  species is evident from UV-vis diffuse reflectance spectroscopy.
- \* Measurement of surface acid amount indicates an enhancement in surface acidity, especially the Lewis acidity upon modification. There is good correlation among the surface acidity values measured by ammonia TPD, perylene adsorption studies, thermodesorption studies of 2, 6-DMP adsorbed samples and catalytic test reactions like cumene cracking and cyclohexanol decomposition reaction.
- \* In the acetalization of cyclohexanone with methanol, dimethoxy cyclohexane was formed as the exclusive product. Most of the systems possess the ability to hydrolyze the dimethoxy cyclohexane to cyclohexanone completely thereby acting as versatile materials in protecting and deprotecting carbonyl groups during organic synthesis. The catalytic activity of the systems towards the acetalization reaction found to vary in accordance with the amount of medium and strong acid sites possessed by them.
- \* Vapour-phase oxidative dehydrogenation of ethylbenzene over the catalytic systems yielded styrene as the major product along with small amounts of benzene, toluene and C-oxides. In this reaction the amount of medium strong acid sites are found to determine the catalytic activity of the systems.
- \* In the Beckmann rearrangement of cinnamaldoxime, isoquinoline and cinnamonitrile are formed as the predominant products. The catalytic systems

are highly effective for the production of benzoxazole by the beckmann rearrangement of salicylaldoxime. Reaction conditions such as temperature of the reaction, flow rate, time on stream etc. are found to have great significance in determining the catalytic activity and product selectivity.

**Future outlook**

The observations we have obtained during the research work on “Catalysis by nanocrystalline ceria modified with transition metals” points to the importance of modified ceria catalysts in improving the environmental quality mainly by the reduction of industrial waste. Since these catalysts have proved to be efficient for the production of heterocyclic compounds, which has great medicinal value, further research work can be made in the field of rearrangements to obtain valuable products. The redox features of the modified ceria systems can also be investigated in detail, in the direction of improving its performance as an automotive catalyst.

\*\*\*\*\*